

**Cutaneous Metabolism, Tissue Binding, Lipophilicity
and Electroosmosis:
Relevance for iontophoretic Enhancement**

Submitted to the faculty of natural sciences
of the University of Basel, Switzerland
for the fulfilment of the requirements
for a Ph.D. Degree

by

Melanie Pamela Altenbach
from Basel (BS)

Riehen, 2005

Accepted by the faculty of natural sciences
on the proposal of

Prof. Dr. H. Leuenberger

PD Dr. G. Imanidis

PD Dr. P. Van Hoogevest

Basel, 6. April 2004

Prof. Dr. M. Tanner

Dean

Acknowledgments

I would like to express my gratitude to **Prof. Dr. Hans Leuenberger** for giving me the opportunity to work as a member of his team and as a Ph.D. student on my thesis at the Institute of Pharmaceutical Technology, Department of Pharmacy, University of Basel.

Especially, I would like to thank my supervisor **PD Dr. Georgios Imanidis** for his support and interest throughout this work. He taught me that also patience and calmness belong to the work of a scientist and how important a detail can be in an entire picture.

I thank **PD Dr. P. van Hoogevest** from Phares, Inc. for acting as co-examiner.

I would like to thank **R. Mirsaidi, N. Schnyder and Ch. Zimmermann** for the work they did on the basis of their diploma thesis.

Many thanks go to **Stefan Winzap** for being ‘die gute Seele des Instituts’ and for his technical support and **Sonja Reutlinger** for being a real friend with good advice.

Furthermore, I express my sincere thanks to all **my colleagues** at the Institute of Pharmaceutical Technology, University of Basel, for giving me support and a friendly atmosphere during my education.

My gratitude goes also to **Ioanna Kotsaka** from Novartis Pharma AG, Basel, who encouraged and supported me concerning further carrier steps during my education.

My deepest thanks go to my mother and Frank for their love, confidence, patience and support.

A	ABSTRACT	1
B	INTRODUCTION AND OBJECTIVES	3
C	THEORETICAL INTRODUCTION	5
C.1	Skin	5
C.1.1	Anatomy of the skin.....	5
C.1.1.1	Epidermis	5
C.1.1.2	Dermis.....	7
C.1.1.3	Hypodermis.....	7
C.1.1.4	Appendages.....	8
C.1.2	The main barrier of the skin.....	9
C.1.3	Penetration pathways across the stratum corneum.....	9
C.1.4	Metabolism of the skin.....	10
C.1.4.1	Localization of the enzyme activity	10
C.1.4.2	Models for skin metabolism studies	11
C.1.4.3	Inhibition of cutaneous metabolism	11
C.2	Transdermal iontophoresis: Theoretical model	13
C.2.1	Passive diffusion	13
C.2.2	Nernst-Planck Equation.....	13
C.2.3	Modified Nernst-Planck Equation incorporating convective solvent flow	14
C.2.4	Extended model incorporating lipid pathways	15
C.2.5	Extended model incorporating membrane alterations	15
C.3	Convective solvent flow	16
C.3.1	Measurement of convective solvent flow	16
C.3.1.1	Direct / Indirect methods	16
C.3.2	Permselectivity of the skin.....	17
C.3.3	Factors affecting convective solvent flow	17
C.3.3.1	Molecular weight of the permeant	17
C.3.3.2	Structure of the permeants.....	18
C.3.3.3	Current density and ionic strength.....	19
C.3.3.4	pH	19
C.4	Membrane alterations following iontophoresis.....	20
C.5	Reverse iontophoresis	21
C.6	In vitro model used for permeation	22
C.6.1	Potentiostat used.....	22
C.6.2	Diffusion cells	22
C.6.3	Electrodes	23
C.6.4	Membrane	24
C.6.5	The model substances	24
C.6.5.1	Tyrosine-Phenylalanine.....	25
C.6.5.2	Tyrosine- β -Naphthylamide	26
C.6.5.3	Benzyl-2-Acetamido-2-deoxy- α -D-glucopyranoside.....	26
C.6.5.4	o-Phenanthroline HCl (Monohydrate).....	27

C.7	Applications of iontophoresis	27
C.8	References	28
D	ORIGINAL PUBLICATIONS	34
D.1	Effect of cutaneous metabolism of a dipeptide on the iontophoretic flux of an uncharged electroosmosis marker.....	34
D.2	Simultaneous assessment of tissue retention, lipophilicity of permeant and electroosmosis as factors affecting iontophoretic enhancement	55
E	APPENDIX	74
E.1	Assay of TyrPhe, Tyrβ-NA, BAd-α-Glc, Tyr, Phe and Benzyl alcohol.....	74
E.2	Physico-chemical characterization of TyrPhe, Tyrβ-NA and BAd-α-Glc.	77
E.2.1	Ionization constants.....	77
E.2.2	Solubility of TyrPhe and Tyr β -NA	78
E.2.3	Stability.....	78
E.2.3.1	Chemical stability	78
E.2.3.2	Enzymatic stability of TyrPhe	79
E.2.3.3	Enzymatic stability of BAd- α -Glc.....	81
E.2.3.4	Stability during voltage application of 250 mV.....	81
E.2.4	Partition coefficient.....	82
E.3	Validation for transport studies.....	83
E.4	Experimental determinations.....	84
E.4.1	Determination of the transport area.....	84
E.4.2	Determination of the thickness of heat-separated epidermal membrane ...	84
E.4.3	Osmolarity and pH during permeation experiment	85
E.4.4	Pulverization of skin	85
E.4.4.1	Determination of the membrane extraction	85
E.4.4.2	Recovery from epidermal membrane	85
E.4.5	Time dependent resistance changes of the membrane.....	85
E.4.6	Procedure of the permeation experiments	86
E.4.7	Cumulative amount permeation	88
E.5	List of instruments.....	96
E.6	References	97

A Abstract

In this work passive and iontophoretic transport of a dipeptide, Tyrosine-Phenylalanine (TyrPhe), a protected amino acid, Tyrosine- β -Naphthylamide (Tyr β -NA), and a glucose derivative, Benzyl-2-Acetamido-2-deoxy- α -D-glucopyranoside (BAd- α -Glc), was investigated across heat-separated human epidermis in vitro. The modified Nernst-Planck Equation was used to theoretically describe permeation of these compounds. Permeation experiments were carried out with custom-made glass diffusion cells connected to a four-electrode system developed in our laboratories to generate constant voltage. Ag/AgCl electrodes with the anode in the donor compartment were used to apply the potential difference across the skin and reference Ag/AgCl electrodes, reaching either side of the membrane with Luggin capillaries, were used to precisely control and maintain constant the potential drop across the membrane. Permeation was studied at pH 3 and 4.5, for which the TyrPhe and Tyr β -NA are positively charged.

The contribution of charge, lipophilicity, skin retention, electroosmosis and the influence of skin metabolism on the permeation rate of the above mentioned substances was examined.

pK_a of TyrPhe and Tyr β -NA was determined by potentiometric titration to be 3.50 and 4.78, respectively. The average net ionic valence of TyrPhe was 0.76 and 0.091 at pH 3 and 4.5, respectively and that of Tyr β -NA was 0.98 and 0.66 at pH 3 and 4.5, respectively. n-octanol/aqueous buffer partition coefficients were determined using shaking flask method to be for BAd- α -Glc 0.13 and 0.11 at pH 3 and 4.5, respectively and for TyrPhe 0.80 and 0.61 at pH 3 and 4.5, respectively and for Tyr β -NA 4.81 and 7.28 at pH 3 and 4.5, respectively. Enzymatic stability of TyrPhe was determined by reflection boundary set-up. A degradation of 12% at pH 3 and 45% at pH 4.5 was measured over 69 hours at 37°C. For BAd- α -Glc the generation of less than 0.5% of benzyl alcohol, the product of glycosidase action, was found. Tyr β -NA was stable because of the side-chain protecting group.

A typical permeation experiment involved three experimental stages. After a first passive stage over 44 hours, 250 mV were applied for 3 hours followed by a second passive stage of 22 hours.

Membrane resistance during the three hours of iontophoresis remained constant or showed only small decline. These results guaranteed the integrity of the membrane under the present experimental conditions.

The influence of TyrPhe skin metabolism on its own permeation rate and skin retention as well as on the permeation rate and skin retention of BAd- α -Glc was examined. No reproducible permeation of TyrPhe at pH 3 and no permeation at all at pH 4.5 was measured when the dipeptide was used alone or in combination with BAd- α -Glc. Additionally, higher fluxes of the degradation products Tyrosine (Tyr) and Phenylalanine (Phe) were observed and higher levels of Tyr and Phe were recovered from the epidermis compared to blank runs. Blank runs reflected endogenous levels of Tyr and Phe. Degradation was inhibited by the use of o-phenanthroline at pH 3 but not at pH 4.5 and at both pH values at low temperature (4°C). Inhibition was verified by reproducible TyrPhe permeation and blank level Tyr and Phe fluxes and tissue recovery. These results confirm degradation of TyrPhe by cutaneous metabolism in heat-separated human epidermis, that was stronger at pH 4.5 compared to pH 3. BAd- α -Glc showed at both pHs smaller iontophoretic fluxes compared to the passive ones, indicating an electroosmotic flux from cathode to anode. In combination with TyrPhe, iontophoretic fluxes of BAd- α -Glc increased significantly when TyrPhe was metabolized in the tissue, while no such decrease was observed when TyrPhe metabolism was inhibited. This increase of BAd- α -Glc iontophoretic flux was accompanied by a considerable decrease of BAd- α -Glc amount retained in the epidermis. The generated Tyr and Phe appear, therefore, to decrease BAd- α -Glc amount retained in the epidermis and enhance iontophoretic flow. Thus, an interaction between the concurrent permeants at the level of tissue retention induced by metabolism can influence iontophoretic permeation of these poorly permeable compounds. So far only Tyr and Phe were able to show this effect. On the other hand, Tyr and Phe did not affect iontophoretic permeation of TyrPhe and Tyr β -NA. This demonstrates that the effect of Tyr and Phe is not universal but depends on the permeant.

The effect of lipophilicity and electroosmosis was assessed simultaneously for all three permeants, which spanned a 70-fold range of lipophilicity, in the absence of extraneous Tyr and Phe using a theoretical model for the enhancement factor. This was based on the modified Nernst-Planck Equation, extended by the ratio of permeability coefficients for lipid and aqueous pathway and including an estimate of the ionic valence of permeants in the aqueous domain of the tissue. At pH 4.5 a very weak electroosmotic flow from cathode to anode was observed, indicating an isoelectric point of the skin slightly above 4.5. At pH 3 electroosmotic flow was approximately 10-fold stronger than at pH 4.5. The ratio of the permeability coefficients for lipid and aqueous pathways resulted for all compounds at both pHs in values much smaller than 1, indicating that the aqueous pathway dominated transepidermal permeation. The simultaneous analysis of the results of all substances shows that the applied model evaluation affords a quantitative assessment of the effect of ionic valence, lipophilicity and electroosmosis and makes possible to predict the outcome of iontophoresis.

B Introduction and Objectives

Ongoing progress in biotechnology and continuing efforts in peptide and protein chemistry provide a steady source of new peptide drug candidates. These drugs are currently delivered mostly by injection because of the proteolytic enzymes in the gastro-intestinal tract and the extensive first-pass hepatic metabolism. Alternatives to the classical parenteral application are desirable, because the peptides with their short half-life need to be injected frequently. Transdermal permeation of peptides into and through the skin proceeds only to a small extent due to their hydrophilicity and large molecule size and due to the lipophilic nature of the stratum corneum. To overcome the problem of poor transport, the use of physical methods, like iontophoresis, has been examined.

Iontophoresis is a method to enhance and regulate transdermal drug permeation and delivery by application of an electric field on the skin. Next to the direct effect of the electrical field driving ionic permeants into the skin, secondary phenomena such as electroosmosis and membrane alterations contribute to iontophoretic flux of charged and uncharged permeants. Since almost 30 years the interest in systemic delivery by transdermal iontophoresis has increased strongly. Numerous groups investigated the mechanisms of iontophoretic enhancement, especially electroosmosis (Burnette and Ongpipattanakul 1987, Burnette and Ongpipattanakul 1988, Sims et al. 1991, Delgado-Charro and Guy 1994). One point of interest was the determination of the isoelectric point of the skin (Hoogestraate et al. 1994, Luzardo-Alvarez et al. 1998, Marro et al. 2001) and consequently the behavior of the electroosmotic flow at different net charges of the skin. Mainly the permeation behavior of drugs at physiological pH, where the skin carries a net negative charge indicating an electroosmotic flow in the same direction as current flow, has been examined (Hirvonen et al. 1996, Peck et al. 1996, Kirjavainen et al. 2000).

Important factors for transdermal permeation are the skin structure and the nature of the permeant. In the simplest theory, the stratum corneum consists of an aqueous and lipid pathway, whereas the aqueous pathway essentially contributes to iontophoretic transport. Generally hydrophilic compounds prefer to permeate through aqueous pathways and result in higher iontophoretic enhancement than lipophilic permeants (Del Terzo et al. 1989, Hirvonen et al. 1998). Partitioning of a permeant between aqueous and lipid pathway, and consequently iontophoretic permeation, are pH-dependent (Lütolf 1997).

Skin structure and physico-chemical characteristics of the permeant are not only relevant for skin permeation but also for skin accumulation. Permeants crossing the skin may adsorb at skin components such as proteins. These interactions can result from physical attraction like weak non-covalent bonding up to strong covalent bonding (Barry 1983). The accumulation of permeants in the skin is known from various drugs like steroids, methotrexate (Alvarez-

Figuroa et al. 2001), fentanyl (Thysman et al. 1995) and insulin (Banga and Chien 1993b). A higher amount of fentanyl was brought into the skin by iontophoretic application, which was slowly released after cutting off the current.

Transdermal application was considered for a long time as the most important alternative to parenteral application, because cutaneous metabolism was underestimated and/or ignored. Many different kinds of enzymes, such as dipeptidase, carboxypeptidase and aminopeptidase, were found in the skin, which potentially catalyze the metabolism of, for example, peptides (Steinsträsser and Merkle 1995). Today opinions still differ about where and to what extent cutaneous metabolism occurs. It is assumed that both the epidermis, because of the cell differentiation existing in this layer, as well as the dermis, with hair follicles and sebaceous glands, play an important role in metabolic degradation (Bucks 1984, Steinsträsser and Merkle 1995). Metabolism may be used for the application of so-called prodrugs, substances with good physico-chemical characteristics for transdermal permeation, which are converted to the active drug by cutaneous metabolism (Loftsson et al. 1981, Sloan and Bordon 1982).

The aim of this thesis was to establish a quantitative understanding of the influence of charge, lipophilicity, cutaneous metabolism and tissue retention of permeants on iontophoretic transport. The dipeptide Tyrosine-Phenylalanine and the protected amino acid Tyrosine (Tyrosine- β -Naphthylamide) were used as model permeants, Benzyl-2-Acetamido-2-deoxy- α -D-glucopyranoside, a glucose derivative, as electroosmotic flow marker. These compounds varied widely in their lipophilicity and could have been susceptible to enzymatic degradation. Formulation pH was used as a means to control ionic valence of the compounds and electroosmotic flow. pH values were chosen in the area of the isoelectric point of the skin that determines skin charge and therefore the direction of electroosmotic flow. Enzymatic degradation and its effect on iontophoresis were validated with inhibition experiments. Iontophoretic transport was investigated in part simultaneously for the above permeants in order to detect possible interactions between them and/or their metabolic products. These experiments, supported by a theoretical model analysis, were designed for the purpose of providing a framework for predicting iontophoretic delivery. Studies were carried out *in vitro* across heat-separated human epidermis using horizontal glass cells connected to a four-electrode system (constant voltage). Fluxes of the permeants and their degradation products across the epidermis and their accumulation in the epidermis were measured. Changes of the electrical characteristics of the skin during experiments were constantly monitored.

C Theoretical Introduction

C.1 Skin

C.1.1 Anatomy of the skin

The skin is the largest and most accessible organ of the body with a surface area of 1.5-1.8 m² (Junqueira and Carneiro 1996). This great amount of exposed area acts as a permeability barrier to the environment reduces water loss and provides protection against abrasive action and microorganisms (Schaefer and Redelmeier 1996a). It contains a varied complement of different cells, but it is generally described in terms of three tissue layers: the epidermis, the dermis and the hypodermis. Figure 1 shows the viable epidermis with the outmost layer, the stratum corneum and the dermis (Banga and Chien 1993a).

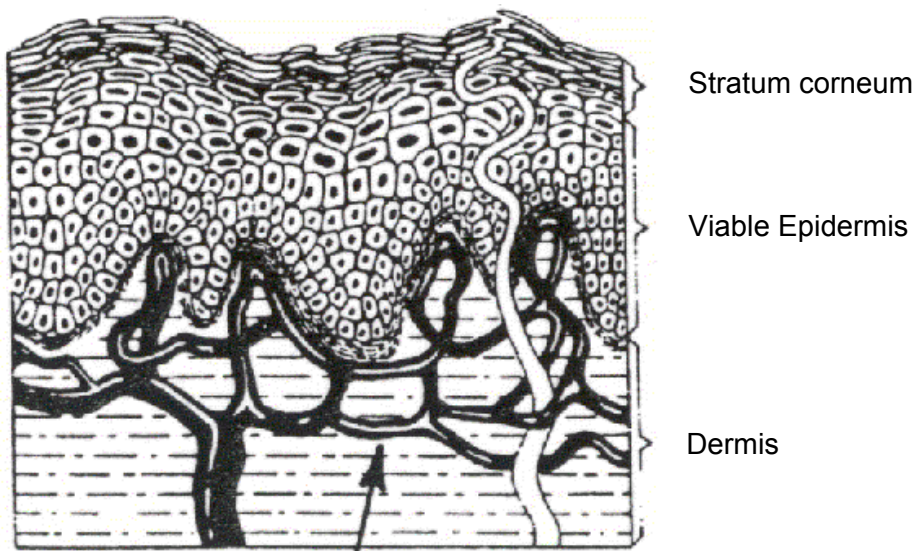


Figure 1. The composition of human skin

C.1.1.1 Epidermis

The epidermis is a continually renewing, stratified, squamous epithelium that keratinizes and is penetrated by appendages like hair, nails, sweat and sebaceous glands.

The majority of cells are keratinocytes, which contain keratin filaments in the cytoplasm and form desmosomes with adjacent cells. The keratinocytes are organized into several layers, which represent different stages of differentiation (Holbrook and Wolff 1993), see Figure 2.

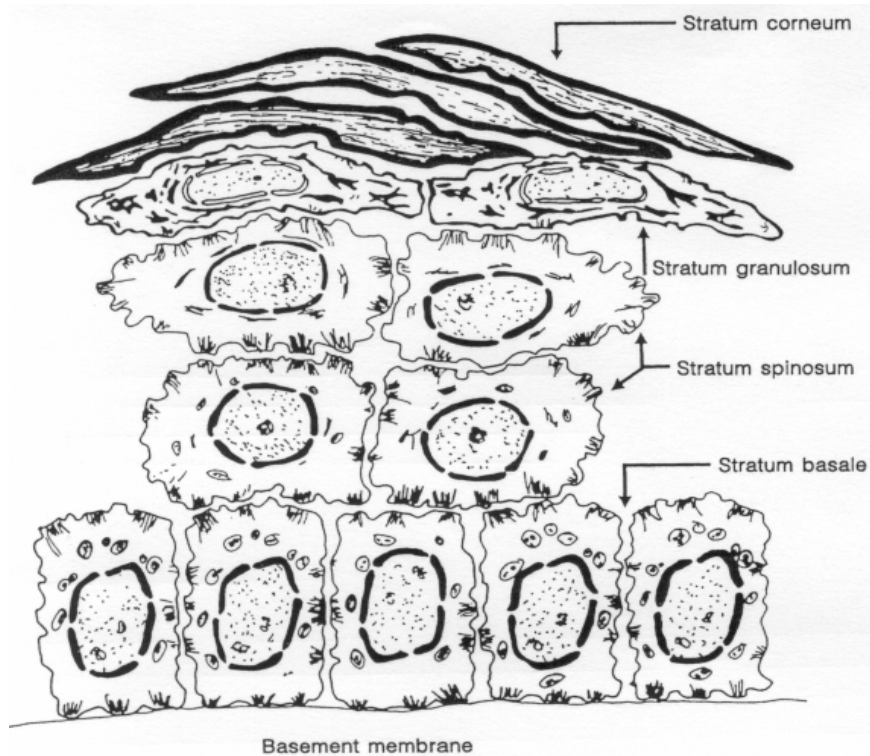


Figure 2. Different layers of the epidermis

The outmost layer, the stratum corneum, is about 20 μm thick. It consists of corneocytes or horny cells, which are remnants of the terminus differentiation of the viable epidermis. During the process of cornification the cellular organelles and cytoplasm disappear so that the corneocytes are built of insoluble bundled keratins surrounded by a cell envelope stabilized by cross-linked proteins and covalently bound lipids. The physical properties are supported and maintained by low-molecular-weight components such as amino acids, sugars, salts and water. A great variety of the low-molecular-weight compounds may derive from metabolism as well as other sources including sweat (Schaefer and Redelmeier 1996b).

The intercellular region is generated from exocytosis of lamellar bodies (Wertz et al. 1989). This intercellular domain is the only continuous domain and forms the skin barrier (Schaefer and Redelmeier 1996a). The principal lipids are ceramides, saturated free fatty acids and cholesterol.

The stratum corneum can be subdivided in two layers, the stratum compactum and the stratum disjunctum. The interface between the terminally differentiated keratinocytes (stratum lucidum) and the lower layer the stratum compactum is a zone of transition and rapid transformation and is very important for metabolic activity. In the stratum disjunctum, reductions in the number of corneodesmosomes reflect changes in the composition of the stratum corneum during the latter stages of desquamation (Schaefer and Redelmeier 1996a).

The horny cells are formed and continuously replenished by the slow upward migration of cells, produced by the stratum basale, which is the regenerative layer of the epidermis. The transition from the living cells to the dead, cornified cells of the stratum corneum is made prominent by two layers, the stratum spinosum and stratum granulosum. In the process of degradation, which occurs in this transition zone, granules of keratohyaline appear in the cells. When these granules have completely changed into keratin, the cells assume a homogeneous appearance to form the stratum lucidum (Chien 1992).

The epidermis also contains melanocytes involved in skin pigmentation, Langerhans cells which are important for antigen presentation and immune responses and Merkel cells which play a role in sensory reception (Schaefer and Redelmeier 1996a).

C.1.1.2 Dermis

The stratum basale is connecting the epidermis with the dermis. The dermis is an integrated system of fibrous, filamentous and amorphous connective tissue that accommodates nerve and vascular networks (Holbrook and Wolff 1993). This system determines the tensile strength and elasticity of the skin (Schaefer and Redelmeier 1996a), protects the body from mechanical injury, binds water, functions as a water storage organ and as a receptor of sensory stimuli, participates in thermal regulation and in immunological protection. Cellular residents include fibroblasts, endothelial cells and mast cells. A variety of appendages, which permeate the epidermis, are derived from this tissue.

The dermis is generally described in terms of two tissue layers: stratum papillare and stratum reticulare. The two layers only differ in the density and organization of their fibrous connective tissue. Both layers are rich in proteoglycans and glycosaminoglycans (Junqueira and Carneiro 1996).

C.1.1.3 Hypodermis

The hypodermis contains loose connective tissue and adipocytes, which are responsible for the energy storage and metabolism as well as for the cushion and protection of the skin (Holbrook and Wolff 1993). The intercellular fat droplets may act as reservoirs for hydrophobic compounds. However, the hypodermis contains also an extensive circulatory network, so that most permeating compounds can be considered to be distributed throughout the body (Schaefer and Redelmeier 1996a).

C.1.1.4 Appendages

Various appendages penetrate the stratum corneum and epidermis providing different functions. Although they account for no more than 0.1% of the total skin surface area, they cannot be neglected in considering possible routes of percutaneous absorption.

C.1.1.4.1 Sweat glands

Sweat glands are distributed almost over the whole body at a density of approximately 400 glands /cm². They decrease the skin temperature by secreting a nearly isotonic solution.

C.1.1.4.2 Hair follicles

Hair follicles extend between less than 1 mm into the dermis and more than 3 mm into the hypodermis. The average density is about 40-50/cm², which is less than the density for sweat glands, but their average surface area may be larger (Chien 1992).

Associated with the hair follicle is a sebaceous gland. The ducts of sebaceous glands join the hair follicles approximately 0.5 mm below the surface of the skin (Schaefer and Redelmeier 1996a).

In the initial diffusion state hair follicles are one of the most important sites for percutaneous penetration (Chien 1992). The inner root sheath surrounding the hair shaft presents an opportunity for molecules to diffuse along the hair follicle. This compartment is filled with sebum, which does not form a barrier to diffusion (Schaefer and Redelmeier 1996a). When a steady diffusion state has been reached, diffusion through the stratum corneum becomes the dominant pathway (Chien 1992).

C.1.1.4.3 Sebaceous glands

Sebaceous glands are found except on the palms of the hands and sole of the feet in all regions of the body. They are connected with a duct to the hair follicle where they deliver the sebum. During this secretion the entire sebaceous cell breaks down (Junqueira and Carneiro 1996). The sebum is composed primarily of triglycerides and free fatty acids with fewer amounts of squalene and waxes.

It is generally accepted that sebum does not participate in the barrier function of the skin. It has to be considered that there may be a possibility of influence to percutaneous absorption by a mix of sebum with topically applied formulations (Schaefer and Redelmeier 1996a).

C.1.2 The main barrier of the skin

The primary barrier to percutaneous absorption is located within the superficial layer, the stratum corneum. The formation of the stratum corneum is under homeostatic control. That means the processes of cornification and desquamation are intimately linked.

The structure of corneocytes and intercellular lipid forms the physical basis for the barrier function ('brick and mortar'-model).

The most satisfying proof of stratum corneum being the main barrier to permeation is provided by the simple demonstration that physically stripping of the outermost layers of the skin results in a dramatic increase in permeability to water (Scheuplein and Blank 1971) and other compounds (Schaefer et al. 1982). A sequential increase in transepidermal water loss is observed as the stratum corneum is progressively removed, indicating that the whole of the stratum corneum provides the barrier of diffusion (Bommannan et al. 1990). An entire removal of this layer results in a significant, but not complete reduction in barrier properties (Schaefer and Redelmeier 1996b).

The stratum corneum contains approximately 15% water, 70% protein and 15% lipid. In comparison, the composition of a keratinocyte in the viable epidermis is approximately 70% water, 15% protein, 5% nucleic acid and 5% lipid.

C.1.3 Penetration pathways across the stratum corneum

The stratum corneum contains protein-rich regions corresponding to the corneocytes and lipid-rich regions, which correspond to the intercellular lipid ('brick and mortar'-model).

This morphological organization of the stratum corneum determines possible penetration pathways (Schaefer and Redelmeier 1996b).

There are three possible routes to percutaneous absorption: transcellular, intercellular and appendageal. These pathways are not mutually exclusive and the importance of each route depends on their frequency (area) and path length as well as the diffusivity and solubility of the compound in each domain (Schaefer and Redelmeier 1996b).

- (a) Transcellular diffusion, in which the drug diffuses through the cornified cells is one possibility. The whole thickness of the stratum corneum contributes to the diffusional resistance. The main arguments against this route are that the cornified cells themselves are dense and offer a large diffusional resistance (Hadgraft 1983).
- (b) Intercellular lipid domain is the only continuous region within the stratum corneum. Although it has a small surface area, the diffusional resistance is fairly low compared to the dead cells (Hadgraft 1983).

The intercellular lipid can be modeled as flattened multilamellar vesicles. Therefore the diffusion of compounds occurs along lipid lamellae. An alternative model is that the lamellae form a continuous barrier, which surround the corneocytes. In this case the compounds transverse the lamellae.

- (c) Hair follicles are the most important appendage in terms of surface area. This transfollicular route has been suggested as being significant particularly in the early stages of penetration (Hadgraft 1983). Iontophoresis appears to dramatically increase the flux of compounds through hair follicles (Schaefer and Redelmeier 1996b).

No active transport process has been shown to be involved in skin permeation (Chien 1992). It also has to be mentioned that percutaneous absorption varies widely between individuals (Schaefer and Redelmeier 1996b).

C.1.4 Metabolism of the skin

In the last several years skin metabolism received more attention because evidence grew that skin is not only a barrier for passive diffusion but also an enzymatic barrier being capable of metabolizing drugs. That led to the fact that clearance by cutaneous metabolism can also be understood as another line of defense to shield the body from uptake of xenobiotics. Therefore skin metabolism may have a strong impact on transdermal delivery of drugs.

Although the skin is well understood nowadays, the extent and the exact localization of enzyme activity remain still uncertain.

C.1.4.1 Localization of the enzyme activity

The viable epidermis and the dermis are sites of high metabolic activity. The epidermis contains many enzymes, which are necessary for the differentiation process in the viable layers. The activity in the dermis is primarily associated with the sebaceous glands and the hair follicles. Sebaceous glands synthesize a complex series of lipids, whereas hair follicles synthesize large amounts of protein.

Täuber and Rost (1987) demonstrated that incubated methylprednisoloneacetate (MPA) with minced stratum corneum of hairless mice showed no degradation and supported the general meaning of stratum corneum being with its dead horny cells a metabolically inert layer. On the other hand they could detect a time-dependent decrease of MPA in minced dermis. They could also show that heat separated epidermis led to a lower metabolization

than epidermis separated by enzymes. This indicates that the enzymatic separation is more gentle and the activity of the enzymes is better preserved.

Although a higher enzyme activity is found in skin appendages, the extent of their contribution to the overall skin metabolism is still unknown.

The exact anatomic distribution of the enzyme systems also remains uncertain. High levels of testosterone-5 α -reductase were found in scrotal skin, causing metabolism of testosterone to hydrotestosterone (Hsia and Hao 1996). On the other side, application of testosterone on the skin of, e.g., abdomen, chest, legs or arms appeared to be free of any metabolism (Mazer et al. 1992).

C.1.4.2 Models for skin metabolism studies

There are several in vitro models to study skin metabolism. Next to isolated cells, cell cultures and histochemical and immunohistochemical detection, the possibility to determine metabolism in homogenates or with mammalian skin fragments exists.

Due to the resistance of the skin to homogenization, the harsh preparation required to disrupt the cells, may completely destroy the enzyme activities.

Homogenization destroys compartmentation and the natural environment of the enzyme. So the metabolizing effect tested in skin homogenates may not directly reflect the mass transport and metabolism in organized tissue.

There are different ways to investigate metabolism with mammalian skin fragments like isolated perfused porcine skin flap, full-thickness skin in organ culture and skin preparations in diffusion chambers (Steinsträsser and Merkle 1995). Here a defined area of skin is exposed to well-stirred donor and receiver compartment. It is also possible to organize the experiments under reflection boundary kinetics, e.g. the viable epidermis is side facing the donor chamber, whereas the receiver chamber is removed and replaced by an impermeable block resulting in reflection of both substrate and metabolite transport (Boderke et al. 1998).

C.1.4.3 Inhibition of cutaneous metabolism

Peptidase inhibitors

Peptidases are enzymes, which catalyze the hydrolysis of proteins and peptides. They rarely show absolute specificity in their action, hence any peptidase has the potential to hydrolyze more than one substrate (Lee et al. 1991). The peptidases can be subdivided into two classes regarding their site of cleavage: endopeptidases, enzymes that cleave peptides and proteins at an internal peptide bond and exopeptidases that only cleave near the end of peptide chains. Exopeptidases are divided concerning their site of cleavage; for example

carboxypeptidase (removes a single amino acid from the C-terminus), peptidyl-dipeptidase (removes a dipeptide from the C-terminus), aminopeptidase (removes one amino acids from the N-terminus), dipeptidyl-peptidase (removes a dipeptide from the N-terminus) etc. Endopeptidases are further subdivided into subclasses based on their site of activity: serin-, cystein-, aspartic- and metalloproteases. But there are also endopeptidases of unknown enzymatic mechanism (Boderke 1998).

Numerous agents could act as a peptidase inhibitor by a variety of mechanisms, e.g. by tightly binding to a covalent modification of the active sites of peptidases or by chelating the metal ions which are essential for the proteolytic activity. Chiang et al. (1998) tested inhibitors like o-phenanthroline, ethylenediaminetetraacetic, dilucine and sodium deoxycholate on the enzymatic stability of delta sleep-inducing peptide (DSIP). All four inhibitors could inhibit the degradation of DSIP to a certain extent in skin homogenate. By using 0.2 mM o-phenanthroline iontophoretic flux of DSIP was about three times as high as control (without inhibitor). The selection of an appropriate peptidase inhibitor could be guided by studying the principal peptidases responsible for the degradation of the peptide, their subcellular compartmentalization and the mechanism of the transport of the peptide (Banga and Chien 1993a).

Temperature

Higo et al. (1992) investigated the effect of skin storage and preparation on cutaneous metabolism of nitroglycerin. The skin was excised immediately postmortem and stored at 4°C for 10 days or put in a plastic bag and immersed in boiling water for 5 minutes. Storage at low temperature did not alter barrier function to the total nitrate flux whereas metabolic function was significantly impaired and suggested at least fivefold loss of the enzyme activity. Across heated skin total nitrate flux was significantly greater compared to the control membrane indicating damage on the skin barrier function. Additionally the ability to hydrolyze nitroglycerin was still present.

Other groups could show inhibition of specific enzymes at temperatures below the freezing point (Kozlova-Lavrinenko and Sokolova 1976), at temperatures higher than 37°C (Smallridge et al. 1986) or inhibition of the enzyme activation at 81°C in the presence of metal ions by denaturation (Ilhan and Gulen 1993).

C.2 Transdermal iontophoresis: Theoretical model

Iontophoresis is a method to enhance and regulate transdermal drug permeation and delivery by application of an electric field to the skin.

The iontophoretic flux of a substance takes place by the following five mechanisms:

- Passive diffusion
- Direct effect of the electric field on ionized drug species (Nernst-Planck Equation)
- Electroosmotic solvent flow which carries ions and neutral species with the solvent stream (modified Nernst-Planck Equation)
- Permeation through aqueous versus lipid domains
- Increase of the skin permeability by the electric field

C.2.1 Passive diffusion

Passive diffusion is a process, which can be described by the 1. Fick's law.

$$J = \frac{dm}{dt} \frac{1}{S} = -D \frac{dc}{dx}$$

where J is the flux, m the mass, t the time, S the surface area of the skin and D the diffusion coefficient. The flux is directly proportional to the concentration gradient dc/dx .

For diffusion through a membrane with a thickness h and a donor concentration c_D , the partition coefficient K between membrane and donor/receiver solution must be introduced.

$$J = \frac{DK}{h} c_D = P c_D$$

The same composition of the donor and the receiver solution, a homogeneous membrane and sink conditions (concentration in the receiver is zero and therefore negligible) are assumed under steady state conditions.

The permeability coefficient P is a measure for the barrier function of the membrane for a specific substance.

C.2.2 Nernst-Planck Equation

Iontophoresis is a process, which involves movement of charged compounds through a membrane under the influence of an electric field. The Nernst-Planck Equation describes a model for a flux, driven entirely by an electrochemical potential gradient.

For iontophoretic transport across a membrane under steady state conditions at constant temperature, it is given by

$$J = -D \frac{dc}{dx} - D \frac{zFc}{RT} \frac{d\psi}{dx}$$

where c is the concentration of the permeant at any point x in the membrane, D the diffusion coefficient, z the ionic valence of the permeant, F the Faraday constant, R the gas constant, T the absolute temperature and ψ the electric potential at any point x in the membrane.

J is the same at all points in the membrane under steady state conditions.

This model assumes that iontophoretic flux is driven entirely by the electrochemical potential gradient and ignores the contributions of current induced convective solvent flow and skin permeability increase due to alterations by the applied electrical potential gradient.

C.2.3 Modified Nernst-Planck Equation incorporating convective solvent flow

As consequence of the above made assumptions, the Nernst-Planck Equation predicts that the flux of uncharged molecules should not be affected by iontophoresis. However convective solvent flow comes to exist when electrical field is applied across a charged membrane (Gangarosa et al. 1980). To take this phenomenon into account, Nernst-Planck Equation was modified by Srinivasan and Higuchi (1990) to include a linear convective solvent term.

$$J = -D \frac{dc}{dx} - D \frac{zFc}{RT} \frac{d\psi}{dx} \pm vc$$

where c is the concentration of the permeant and v the average velocity of the solvent. If the flux of the solvent takes place from donor to acceptor with the anode in the donor, v is positive and contributes to the iontophoretic flux. If the solvent flux takes place from acceptor to donor, v is negative.

The enhancement factor E quantifies the change of permeation rate by the influence of voltage application across a membrane compared to passive diffusion. Theoretical E can be obtained from the modified Nernst-Planck Equation (Srinivasan and Higuchi 1990).

$$E = \frac{-zB + Pe}{1 - \exp(zB - Pe)}$$

$$\text{where } B = \frac{F\Delta\psi}{RT} \quad \text{and} \quad Pe = \frac{vh}{D}$$

The Peclet number Pe is a dimensionless parameter, which characterizes the effect of the convective solvent flow.

This model ignores the contributions of skin alterations caused by the applied electrochemical potential gradient. The same partition coefficients between membrane and donor and the same diffusion coefficient for passive and iontophoretic phase have been used. This indicates that permeation takes place through the same pathway under passive and iontophoretic conditions.

C.2.4 Extended model incorporating lipid pathways

This modification of the modified Nernst-Planck Equation takes into consideration the possible permeation through lipid pathways. Lütolf (1997) extended the model to induce the ratio of the permeability coefficients through lipid (P_{ld}) and aqueous domains (P_{ad}) under passive conditions.

$$E = \frac{\frac{-\bar{z}_{ad} B + Pe}{1 + (P_{ld}/P_{ad})^{passive}}}{1 - \exp\left[-\frac{-\bar{z}_{ad} B + Pe}{1 + (P_{ld}/P_{ad})^{passive}}\right]}$$

This new model assumes that all ionic forms of a drug might permeate through aqueous and lipid domains, that the diffusion coefficient in the aqueous domain and in the lipid domain, respectively, is the same for all ionic forms and that the application of voltage does not effect permeation through the lipid domains.

C.2.5 Extended model incorporating membrane alterations

For all in this chapter described equations the contribution of membrane alteration during iontophoresis was ignored. For this reason, the ratio ($\varepsilon' / \varepsilon$), where ε' is the porosity arising due to voltage dependent alterations in the membrane and ε is the effective volume fraction of the aqueous domain under passive conditions and the ratio $(P_{ld}/P_{ad})^{passive'}$ under passive conditions after voltage application, was inserted (Kochhar and Imanidis 2003).

$$E = \frac{\frac{\varepsilon'}{\varepsilon} \left(\frac{-\bar{z}_{ad} B + Pe}{1 + (P_{ld}/P_{ad})^{passive}} \right)}{1 - \exp\left[-\frac{-\bar{z}_{ad} B + Pe}{1 + (P_{ld}/P_{ad})^{passive'}}\right]}$$

C.3 Convective solvent flow

Iontophoresis normally refers to the transfer of ionic solutes through biological membranes under the influence of an electric field. However, Gangarosa et al. 1980 have observed increasing transport of nominally neutral species by application of an electric field. Later work by Burnette and Marrero 1986 found enhanced transport of neutral thyrotropin releasing hormone and mannitol.

When an electrical potential difference is applied at physiological pH across a 'porous' membrane containing fixed negative charges, i.e. ionic groups of lipids, fatty acids and cholesterol sulfate immobilized in the membrane, bulk fluid flow occurs in the direction of the anode to the cathode (anode in the donor) and implies a permselectivity to cations (Burnette and Ongpipattanakul 1987).

C.3.1 Measurement of convective solvent flow

C.3.1.1 Direct / Indirect methods

Direct methods

The effect of electroosmosis by applying constant current in vitro on human skin and measuring the flow rate of water was first described by Rein in 1924. He measured the increase in the volume of the acceptor and determined the flow rate by measuring the number of drops falling down per unit time in horizontal position.

By measuring the fluid movement flow in horizontal capillary tubes attached to the anode and cathode compartments by Pikal and Shah 1990a, the convective solvent flow was investigated as a function of pH. The measurements showed pH dependence consistent with the charge on the membrane.

Indirect methods

Different groups have investigated the convective flow with the help of the indirect method by measuring the rate flow of an uncharged molecule like mannitol. It could be shown that iontophoretic flow of mannitol through human skin is increased in comparison to passive diffusion, if the anode is in the donor chamber and the skin carries a net negative charge (Sims et al. 1991). These experiments were carried out at 125 mV and 250 mV, where membrane alterations are not supposed to play any role.

Electroosmotic flow from anode to cathode increased the flux of an uncharged molecule with applied current density and led to a flux decrease in cathode to anode direction (Delgado-Charro and Guy 1994).

Another study was carried out to show that at physiological pH lipophilic and positively charged drug species can neutralize the skin charge and therefore decrease or even change the direction of the convective solvent flow (Hirvonen et al. 1996).

C.3.2 Permselectivity of the skin

The isoelectric point (pI) of the skin is above 4 (Hoogstraate et al. 1994, Luzardo-Alvarez et al. 1998, Marro et al. 2001) and at physiological pH the skin is a negatively charged membrane. This net negative charge may result from a greater number of residues of protein amino acids, fatty acids and ceramides carrying negative charges (e.g. carboxylic groups) as opposed to positive charges (e.g. amine moieties).

This characteristic implies that the skin allows the transport of a positively charged compound to proceed with less resistance than the transport of a comparable-sized negatively charged compound (Burnette and Ongpipattanakul 1987).

Direct proof of this permselectivity was given by measuring passive and iontophoretic transport of Na^+ , Cl^- and mannitol across human cadaver skin at pH 7.4 (Burnette and Ongpipattanakul 1987). When the anode was placed in the donor compartment containing Na^+ and Cl^- , the flux of the anion detected in the receptor compartment containing the cathode was approximately three orders of magnitude smaller than the flux of the cation. In consequence an osmotic flow with a convective movement of the dissolved mannitol occurs from the anode to the cathode chamber. The permselectivity of the skin was also confirmed by other authors using monovalent ions like sodium, potassium and caesium and divalent ions like calcium, magnesium and zinc (De Nuzzio and Berner 1990).

The convective solvent flow can be influenced by different factors, which are discussed in the following chapter.

C.3.3 Factors affecting convective solvent flow

C.3.3.1 Molecular weight of the permeant

For large peptides (molecular weight ≥ 1000 Da), electroosmosis is a significant mechanism for iontophoretic enhancement because the fraction of the total current carried by the molecule is very small compared to smaller, more mobile ions which are typically present,

either comprising part of the peptide formulation (e.g. the buffer), or as endogenous ions within and beneath the cutaneous barrier (Marro et al. 2001).

The influence of permeant molecular weight was determined by analyzing the electroosmotic flux enhancement of urea, mannitol, sucrose and raffinose (molecular range of 60-504). The flux enhancement due to electroosmosis was strongly molecular weight dependent, e.g. the Peclet number was around 4 times greater for raffinose than for urea, and mannitol and sucrose yielded intermediate values. The calculated effective flow velocity showed a linear correlation to the applied voltages of 125, 250, 500 and 1000 mV but was independent of the molecular weight of the permeant. These observations showed a semi-quantitative agreement between the predictions of the model and the experimental results (Peck et al. 1996).

C.3.3.2 Structure of the permeants

Numerous studies have investigated the neutralization of the net negative charge of the skin. It has been suggested that a positively charged peptide like the leutinizing hormone releasing hormone (LHRH) (Delgado-Charro and Guy 1994), leuprolide (Hoogestraate et al. 1994, Kochhar and Imanidis 2003) and also nafarelin (Delgado-Charro and Guy 1994) may be able to reduce, neutralize or even reverse the negative charge of the membrane and decrease or change the direction of the electroosmotic flow.

This reversal of the direction implies that at physiological pH (the anode in the donor compartment) the convective solvent flow would impede the flux of a positively charged and neutral permeant and assist the flux of a negatively charged permeant.

It was shown that the degree of effect was correlated with the initial concentration but also with the molecular size of the permeants employed (Hirvonen and Guy 1998).

The necessity of the presence of a positive charge in close proximity to a hydrophobic portion of the molecule is not clearly defined yet. Studies investigating the effect of LHRH, nafarelin and oligopeptides with different degree of lipophilicity, on the direction of the electroosmotic flow, showed clearly the need of a hydrophobic surface (Hirvonen et al. 1996).

The same effect was shown by delivering β -blockers of different lipophilicity (Hirvonen and Guy 1997).

On the other hand, experiments with tripeptides which differed only in the central amino acid residue and thus in the charge and relative lipophilicity were carried out and resulted in an independence of the permeant lipophilicity (Green et al. 1991).

Studies investigating the influence of divalent ions on electroosmosis such as Ca^{2+} (Burnette and Ongpipattanakul 1987, Santi and Guy 1996b) and Mg^{2+} (Santi and Guy 1996b) showed a decrease of the electroosmotic flow by these ions. Shielding of the net negative charge on the skin is a possible mechanism for this phenomenon, a hypothesis not inconsistent with the ability of certain lipophilic peptides to achieve a similar effect.

Not only the inhibition of the electroosmotic flow by neutralizing the skin was investigated, but also the increase of the already negatively charged skin and thus to an enhanced electroosmotic flow (Hirvonen and Guy 1997, 1998). The experiments to enhance the negative charge of the membrane at pH 7.4 did not significantly improve cathodal extraction of negatively charged NSAIDs. The effect of poly-L-glutamic acids on mannitol flux was no more than a three fold increase.

C.3.3.3 Current density and ionic strength

Under constant current iontophoresis, anodal electrotransport of mannitol as a marker for the electroosmotic flow generally increases proportionally with current density. The electroosmotic flow is coupled with the linearly increased flow of ions, which takes place as the current density is raised. On the other hand, electroosmosis is decreased with increasing ion concentration at a constant current density (Pikal and Shah 1990b).

The maximum electroosmotic flow may be increased by raising the current density is not known yet, but current densities of more than 0.5 mA/cm^2 are regarded as inappropriate for human in vivo use (Delgado-Charro and Guy 1994).

C.3.3.4 pH

Lowering the pH of the compartment solutions near the pI of the skin results in a 'neutralization' of the membrane, lowering under the pI in a positively charged membrane. This leads to a decrease or to a change of the direction of the convective solvent flow from the cathodal to the anodal compartment and thus to a permselectivity for anions.

This change in skin charge was for example confirmed by measuring the mannitol flux at a pH range of 3.5 - 7.4. At physiological pH, mannitol flux dominated in the anode-to-cathode direction. By lowering the pH to 3.5 the direction of the convective solvent flow progressively reversed, indicating the skin becoming net positively charged (Marro et al. 2001).

How much the direction of the electroosmotic flow may be changed by changing the pH is not known yet, but a pH lower than 3.0 is regarded as inappropriate for human in vivo use (Lopez et al. 2001).

C.4 Membrane alterations following iontophoresis

Membrane alterations following the application of an electrical potential difference across a membrane contribute to an increased transport of charged and uncharged species.

Sims et al. (1991 and 1992) investigated skin alteration effects during iontophoresis. Constant current during the application of 125 or 250 mV and the comparable permeability coefficient values before and after the voltage application showed that the membrane was not significantly altered. The application of 1000 mV on the other hand showed increasing current, sometimes different permeability coefficients before and after iontophoresis and a nonlinear increase of the amount of permeant transported across the membrane. Another group measured passive permeation rates before and after an application ≥ 500 mV, which did not completely return in the postiontophoretic phase to the baseline value (Kochhar and Imanidis 2003).

Inada et al. 1994 monitored membrane alterations by measuring the electrical resistance. It was found that the rate of decrease in resistance was dependent upon the applied voltage that reversible recovery times are dependent upon the magnitude and the duration of the applied field and that recovery times were much longer when there were lower voltages applied over a longer range of time.

Repeated iontophoretic application of 250 mV on the same skin piece was investigated with 24 hours or 3 hours of passive phase between several voltage applications over 1 hour. The same enhancement and no membrane alterations could only be found with 24 hours of passive phase between the voltage applications (Kochhar and Imanidis 2003).

It is now generally accepted that electrical breakdown of membranes is based on the formation of pores, so called pore induction, including pore modification like expansion of already existing pores.

The magnitude and the duration of the applied voltage determine the quantity, reversibility and the size of the pore formation (Sims et al. 1992).

Peck et al. (1994) measured effective pore radii of human epidermal membrane of 15-25 Å under passive conditions using urea, mannitol, raffinose and sucrose.

Li et al. (1998) reported that the application of 2.0 V across human epidermal membrane resulted in a large porosity increase. The pore radii of the newly induced pores, calculated using the hindered transport theory, were found to be in the range of 6-12 Å.

Higuchi et al. (1999) found pore radii of 10-20 Å by a new method, which incorporated the determination under steady electroporation conditions (low frequency (12.5 Hz) a.c. at 2-5 V) with hindered transport theory.

C.5 Reverse iontophoresis

Iontophoresis is typically associated with drug delivery across the skin, but the symmetry of the technique permits its application to a noninvasive withdrawal of analytes from within the tissue to the body surface, so called reverse iontophoresis. This technique causes ions and neutral molecules to move in both directions under both electrodes (Gliksfeld et al. 1989).

This approach is used to monitor the subdermal concentration variations of glucose and provides therefore a noninvasive technique by which a diabetic might monitor the daily fluctuations in blood sugar (Rao et al. 1995). Although glucose is an uncharged molecule the passage of this polar sugar can be dramatically increased by electroosmosis.

Another analyte of interest is the amino acid phenylalanine that is used to diagnose Phenylketonuria, a metabolic disease in infants resulting from a mutation in the gene encoding the enzyme phenylalanine hydroxylase.

The reverse iontophoretic extraction was described as rapid, easily detectable and highly linear in the concentration range of 1-10 mM phenylalanine (Merino et al. 1999).

Recently, investigations were carried out to replace therapeutic drug monitoring based on blood sampling by reverse iontophoresis. The results showed that the iontophoretic extractions flux of the investigated valproate was linearly correlated with the subdermal concentration (Delgado-Charro and Guy 2003).

To optimize reverse iontophoresis, mannitol flux was measured as a function of pH, ionic strength and formulation (Santi and Guy 1996a, 1996b). It was found that cathodal extraction was enhanced by increasing the pH and reduced electrolyte ionic strength in the electrode chambers. An anodal composition with CaCl_2 or MgCl_2 instead of NaCl decreased electroosmotic flow towards the anode because of skin neutralization at pH 7.4. Hirvonen and Guy (1997, 1998) tried to increase the already negative charge of the skin at physiological pH to more negative values. The experiments to enhance the negative charge of the membrane at pH 7.4 by applying negatively charged NSAIDs did not significantly improve cathodal extraction. The effect of poly-L-glutamic acids on mannitol flux was no more than a three fold increase.

C.6 In vitro model used for permeation

The advantage of in vitro compared to in vivo models is the possibility of varying parameters to a extent which is impossible in vivo. In vitro models offer also the advantages of being easier and convenient.

Different models have been used to investigate the permeability of the membrane. But mostly two-chamber diffusion cells with a donor and an acceptor representing the delivery system and the body, respectively, have been used.

C.6.1 Potentiostat used

The four-electrode potentiostat system for a two-chamber diffusion cell, developed by Masada et al. 1985 and later modified and validated in our laboratory (Lütolf 1997), was used for the experiments. In this system each half cell has two electrodes, a counter electrode, dipped in the solution and a reference electrode, placed at one end of a Luggin capillary.

The potentiostat maintains the potential drop across two Luggin capillary probes, which are placed very close to the membrane on either side, at a desired value by driving the required current through the cell with the help of the counter electrodes (Masada et al. 1989, Srinivasan et al. 1990). With this it is possible to control precisely and maintain constant the potential drop across the membrane.

C.6.2 Diffusion cells

The cells, with which the experiments were carried out, were of the horizontal type (see Figure 3 (Srinivasan et al.1990)).

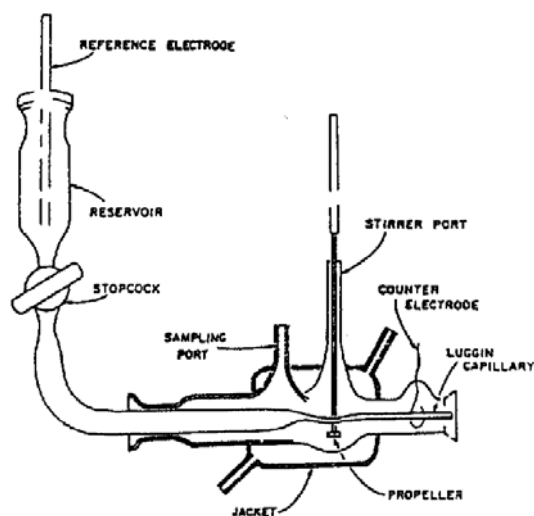


Figure 3. Schematic drawing of one half-cell of the two-chamber diffusion cell

The Luggin capillary, which contains the reference electrode, consists of a long thin glass capillary placed very close to the membrane. It is filled with the same solution as in the two half cells. The use of this capillary eliminates any interfacial potential drops close to the membrane. With this, the voltage drop between the Luggin capillary tips corresponds to the potential drop of the membrane and can be controlled by driving the required current through the counter electrodes.

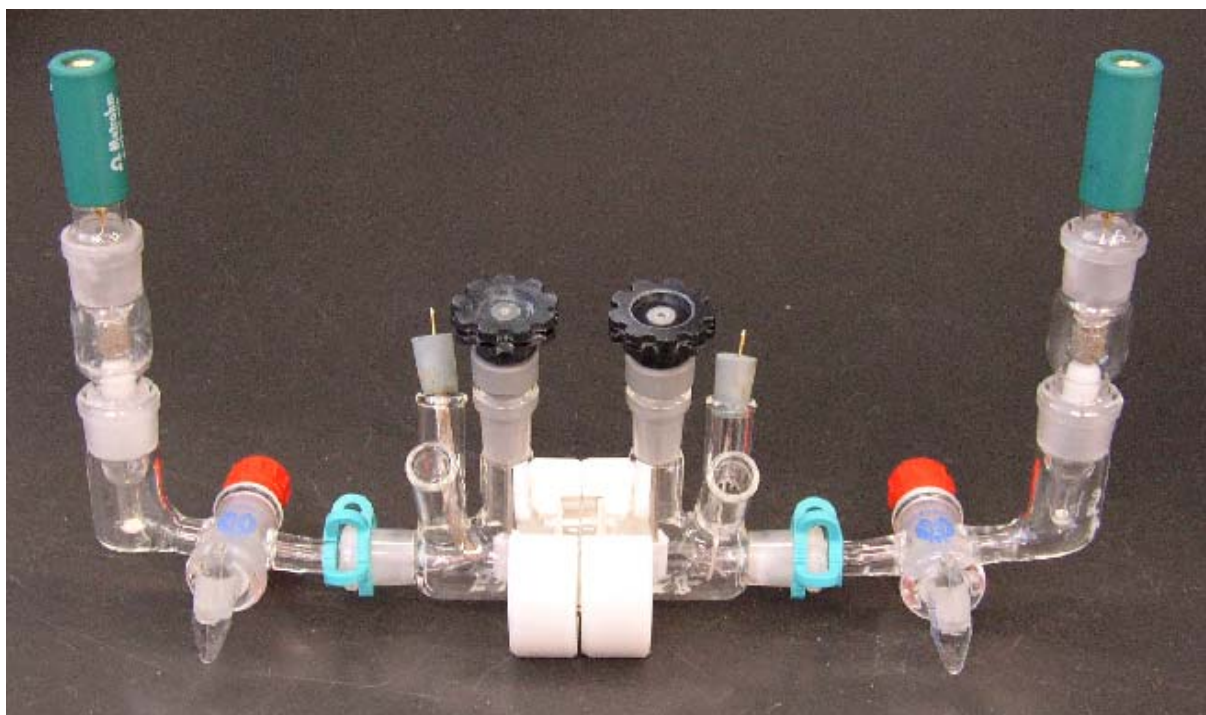
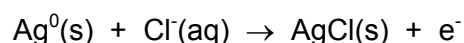


Figure 4. A complete diffusion cell with Luggin capillaries, counter and reference electrodes and stirrers

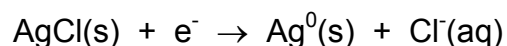
C.6.3 Electrodes

The electrodes used to apply the potential difference across the skin should be inert, work at low voltage, provide a stable environment for the drug and the excipients and minimize the transport of toxic species to the skin (Teillaud 1997). Therefore Ag/AgCl electrodes were used.

The electrochemical sequence of events is as follows: Na^+ is repelled from the anode and enters the skin, leaving a charge imbalance in the solution surrounding the positive electrode. This is resolved by Cl^- , which is attracted to the anode, combining with Ag to form AgCl, and releasing an electron to the electrical circuit:



In the cathodal compartment, the negative electrode attracts Na^+ through the skin into the receptor phase. Again a charge imbalance is created, which is then resolved by dissociation of AgCl(s) from the electrode using an electron from the circuit:



The net transfer of one Na^+ (aq) and one Cl^- (aq) from anode chamber to cathode chamber is effected. While the reverse movement of Cl^- balances the above process, the permselectivity of the skin to Na^+ dictates the net flow of ions as stated (Green et al. 1991).

C.6.4 Membrane

Difficulties in obtaining human skin lead to investigations of model-membranes, like hairless mouse and rat skin, skin of pigs and snakes and synthetic membranes like Nucleopore®.

With human skin, obtained from autopsies or following plastic surgery and stored at freezing temperatures, the best correlation between in vitro and in vivo is given.

Because the stratum corneum plays the main role for the barrier properties of diffusion, heat separated epidermis has become a widely used model. Full thickness skin should be stored within 24 hours of demise at a temperature of the order of -40 to -70°C . Studies showed no influence on the permeability of the skin after storage under -20°C (Barry 1983). After the modified method of Kligman and Christophers (1963) the full thickness skin, being freed of the fat, is heated in a waterbath at 60°C for 2 to 3 minutes and the epidermis peeled of the dermis. Later studies could have shown that good separation can also be achieved by heating the skin for just one minute (Sims et al. 1991). The barrier properties remain unaltered even after heating at 60°C over hours (Schaefer and Redelmeier 1996).

C.6.5 The model substances

The criteria for the selection of the model substances were peptide structure, same molecular weight, which should have been around 300 and a minimal solubility in Teorell-Stenhagen buffer pH 3 and 4.5 of 0.5 mg/ml.

At the same time the model substances, dissolved in Teorell-Stenhagen buffer pH 3, should carry a net positive charge, but they should differ regarding their partition coefficient.

For detailed investigations of the convective solvent flow a substance with the same molecular weight and a minimal solubility of 1 mg/ml, but without carrying a charge at pH 3 and 4.5, was needed.

Because of those criteria the following substances were chosen:

Tyrosine-Phenylalanine (TyrPhe)

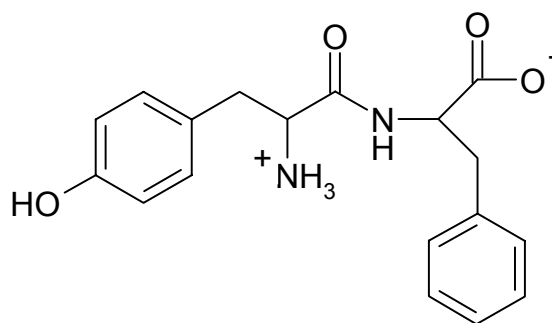
Tyrosine- β -Naphthylamide (Tyr β -NA)

Benzyl-2-Acetamido-2-deoxy- α -D-glucopyranoside (BAd- α -Glc)

Metabolism of peptides is typically catalyzed by enzymes such as aminopeptidase, carboxypeptidase and dipeptidase, which are metallopeptidases. Therefore, o-phenanthroline, a metallopeptidase inhibitor, was chosen as inhibitor for cutaneous metabolism.

C.6.5.1 Tyrosine-Phenylalanine

Tyrosine-Phenylalanine (TyrPhe) is not therapeutically used and acts here as model substance. Chemically, it is a dipeptide and has the following structure:

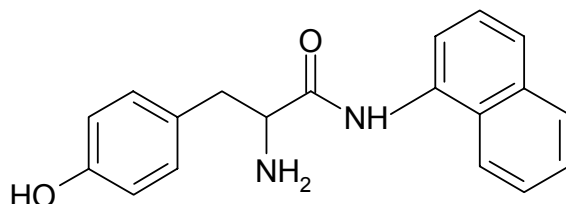


MW=328.4

Bachem AG (4416 Bubendorf, Switzerland)

C.6.5.2 Tyrosine- β -Naphthylamide

Tyrosine- β -Naphthylamide (Tyr β -NA) is not therapeutically used and acts here as model substance. Chemically, it is an amino acid, which is blocked at the C-terminus with naphthylamide and has the following structure:

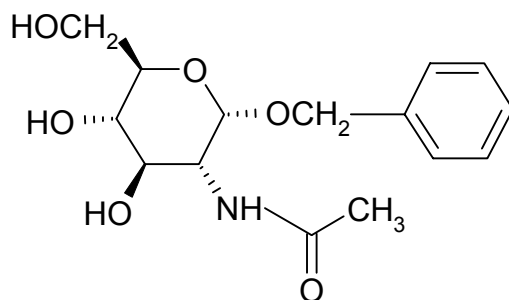


MW=306.4

Bachem AG (4416 Bubendorf, Switzerland)

C.6.5.3 Benzyl-2-Acetamido-2-deoxy- α -D-glucopyranoside

Benzyl-2-Acetamido-2-deoxy- α -D-glucopyranoside (BAd- α -Glc), a glucose derivate, is a hydrophilic molecule, which acts in this work as an electroosmotic marker.

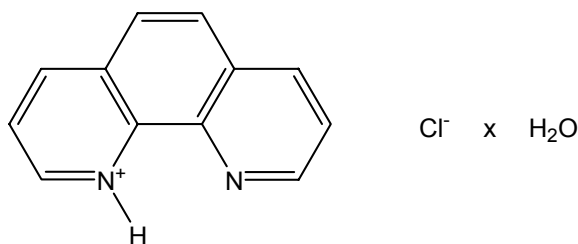


MW=311.3

Toronto Research Chemicals Inc. (North York, Canada)

C.6.5.4 o-Phenanthroline HCl (Monohydrate)

o-Phenanthroline, a metalloproteinase inhibitor, is used here to inhibit cutaneous metabolism.



MW=234.69

Fluka Chemie GmbH (9471 Buchs, Switzerland)

C.7 Applications of iontophoresis

The iontophoretic application of pilocarpine has been approved by the FDA for diagnosis of cystic fibrosis, a disease where the electrolyte concentration of the sweat is augmented. The increase of electrolytes has been used to stimulate the sweat secretion by pilocarpine and then to measure the electrolyte concentration (Gibson and Cooke 1959).

Another diagnostic application is the non-invasive monitoring of diabetics blood glucose levels by reverse iontophoresis (Guy 1995). The wrist-watch, called GlucoWatch®Biographer, received FDA approval in 1991. The watch extracts glucose through the skin by reverse iontophoresis and measures the extracted sample using an electrochemical biosensor. Although GlucoWatch®Biographer measurements generally are consistent with those of traditional finger stick blood glucose tests, results can differ significantly. Because these variations are unpredictable, individual readings should never be used to make changes in insulin dose. Currently the GlucoWatch®Biographer measurements must be used along with finger blood tests to ensure accurate results (FDA 2002).

The most classic use in clinical therapy of iontophoresis is the treatment of Hyperhidrosis, a disease of augmented sweat secretion. There are several anticholinergic substances like poldinmetyhsulfate, glykopyrronium and atropin but also tap water, which proved to be effective. The hands or the feet are dipped in two basins, applied with a current of 20 mA. Although the mechanism of action in Hyperhidrosis is still unknown, this therapy has shown to yield satisfactory results.

Also commonly used in clinical therapy is the application of NSAIDs like diclofenac against inflammatory conditions like rheumatoid arthritis, local anesthetics like lidocaine, corticosteroids like dexamethasonnatriumphosphate, compounds against viral infections like Herpes simplex (idoxuridine) and like Papillomavirus (salicylate sodium) and cisplatin for the treatment of superficial carcinoma of the skin.

An iontophoretic application of apomorphine in the systemic treatment of Parkinson has been investigated in clinical studies (Junginger 2002).

Also the systemic treatment of hypertension was analyzed by an application of metoprolol (Okabe et al. 1986).

Important for all these applications is a good cutaneous tolerance with as less as possible side effects. Generally speaking, iontophoresis is very tolerant and does not result in modifications of major physiological parameters (Guillot 1997). Even though there have been reported some side effects in literature like irritation, itching or pain and erythemas. Irritations are often related to pH changes that take place due to electrolysis of water by the use of metal/metal salt electrodes (Teillaud 1997). Itching and pain varies from one person to another and from different body locations, sometimes even from anode to cathode. Modification of the current density, the frequency and application time often reduces these side effects. The appearance of erythemas, which is due to the release of cytokines and prostaglandins that trigger vasodilatation, is reversible within hours (Thysman et al. 1995).

C.8 References

Alvarez-Figueroa MJ, Delgado-Charro BM, Blanco-Mendez J. 2001. Passive and iontophoretic transdermal penetration of methotrexate. *Int J Pharm* 212: 101-107

Banga AK, Chien YW. 1993a. Dermal absorption of peptides and proteins. In *Biological barriers to protein delivery*. Audus KL and Raub TJ (Eds). New York. Plenum Press, 179-197

Banga AK, Chien YW. 1993b. Characterization of in vitro transdermal iontophoretic delivery of insulin. *Drug Dev and Ind Pharm* 19: 2069-2087

Barry BW. 1983. Methods of studying percutaneous absorption. In *Dermatological Formulations-Percutaneous Absorption*. New York. Marcel Dekker, 234-295

Boderke PA, Boddé HE, Ponce M, Wolf M and Merkle HP. 1998 Mechanistic and quantitative prediction of aminopeptidase activity in stripped human skin based on the HaCaT cell sheet model. *J Invest Dermatol* 3: 180-184

Boderke PA. 1998. Aspects of epidermal peptide metabolism for transdermal drug delivery: Localization, modeling and prediction. Ph D Thesis, Swiss Federal Institute of Technology Zuerich

Bommannan D, Potts RO, Guy RH. 1990. Examination of the stratum corneum barrier function in vivo by infrared spectroscopy. *J Invest Derm* 95: 403-408

Bucks DA. 1984. Skin structure and metabolism: relevance to the design of cutaneous therapeutics. *Pharm Res* 4: 148-153

Burnette RR, Marrero D. 1986. Comparison between the iontophoretic and passive transport of thyrotropin releasing hormone across excised nude mouse skin. *J Pharm Sci* 8: 738-743

Burnette RR, Ongpipattanakul B. 1987. Characterization of the permselectivity properties of excised human skin during iontophoresis. *J Pharm Sci* 76: 765-773

Burnette RR, Ongpipattanakul B. 1988. Characterization of the pore transport properties and tissue alteration of excised human skin during iontophoresis. *J Pharm Sci* 77: 132-137

Chiang C-H, Shao C-H, Chen J-L. 1998. Effects of pH, electric current, and enzyme inhibitors on iontophoresis of delta sleep-inducing peptide. *Drug Del and Ind Pharm* 24(5): 431-438

Chien YW. 1992. Transdermal drug delivery and delivery systems. In *Novel drug delivery systems*. New York. Marcel Dekker, 301-380

Delgado-Charro MB, Guy RH. 1994. Characterization of convective solvent flow during iontophoresis. *Pharm Res* 11: 929-935

Delgado-Charro MB, Guy RH. 2003. Transdermal reverse iontophoresis of valproate: A noninvasive method for therapeutic drug monitoring. *Pharm Res* 20: 1508-1513

Del Terzo S, Behl CB, Nash RA. 1989. Iontophoretic transport of a homologous series of ionized and nonionized model compounds: Influence of hydrophobicity and mechanistic interpretation. *Pharm Res* 6: 85-90

De Nuzzio JD, Berner B. 1990. Electrochemical and iontophoretic studies of human skin. *J Cont Rel* 11: 105-111

FDA News 2002 www.fda.gov/bbs/topics/NEWS/2002NEW00830

Gangarosa LP, Park N, Wiggis C, Hill J. 1980. Increased penetration of nonelectrolytes into mouse skin during iontophoretic water transport. *J Pharmacol Exp Ther* 212: 377-381

Gibson LEE, Cooke RE. 1959. A test for the concentration of electrolytes in sweat in cystic fibrosis of the pancreas utilizing pilocarpine by iontophoresis. *Pediatrics* 23: 545-549

Glikfeld P, Hinz RS, Guy RH. 1989. Non invasive sampling of biological fluids by iontophoresis. *Pharm Res* 6: 988-990

Green PG, Hinz RS, Kim A, Szoka FC, Guy RH. 1991. Iontophoretic delivery of a series of tripeptides across the skin in vitro. *Pharm Res* 8: 1121-1127

Guillot B. 1997. Clinical applications of iontophoresis: Efficacy and tolerance. In *Transdermal administration, A case study, Iontophoresis*. Couvrer P, Duchene, Green P, Junginger HE. Paris. Editions de Santé, 127-135

Guy RH. 1995. A sweeter life for diabetics? *Nat Med* 11: 1198-1201

- Hadgraft J. 1983. Percutaneous absorption: Possibilities and problems. *Int J Pharm* 16: 255-270
- Higo N, Hinz RS, Lau DTW, Benet LZ, Guy RH. 1992 Cutaneous metabolism of nitroglycerin in vitro. II. Effects of skin condition and penetration enhancement. *Pharm Res* 9: 303-306
- Higuchi WI, Li KS, Ghanem A-H, Zhu H, Song Y. 1999. Mechanistic aspects of iontophoresis in human epidermal membrane. *J Cont Rel* 62: 13-23
- Hirvonen J, Yogeshvar NK, Guy RH. 1996. Transdermal delivery of peptides by iontophoresis. *Nat Biotech* 14: 1710-1713
- Hirvonen J, Guy RH. 1997. Iontophoretic delivery across the skin: Electroosmosis and its modulation by drug substances. *Pharm Res* 14: 1258-1263
- Hirvonen J, Guy RH. 1998. Transdermal iontophoresis: Modulation of electroosmosis by polypeptides. *J Cont Rel* 50: 283-289
- Hirvonen J, Murtomäki L, Kontturi K. 1998. Experimental verification of the mechanistic model for transdermal transport including iontophoresis. *J Cont Rel* 56: 169-174
- Hoogstraate AJ, Srinivasan V, Sims SM, Higuchi WI. 1994 Iontophoretic enhancement of peptides: Behavior of leuprolide versus model permeants. *J Cont Rel* 31: 41-47
- Holbrook KA, Wolff K. 1993. The structure and development of skin. In *Dermatology in general medicine*. Fitzpatrick TB, Eisen AZ, Wolff K, Freedberg IM, Austen KF (Eds). New York. McGraw Hill, 97-154
- Hsia SL, Hao YL. 1966. Metabolic transformations of cortisol-4- ^{14}C in human skin. *Biochem* 5: 1469-1474
- Ilhan N, Gulen S. 1993. The stability of arginase activity of thyroid tissue against heat in the presence of different metallic ions. *Biyokimya Dergisi* 18 (4): 59-67
- Inada H, Ghanem AH, Higuchi WI. 1994. Studies of the effects of applied voltage and duration on human epidermal membrane alteration/recovery and the resultant effects upon iontophoresis. *Pharm Res* 11: 687-697
- Junginger HE. 2002. Iontophoretic delivery of apomorphine: From in vitro modeling to Parkinson patient. *Bulletin technique Gattefossé* 95: 61-77
- Junqueira LC, Carneiro J. 1996. *Histologie*. Springer, 412-430
- Kirjavainen M, Urtti A, Mönkkönen J, Hirvonen J. 2000. Influence of lipids on the mannitol flux during transdermal iontophoresis in vitro. *Europ J Pharm Sci* 10: 97-102
- Kligman AM, Christophers E. 1963. Preparation of isolated sheets of human stratum corneum. *Arch Dermatol* 88: 702-705
- Kocchar C, Imanidis G. 2003. In vitro transdermal iontophoretic delivery of leuprolide-Mechanism under constant voltage application. *J Pharm Sci* 92: 84-96
- Kozlova-Lavrinenko TE, Sokolova NB. 1976. Determination of the effectiveness of low-temperature preservation by the detection of enzymes in tissues. *Biol Struct*: 55-58

Lee VHL, Traver RD, Taub ME. 1991. Enzymatic barriers to peptide and protein drug delivery. In Peptide and protein drug delivery. Lee VHL (Eds). New York. Dekker, 303-310

Li KS, Ghanem A-H, Peck KD, Higuchi WI. 1998. Characterization of the transport pathways induced during low to moderate voltage iontophoresis in human epidermis membrane. *J Pharm Sci* 87: 40-48

Loftsson T, Kaminski JJ, Bodor N. 1981. Improved delivery through biological membranes. VIII. Design, synthesis, and in vivo testing of prodrugs of aspirin. *J Pharm Sci* 70: 743-749

Lopez RFV, Bentley MVLB, Delgado-Charro MB, Guy RH. 2001. Iontophoretic delivery of 5-Aminolevulinic acid: effect of pH. *Pharm Res* 18: 311-315

Lütolf P. 1997. Transdermale Iontophorese einer amphoteren Verbindung: Einfluss der Molekülladung und Interaktion mit menschlicher Epidermis. Ph D Thesis, University of Basel

Luzardo-Alvarez A, Rodriguez-Fernandez M, Blanco-Méendez J, Guy RH, Delgado-Charro MB. 1998. Iontophoretic permselectivity of mammalian skin: Characterization of hairless mouse and porcine membrane models. *Pharm Res* 15: 984-987

Marro D, Guy RH, Delgado-Charro MB. 2001. Characterization of the iontophoretic permselectivity properties of human and pig skin. *J Cont Rel* 70: 213-217

Masada T, Rohr U, Higuchi WI, Fox J, Behl CR, Malick AW, Goldberg AH, Pons S. 1985. Examination of iontophoretic transport of drugs across skin I. Baseline studies with the four electrode system, presented at the AphA Academy of Pharmaceutical Sciences 39th National Meeting, Minneapolis, MN, Oct. 18-24, 1985

Masada T, Higuchi WI, Srinivasan V, Rohr U, Fox J, Behl CR, Pons S. 1989. Examination of iontophoretic transport of drugs across skin: baseline studies with the four electrode system. *Int J Pharm* 49: 57-62

Mazer NA, Heiber WE, Moellmer JF, Meikle AW, Stringham JD, Sanders SW, Tolman KG, Odell WD. 1992. Enhanced transdermal delivery of testosterone: A new physiological approach for androgen replacement in hypogonadal men. *J Cont Rel* 19: 347-362

Merino V, Lopez A, Hochstrasser D, Guy RH. 1999. Noninvasive sampling of phenylalanine by reverse iontophoresis. *J Cont Rel* 61: 65-69

Okabe K, Yamaguchi H, Kawa Y. 1986. New iontophoretic transdermal administration of the beta blocker metoprolol. *J Cont Rel* 4: 79

Peck KD, Ghanem A-H, Higuchi WI. 1994. Hindered diffusion of polar molecules through and effective pore radii estimates of intact and ethanol treated human epidermal membrane. *Pharm Res* 11: 1306-1314

Peck KD, Srinivasan V, Li SK, Higuchi I, Ghanem A-H. 1996. Quantitative description of the effect of molecular size upon electroosmosis flux enhancement during iontophoresis for a synthetic membrane and human epidermal membrane. *J Pharm Sci* 85: 781-788

Pikal MJ, Shah S. 1990a. Transport mechanisms in iontophoresis. II. Electroosmotic flow and transference measurements for hairless mouse skin. *Pharm Res* 7: 213-221

Pikal MJ, Shah S. 1990b. Transport mechanisms in iontophoresis. III. An experimental study of the contribution of electroosmotic flow and permeability change in transport of low and high molecular weight solutes. *Pharm Res* 7: 222-229

- Rao G, Guy RH, Glikfeld P, LaCourse WR, Leung L, Tamada J, Potts RO, Amizi N. 1995. Reverse iontophoresis: Noninvasive glucose monitoring in vivo in humans. *Pharm Res* 12: 1869-1873
- Rein H. 1924. Experimentelle Studien über Elektroendosmose an überlebender menschlicher Haut. *Zeitschrift für Biologie* 81: 125-140
- Samec Z, Marecek V, Weber J. 1979. Charge transfer between two immiscible electrolyte solutions. *J Electroanal Chem* 100: 841-852
- Santi P, Guy RH. 1996a. Reverse iontophoresis – Parameters determining electroosmotic flow. I. pH and ionic strength. *J Cont Rel* 38: 159-165
- Santi P, Guy RH. 1996b. Reverse iontophoresis – Parameters determining electroosmotic flow. II. Electrode chamber formulation. *J Cont Rel* 42: 29-36
- Schaefer H, Redelmeier TE. 1996a. Structure and dynamics of the skin barrier. In *Skin barrier: Principles of percutaneous absorption*. Basel. Karger, 1-42
- Schaefer H, Redelmeier TE. 1996b. Composition and structure of the stratum corneum. In *Skin barrier: Principles of percutaneous absorption*. Basel. Karger, 43-86
- Schaefer H, Zesch A, Stuttgen G. 1982. In *Skin permeability*, Berlin Springer
- Scheuplein RJ, Blank IH. 1971. Permeability of the skin. *Physiol Rev* 51: 702-747
- Sims SM, Higuchi WI, Srinivasan V. 1991. Skin alteration and convective solvent flow effects during iontophoresis. I. Neutral solute transport across human skin. *Int J Pharm* 69: 109-121
- Sims SM, Higuchi WI, Srinivasan V. 1992. Skin alteration and convective solvent flow effects during iontophoresis. II. Monovalent anion and cation transport across human skin. *Pharm Res* 9: 1402-1409
- Sloan KB, Bordor N. 1982. Hydroxymethyl and acyloxymethyl prodrugs of theophylline: Enhanced delivery of polar drugs through skin. *J Pharm Sci* 12: 299-313
- Smallridge RC, Ganblin GT, Eli C. 1986. Angiotensin-converting enzyme: characterization in human fibroblasts. *Metabolism, Clinical and Experimental* 35(10): 899-904
- Srinivasan V, Higuchi WI. 1990. A model for iontophoresis incorporating the effect of convective solvent flow. *Int J Pharm* 60: 133-138
- Srinivasan V, Sims SM, Higuchi WI, Behl CR, Malick AW, Pons S. 1990. Iontophoretic transport of drugs: A constant voltage approach. In *Pulsed and self-regulated drugs delivery*, Boca Raton/USA, CRC Press, 65-88
- Steinrässer I, Merkle HP. 1995. Dermal metabolism of topically applied drugs: Pathways and models reconsidered. *Pharm Acta Helv* 70: 3-24
- Täuber U, Rost KL. 1987. Esterase activity of the skin including species variations. In *Skin pharmacokinetics*. Shroot B, Schaefer H. (Eds) Basel. Karger, 170-183
- Teillaud E. 1997. Effects of iontophoretic currents on human local skin tolerance. In *Transdermal administration, A case study, Iontophoresis*; Couvreur P, Duchene, Green P, Junginger HE. Paris. Editions de Santé, 7-29

Thysman S, van Neste D, Pr at V. 1995. Non invasive investigation of human skin after in-vivo iontophoresis. *Skin Pharmacol* 8: 229-236

Wertz PW, Madison KC, Downing DT. 1989. Covalently bound lipids of human stratum corneum. *Inv Derm* 92: 109-111

D Original publications

D.1 Effect of cutaneous metabolism of a dipeptide on the iontophoretic flux of an uncharged electroosmosis marker

Abstract

Passive and iontophoretic transport of the dipeptide Tyrosine-Phenylalanine (TyrPhe) and a glucose derivative, Benzyl-2-Acetamido-2-deoxy- α -D-glucopyranoside (BAd- α -Glc), across heat-separated human epidermis *in vitro* was investigated at pH 3 and 4.5. TyrPhe and BAd- α -Glc, an electroosmosis marker, were used separately and in combination. The influence of TyrPhe skin metabolism on its own permeation rate and skin retention as well as on the permeation rate and skin retention of BAd- α -Glc was examined. TyrPhe was found to be chemically and electrochemically stable. Incubation of TyrPhe with epidermis under reflection boundary conditions resulted in degradation of 12 % at pH 3.0 and 45 % at pH 4.5 over 70 hours. No reproducible permeation of TyrPhe at pH 3 and no permeation at all at pH 4.5 was measured when the dipeptide was used alone or in combination with BAd- α -Glc. Additionally, higher fluxes of the degradation products Tyrosine (Tyr) and Phenylalanine (Phe) were observed and higher levels of Tyr and Phe were recovered from the epidermis compared to blank runs. Blank runs reflected endogenous levels of Tyr and Phe. Degradation was inhibited by the use of o-phenanthroline at pH 3 but not at pH 4.5 and at both pH values at low temperature (4°C). Inhibition was verified by reproducible TyrPhe permeation and blank level Tyr and Phe fluxes and tissue recovery. These results confirm degradation of TyrPhe by cutaneous metabolism in heat-separated human epidermis, that was stronger at pH 4.5 compared to pH 3. BAd- α -Glc showed at both pHs smaller iontophoretic fluxes compared to the passive ones, indicating an electroosmotic flux from cathode to anode. In combination with TyrPhe, iontophoretic fluxes of BAd- α -Glc increased significantly when TyrPhe was metabolized in the tissue, while no such decrease was observed when TyrPhe metabolism was inhibited. This increase of BAd- α -Glc iontophoretic flux was accompanied by a considerable decrease of BAd- α -Glc amount retained in the epidermis. The generated Tyr and Phe appear, therefore, to decrease BAd- α -Glc amount retained in the epidermis and enhance iontophoretic flow. Thus, an interaction between the concurrent permeants at the level of tissue retention induced by metabolism can influence iontophoretic permeation of these poorly permeable compounds.

Introduction

The skin, especially the stratum corneum, is an excellent barrier to the passive transport of topically applied drugs. Peptides penetrate the stratum corneum barrier with difficulty due to their hydrophilicity and large molecule size and due to the lipophilic nature of the stratum corneum. To overcome the problem of poor transport, the use of chemical and physical methods has been examined. Iontophoresis is a non-invasive process of increasing the permeation rate of charged and uncharged compounds into or through a membrane by the application of an external electric field across the membrane. The skin is a permselective membrane with an isoelectric point (pI) above 4^{1,2,3}, indicating a negative charge at physiological pH⁴. This characteristic implies that the skin at physiological pH allows the transport of a positively charged compound to proceed with less resistance than the transport of a comparable-sized negatively charged compound. In consequence an osmotic flow with a convective movement of the dissolved permeants (charged and uncharged) occurs from the anode to the cathode chamber. Convective solvent flow is predominant during iontophoresis of neutral, polar compounds or compounds with a high molecular weight⁵⁻⁷. Lowering the pH of the compartment solutions near the pI of the skin results in a neutralization of the membrane, lowering it under the pI in a positively charged membrane. This leads to an inhibition respectively to a change of the direction of the convective solvent flow from the cathodal to the anodal compartment and thus to a permselectivity for anions^{1,8,9}.

Apart from the function as physical barrier the skin plays also an important role as metabolic barrier capable of degrading a wide range of substances upon permeation. Although the skin is well known nowadays, the extent and the exact localization of enzyme activity remains still uncertain. Cutaneous metabolism was found in epidermal as well as in dermal tissue^{10,12}. The epidermis contains many enzymes, which are necessary for the differentiation process in its viable layers. In the stratum corneum a great variety of low-molecular-weight compounds such as amino acids and sugars may derive from metabolism¹⁹. The activity in the dermis is primarily associated with the sebaceous glands and the hair follicles. Detailed investigations resulted in lower metabolization in heat-separated epidermis than epidermis separated by enzymes¹³.

In this report, separate and combined iontophoresis of the dipeptide Tyrosine-Phenylalanine (TyrPhe) and the glucose derivative Benzyl-2-Acetamido-2-deoxy- α -D-glucopyranoside (BAd- α -Glc), used as electroosmosis marker, across heat-separated human epidermis in vitro at pH 3 and 4.5 was investigated. A number of issues that influence iontophoretic transport of BAd- α -Glc were examined: (a) cutaneous metabolism of TyrPhe, (b) inhibition of TyrPhe metabolism, (c) electroosmosis and (d) skin retention.

Materials and Methods

Materials

Substances

Tyrosine-Phenylalanine (TyrPhe) a dipeptide with a molecular weight of 328.4 and a pK_a of 3.5 was purchased from Bachem AG (Bubendorf, Switzerland). TyrPhe concentration used in the donor was 3 mM at pH 3.0 and 2 mM at pH 4.5.

Metabolic degradation products of TyrPhe, Tyrosine (Tyr) with a molecular weight of 181.2 (pK_a 2.2, 9.1, 10.1) and Phenylalanine (Phe) with a molecular weight of 165.2 (pK_a 2.2, 9.2) were purchased from Fluka BioChemika (Buchs, Switzerland) and Sigma Chemical CO (St. Louis, USA), respectively. The used donor concentrations for both amino acids were 3 mM at pH 3.0 and 2 mM at pH 4.5.

Benzyl-2-acetamido-2-deoxy- α -D-glucopyranoside (BAd- α -Glc), neutral at all three pHs (3.0, 4.5 and 7.2), was used as electroosmosis marker and added in a concentration of 13 mM to the donor solution. BAd- α -Glc (MW = 311.3) was purchased from Toronto Research Chemicals, North York, Canada.

To inhibit cutaneous metabolism o-phenanthroline HCl (monohydrate), a metallopeptidase inhibitor, was used in a concentration of 0.5 mM at pH 3.0 and 4.5. The inhibitor was purchased from Fluka BioChemika (Buchs, Switzerland).

Buffer

Universal buffer was used at pH 3.0, 4.5 and 7.2. It was composed of citric and phosphoric acid (6.67 mM each), and boric acid (11.5 mM). They were all dissolved in double distilled water and the mixture was titrated to the desired pH using sodium hydroxide. For an osmolarity of 300 mosmol the adequate amount of sodium chloride was added to the donor and acceptor solutions. All the chemicals used were of analytical reagent grade or better.

Skin

The skin membrane used was human cadaver skin of only female donors, excised postmortem within 24 h of demise from the abdominal region by the Department of Pathology, University Hospital, Basel. The membrane, which included the stratum corneum and a part of the epidermis, was separated from the underlying dermis by heat-separation^{11,16}.

Preparation of the membrane, its fitting in the diffusion cell, a gravitational leaking and an electrical test of the membrane integrity, were made using the same procedures reported by Kochhar and Imanidis¹¹.

Diffusion cells and iontophoretic equipment

Custom-made glass diffusion cells connected to a four-electrode system developed in our laboratories¹¹ were used for the permeation experiments. The anode was placed in the donor, the cathode in the acceptor compartment.

The current source (built in the Department of Physics, University of Basel) supplied direct current only and could maintain voltage constant. While keeping voltage constant, the current was measured and recorded on a disk with Digital Chart Recorder (DCR 520, W + W Instruments AG, Basel, Switzerland).

Methods

Assay

TyrPhe, the degradation products Tyr and Phe and BAd- α -Glc were assayed by LC/MS (Agilent 1100 and Hewlett Packard 1100 system). A chiral chromatography column (125 x 2 mm, 5 μ m, Spherisorb) was used for quantification. MS parameters were as followed: Mode: SIM, Polarity: Positive, Ionization mode: API-ES, Peak width: 0.2 min, Cycle time: 1.2 s/cycle, Mass range: TyrPhe 329, Tyr 182, 204, 226, Phe 166, BAd- α -Glc 312, Fragmentor: 40-80 Volt, Drying gas flow: 10l/min, Nebulizer pressure: 30 psig, Drying gas temperature: 350°C, Capillary Voltage: 4000, mobile phase: acetonitrile 5%, double distilled water 95%, ammonium acetate 10 mM and acetic acid 50% to pH 3.2

Benzyl alcohol to determine the stability of BAd- α -Glc was analyzed by HPLC (Hewlett Packard 1100 system; ICC 125/2 Lichrospher 100-5 RP-18ec). HPLC parameters were as followed: Wavelength: 258 nm, mobile phase: acetonitrile 15% and double distilled water 85%.

Protocol of permeation experiments

A typical experiment involved three experimental stages. Passive I was a passive stage over 44 hours during which steady state permeant flux was measured by collecting samples of 0.2 ml every 90 minutes from the receiver chamber. The volume was replenished with fresh buffer. During three hours a fixed voltage of 250 mV was applied across the membrane. Samples of 0.2 ml were taken every 20 minutes from the receiver chamber and replaced with 0.2 ml fresh buffer. Passive II was a second passive run over 22 hours taking samples of 0.2 ml every 90 minutes from the receiver chamber and replacing them with 0.2 ml fresh buffer. All the samples were analyzed with no previous treatment against a set of standard solutions by LC/MS. At the beginning of each stage 0.05 ml were taken of the donor chamber and not replenished. These samples were diluted 400 fold before analyzed.

At the end of Passive I and II a voltage drop of 250 mV was applied for 5 minutes to record the electrical resistance and to check the integrity of the barrier. At the end of each

experiment the absence of significant pH and osmolarity changes in both chambers was verified.

The cumulative amount of the substances permeating the membrane was determined as a function of time. Fluxes for TyrPhe and BAd- α -Glc were determined during each experimental stage and for Tyr and Phe during the whole experiment.

Protocol of permeation experiments with inhibition

The enzyme inhibitor o-phenanthroline was added in a concentration of 0.5 mM to the donor and the receiver solution to determine the effect of inhibition on skin enzyme activities and thus on the degradation of TyrPhe. The same procedure as described above was carried out. As a second method the above described experiments were carried out at 4°C¹⁵ instead of 37°C.

Stability of TyrPhe

During passive and iontophoretic phase peptide breakdown via chemical, electrochemical or enzymatic degradation may be envisaged. Therefore experiments were undertaken to determine whether these reactions, and to what extent, were occurring. To determine chemical stability 4 mM solutions of TyrPhe at pH 3.0 and 4.5 were shaken continuously by magnetic stirrer at 37°C over a period of 95 hours. Samples were withdrawn every 10-12 hours.

75 membrane filters (Isopore™ Membrane Filter, Filter Type 0.1 μ m VCTP, Milipore AG) with a pore size of 0.1 μ m were used instead of human epidermal skin to investigate electrochemical degradation of TyrPhe. Analogue to the permeation experiments a TyrPhe solution at pH 4.5 was used, but filled in both half-cells. During 8 hours a voltage of 250 mV was applied and each hour a sample was withdrawn.

Reflection boundary set-up¹⁴ was performed to investigate cutaneous metabolism of TyrPhe. Therefore heat-separated epidermis, the viable epidermis facing the donor compartment, and, at the side of the stratum corneum, a plastic foil, as an impermeable barrier, were sandwiched between donor and receiver compartment (see Figure 1).

All the samples withdrawn from these different stability experiments were analyzed with no previous dilution of TyrPhe and its degradation products Tyr and Phe by LC/MS.

Stability of BAd- α -Glc

1 ml of BAd- α -Glc solution (1.5 mM) was added to a piece of heat-separated epidermis of the same size like those of the permeation experiments. During 70 hours every 8-17 hours samples of 100 μ l were withdrawn and analyzed as described above.

Skin extraction

After each permeation experiment, the skin specimens were pulverized and extracted in order to determine the amount of the substances, which were dissolved in the donor solution and their possible degradation products, in the skin. The skin specimens were pulverized by a freezer mill, type 6750. The following settings were used for the pulverization: P Cool T3 (freezing time 10 min), Run T1 (milling time 2-5 min), Cycles (1 cycle). After the milling the pulverized skin was dispersed in its HPLC eluant, put in the ultrasonic bath and centrifuged (10'000 rpm, 10 min). The over standing solution was then quantified for the corresponding substances and their possible degradation products by LC/MS.

Results and Discussion

Integrity of epidermal membrane

The integrity of the epidermis during permeation experiments was monitored by continually measuring the electrical resistance of the membrane. This was possible with the pair of reference electrodes and membrane reaching capillaries of the four-electrode power unit¹¹. Monitoring membrane integrity was essential because of the long duration of the experiments. Electrical resistance is a sensible measure of integrity because it is immediately related to the permeation barrier function of the epidermis and is quite sensitive because it responds to changes of the permeation of small electrolyte ions through the membrane.

In Figure 2, membrane resistance during the three hours of iontophoresis is shown for several epidermis specimens encompassing different experimental conditions. Typically, the resistance remained constant or showed a small decline. In absolute terms, membrane resistance values varied between 20 and 150 kOhm*cm², the majority being around 40 kOhm*cm². These values are in agreement with the established electrical resistance of human epidermis in isotonic electrolyte solution. Experiments that did not comply with this resistance pattern were discarded. These results demonstrate that it was possible to guarantee the integrity of the epidermis under the present experimental conditions.

Permeation and metabolism of TyrPhe

In Table 1, the passive and iontophoretic fluxes of the dipeptide TyrPhe and the amount of the amino acids Tyr and Phe detected in the receiver compartment of the diffusion cells are reported. The amino acid amount increased steadily during the permeation experiment, but no uniform distinction in the pattern between passive and iontophoretic stages could be

made. Therefore, the amino acid results are reported as average fluxes over the entire experimental duration.

No reproducible permeation of TyrPhe was measured at pH 3 when the dipeptide was used alone (not shown) or in the presence of BAd- α -Glc. TyrPhe was either not detectable at all or it first appeared in the receiver at time points that varied strongly between experiments. Under the same conditions at pH 4.5, TyrPhe permeation was never detectable. In the same experiments, the amount of amino acids measured in the receiver solution was elevated compared to the blank runs. It is worth noticing here that a significant amount of endogenous Tyr and Phe is released from the epidermis in the blank runs. The elevated amino acid amounts suggest that the failure to detect dipeptide fluxes was because of hydrolytic cleavage of its peptide bond, whereby the constituent amino acids are formed. No amino acids were detected in the donor solution either because of the strong dilution of this solution prior to the assay or because of limited diffusion through the stratum corneum.

Analysis of the epidermis specimens at the end of the experiment confirms the above view (Table 2). Intact TyrPhe was recovered from the epidermis when it was used alone or in the presence of BAd- α -Glc at both pH values demonstrating that the dipeptide penetrates into the tissue. The levels of Tyr and Phe were again higher compared to those of the blank runs indicating hydrolysis of TyrPhe.

TyrPhe was found to be chemically stable under the employed experimental conditions. Also, electrochemical stability was verified after application of a voltage of 250 mV for eight hours to the solution (data not shown). These results provide evidence that degradation of TyrPhe in the epidermis takes place by enzymatic hydrolysis. The presence of peptidases in the epidermis has already been reported in the literature¹².

The enzymatic degradation of TyrPhe was quantitatively assessed by incubations with epidermal membrane using the reflection boundary experimental arrangement (Figure 1). A decrease of TyrPhe concentration was evident, which was stronger at pH 4.5 than at pH 3 (Figure 3). BAd- α -Glc included as a control showed a marginal concentration change. In separate incubation experiments of BAd- α -Glc with epidermal membrane, the generation of <0.5% benzyl alcohol, the product of glycosidase action on this glucose derivative, in 70 hours was found for both pH values, confirming that under these conditions this compound was practically stable. The mass balance of the enzymatic TyrPhe reaction is given in Table 3. A three-fold greater decrease of concentration was observed at pH 4.5 compared to pH 3. The amount of generated Tyr and Phe accounted exactly for the concentration decrease of TyrPhe after correction for the endogenously produced amino acids.

From these results, substantial metabolism of TyrPhe in human cadaver epidermis can be concluded. The lack of measurable transdermal permeation of this dipeptide is therefore the result of its metabolism in the epidermis. This is more pronounced at pH 4.5 than at pH 3

probably reflecting a difference of enzymatic activity between these two pH values. The amount of the amino acids Tyr and Phe recovered from the tissue at the end of the permeation experiments was, when related to the dipeptide, larger at pH 4.5 than at pH 3; this is in agreement with the more pronounced metabolism at the former pH compared to the latter. The consistently not detectable permeation at pH 4.5 and the in this respect more variable result at pH 3 can also be ascribed to this difference of enzymatic activity between the pH values, considered on average over all skin specimens. Finally, Tyr seems in general to be more abundant than Phe, which is possibly because of conversion of Phe to Tyr by enzymatic hydroxylation.

The metabolism of TyrPhe is potentially catalyzed by enzymes such as dipeptidase, carboxypeptidase and aminopeptidase that have been found in the epidermis¹⁵. These are typically metalloenzymes. Therefore, the addition of o-phenanthroline, a chelating agent, was investigated as a means to inhibit degradation. At pH 3, it was possible to inhibit enzymatic cleavage of TyrPhe by 0.5 mM o-phenanthroline as indicated by the reproducible permeation across epidermis (Table 1) and the nearly blank levels of Tyr and Phe extracted from the tissue (Table 2). At pH 4.5, however, lacking epidermal permeation and elevated tissue levels of Tyr and Phe demonstrate that, at least at this concentration, addition of o-phenanthroline could not inhibit hydrolysis of TyrPhe. This seems to be in line with the stronger metabolism at pH 4.5 compared to pH 3 discussed above.

Metabolic degradation of TyrPhe at both pH values was completely suppressed at 4°C. This is evidenced by the amounts of Tyr and Phe found in the receiver solution and recovered from the epidermis, that were all at the level of the blank runs. Furthermore, TyrPhe permeation was measured in a reproducible fashion and the amount of intact TyrPhe extracted from the tissue was higher compared to the other experiments at the same pH. Therefore, iontophoresis of TyrPhe could be studied only at this low temperature. Flux and epidermal accumulation of TyrPhe as well as the difference of iontophoretic permeation enhancement between the used pH values are addressed elsewhere¹⁷. The present results reassert that the epidermis exhibits marked metabolic activity even under *in vitro* conditions and can elicit considerable first pass drug metabolism in dermal and transdermal delivery.

Iontophoresis of BAd- α -Glc

BAd- α -Glc, a glucose derivative, is used as a reporter of electroosmotic flow in the iontophoresis experiments. Frequently, poly-alcohols such as mannitol being highly hydrophilic and electrically neutral molecules, have been employed for this purpose. In BAd- α -Glc, glucose is substituted with a benzyl group making the compound detectable by UV spectroscopy. The n-octanol/aqueous buffer partition coefficient of BAd- α -Glc was found to be 0.110 and 0.133 at pH 4.5 and 3, respectively¹⁷, confirming that the compound was

quite hydrophilic thus warranting its use as electroosmosis marker. Also, BAd- α -Glc is not subject to glucolysis because of its 2-substitution and is stable towards epidermal glycosidase as shown above. Finally, the pK_a of the acetyl-amino group is typically around unity, which renders the compound practically uncharged at the employed pH values but enables its detection by positive mode electrospray mass spectroscopy.

Passive epidermal permeability of BAd- α -Glc was inversely proportional to the electrical resistance of the membrane regardless of pH as demonstrated in Figure 4. This behavior has also been observed for other hydrophilic molecules^{11,18}. This relationship was used to correct for skin-to-skin variability by referring all passive flux values to a membrane resistance of 60 kOhm*cm² (Table 4). No difference in (adjusted) passive permeability between pH 3, 4.5 and 7.2 was observed within experimental error as would be expected for an unionized compound. The presence of o-phenanthroline or TyrPhe individually did not seem to affect passive BAd- α -Glc fluxes while their combination might have caused a reduction of passive flux; the present data basis, however, is not broad enough to allow a definite conclusion in this respect. Also, no systematic effect of temperature could be observed after the correction based on the 4°C electrical membrane resistance.

The effect of iontophoresis on BAd- α -Glc is evaluated by comparing iontophoretic fluxes with the corresponding (raw, i.e., unadjusted) passive fluxes. Iontophoretic flux at pH 7.2 was higher than the passive one, this being in line with the established notion that at this pH electroosmotic flow takes place in the anode-to-cathode direction due to the negative fixed charges of the epidermal membrane. At pH 4.5 and pH 3, iontophoretic fluxes were diminished compared to the passive ones, which is consistent with a cathode-to-anode direction of electroosmotic flow and the proposed isoelectric point of human epidermis of between 4.5 and 5^{1,2}. At pH 3, in particular, the average iontophoretic fluxes given in Table 4 are the result of partly positive and partly negative values of the individual experiments. Negative flux values reflect a reduction of the permeant concentration in the receiver compartment. This is a remarkable result indicating that the magnitude of the electroosmotic flow was such that it prevailed over the flux due to the concentration gradient between donor and receiver compartment.

The presence of TyrPhe in the donor solution had a striking effect on the iontophoresis of BAd- α -Glc. At both, pH 3 and pH 4.5, iontophoretic fluxes were invariably several fold higher than passive fluxes contrary to the result obtained when BAd- α -Glc was used alone. Given the fact that TyrPhe was metabolized in the epidermis, the question arose of whether TyrPhe itself or its metabolic products were responsible for this effect. For the donor compositions BAd- α -Glc+TyrPhe pH 3, BAd- α -Glc+TyrPhe pH 4.5, and BAd- α -Glc+TyrPhe+o-phenanthroline pH 4.5, a flux enhancement, whereas for all other compositions a flux retardation of BAd- α -Glc was achieved by iontophoresis. For the first group of the three

compositions, a hydrolysis of TyrPhe to Tyr plus Phe was found (previous section) whereas for all other compositions this hydrolysis was inhibited by the low temperature or (at pH 3) by the addition of o-phenanthroline. o-phenanthroline itself did not affect the iontophoretic behavior of BAd- α -Glc (Table 4). These results clearly demonstrate that the generation of the amino acids Tyr and Phe, but not the dipeptide, must be responsible for the change of the effect of iontophoresis on BAd- α -Glc flux.

The iontophoretic enhancement of BAd- α -Glc observed at pH 3 and pH 4.5 when TyrPhe was hydrolyzed to Tyr and Phe might at first be interpreted in terms of the electroosmotic flow taking place in the anode-to-cathode direction. This would entail that the amino acids reversed the direction of the flow in this pH range by shifting the isoelectric point of the epidermis towards lower values. This has been reportedly accomplished by negatively charged compounds which bound to the tissue^{7,11}. Tyr and Phe, however, are unlikely to be exerting this effect because they are partly positively charged at the pH range of interest.

A mechanistic understanding of the observed phenomenon may be gained by considering the accumulation of the compounds in the epidermis (Table 2). For all donor compositions which produced no Tyr or Phe, including BAd- α -Glc alone, and which gave a cathode-to-anode electroosmotic flow at pH 3 and 4.5, the amount of BAd- α -Glc recovered from the tissue was high with an average of >20 μ g per specimen. Also for pH 7.2 and anode-to-cathode electroosmotic flow but no Tyr or Phe production, a high tissue content of BAd- α -Glc was found. For the other compositions, the recovered amount was reduced to less than half of this value. It appears, therefore, that the generated Tyr and/or Phe decreased the amount of BAd- α -Glc retained in the epidermis. Since the amount of permeants accumulating in the epidermis is significant compared to the amount permeating into the receiver solution, a variation of the former can influence the determined flux values.

These results suggest that the apparent iontophoretic permeation enhancement of BAd- α -Glc at pH 3 and 4.5 is due to a promoted release of this compound from the epidermis into the receiver compartment rather than an anode-to-cathode electroosmotic flow. The mechanism by which, firstly, BAd- α -Glc binds to the epidermis and, secondly, it is displaced by Tyr and/or Phe is scantily understood. Nevertheless, some interesting characteristics of the process may be pointed out: (i) the endogenously present Tyr and Phe, representing one third to one half of the total amino acid amount recovered from the tissue, do not seem to produce the same effect; (ii) the dipeptide TyrPhe does not produce the effect of Tyr and Phe; (iii) importantly, displacement of BAd- α -Glc by Tyr and/or Phe is promoted by iontophoresis; (iv) the release of BAd- α -Glc into the receiver solution outweighs by far the cathode-to-anode electroosmotic flow taking place in this pH range for determining the apparent iontophoretic permeation of the compound. Examining this property of the amino acids prospectively using different permeants is subject of subsequent investigations¹⁷.

Conclusions

The dipeptide TyrPhe is extensively metabolized in the epidermis. The generated metabolic products Tyr and Phe enhance iontophoretic transport at pH 3 and pH 4.5 of the glucose derivative BAd- α -Glc used as an unionized electroosmosis marker. This appears to take place by an interference of the amino acids with the distribution and/or binding process of BAd- α -Glc in the epidermal tissue during iontophoresis. The results underline the possibility of permeability interactions in iontophoretic delivery between permeants or the products of their cutaneous metabolism.

Acknowledgments

We wish to thank Ralf Schoch (Department of Pathology, University Hospital, Basel, Switzerland) for the generous donation of human cadaver skin.

References

1. Marro D, Guy RH, Delgado-Charro MB. 2001. Characterization of the iontophoretic permselectivity properties of human and pig skin. *J Cont Rel* 70: 213-217
2. Luzardo-Alvarez A, Rodriguez-Fernandez M, Blanco-Ménedez J, Guy RH, Delgado-Charro MB. 1998. Iontophoretic permselectivity of mammalian skin: characterization of hairless mouse and porcine membrane models. *Pharm Res* 15: 984-987
3. Hoogestraate AJ, Srinivasan V, Sims SM, Higuchi WI. 1994. Iontophoretic enhancement of peptides: behaviour of leuprolide versus model permeants. *J. Cont Rel* 31:41-47
4. Brunette RR, Ongpipattanakul B. 1987. Characterisation of the permselective properties of excised human skin during iontophoresis. *J of Pharm Sci* 76:765-773
5. Kirjavainen M, Urtti A, Mönkkönen J, Hirvonen J. 2000. Influence of lipids on the mannitol flux during transdermal iontophoresis. *Pharm Sci* 10:97-102
6. Pikal MJ, Shah S. 1990. Transport mechanisms in iontophoresis. III. An experimental study of the contributions of electroosmotic flow and permeability change in transport of low and high molecular weight solutes. *Pharm Res* 7:222-229

7. Hirvonen J, Guy RH. 1998. Transdermal iontophoresis: modulation of electroosmosis by polypeptides. *J Control Rel* 50:283-289
8. Delgado-Charro MB, Guy RH. 1994. Characterization of convective solvent flow during Iontophoresis. *Pharm Res* 11:929-935
9. Lopez RFV, Bentley MVLB, Delgado-Charro MB, Guy RH. 2001. Iontophoretic delivery of 5-Aminolevulinic acid: effect of pH. *Pharm Res* 18:311-315
10. Bucks DA. 1984. Skin structure and metabolism: relevance to the design of cutaneous therapeutics. *Pharm Res* 4:148:153
11. Kochhar C, Imanidis G. 2003. In vitro transdermal iontophoretic delivery of leuporlide- Mechanisms under constant voltage application. *J of Pharm Sci* 92: 84-96
12. Steinsträsser I, Merkle HP. 1995. Dermal metabolism of topically applied drugs: Pathways and models reconsidered. *Pharm Act Helv* 70:3-24 14
13. Täuber U, Rost KL. 1987. Esterase activity of the skin including species variations. In Shroot B, Schaefer H, editors. *Skin pharmacokinetics*, Basel: Karger, p 170-183
14. Boderke P, Boddé HE, Ponce M, Wolf M, Merkle HP. 1998. Mechanistic and quantitative prediction of aminopeptidase activity in stripped human skin based on the HaCaT cell sheet model. *J Invest Dermatol* 3:180-184
15. Higo N, Hinz RS, Lau DTW, Benet LZ, Guy RH. 1992. Cutaneous metabolism of nitroglycerin in vitro. II. Effects of skin condition and penetration enhancement. *Pharm Res* 9:303-306
16. Sims SM, Higuchi WI, Srinivasan V. 1991. Skin alteration and convective flow effects during iontophoresis I. Neutral solute transport across human skin. *Int J Pharm* 69:109-121
17. Altenbach MP, Imanidis G, Schnyder N, Zimmermann C. Simultaneous assessment of tissue binding, lipophilicity and electroosmosis as factors affecting iontophoretic enhancement. *J Pharm Sci* to be submitted

18. Peck KD, Ghanem AH, Higuchi WI. 1995. The effect of temperature upon the permeation of polar and ionic solutes through human epidermal membrane. *J Pharm Sci* 84:975-982

19. Schaefer H, Redelmeier TE. 1996. Composition and structure of the stratum corneum. In *Skin barrier: Principles of percutaneous absorption*. Basel: Karger, p 43-86

Table 1. Flux, J, of TyrPhe, Tyr and Phe at pH 3.0 and 4.5 with Standard Error of the Mean, SEM, (n=2-8)

pH	Donor composition	J of TyrPhe and SEM x 10 ⁶ (in ug/s/cm ²)			J _{69h} ^d of Tyr and Phe and SEM x 10 ⁶ (in ug/s/cm ²)	
		Passive I	Iontophoresis	Passive I ^e	Tyr	Phe
3.0	TyrPhe + BAd- α -Glc	ND ^a	ND ^a	ND ^a	1.87 (0.40)	1.67 (0.11)
3.0	TyrPhe + BAd- α -Glc + Phenanthroline	1.11 (0.48)	3.04 (2.49)	0.95 (0.44)	NM ^b	NM ^b
3.0	TyrPhe + BAd- α -Glc at 4°C	1.33 (0.32)	2.31 (0.94)	1.08 (0.36)	1.21 (0.21)	0.92 (0.13)
3.0	Blank	NA ^c	NA ^c	NA ^c	1.02 (0.23)	0.74 (0.012)
4.5	TyrPhe + BAd- α -Glc	ND ^a	ND ^a	ND ^a	3.17 (1.06)	1.27 (0.43)
4.5	TyrPhe + BAd- α -Glc + Phenanthroline	ND ^a	ND ^a	ND ^a	NM ^b	0.93 (0.20)
4.5	TyrPhe + BAd- α -Glc at 4°C	2.69 (1.69)	1.08 (0.77)	1.01 (0.37)	1.94 (0.53)	0.72 (0.11)
4.5	Blank	NA ^c	NA ^c	NA ^c	1.91 (0.21)	0.84 (0.14)

^a ND - not detectable^b NM - not measured^c NA - not applicable^d Flux over 69 hours^e Flux of Passive I phase interpolated to a membrane resistance of 60 kOhm*cm². Regression through the points gave a slope of -1.04 and r=0.67 for pH 3.0 and 4.5.

Table 2. Skin extractions of permeation experiments with different donor compositions, temperatures and pHs with Standard Error of the Mean, SEM, (n=3-11)

pH	Donor composition	Amount ug/skin sample (SEM)			
		TyrPhe	Tyr	Phe	BAd- α -Glc
3.0	TyrPhe + BAd- α -Glc	4.96 (0.60)	2.39 (0.71)	2.54 (0.81)	4.97 (1.67)
3.0	TyrPhe + BAd- α -Glc + Phenanthroline	10.20 (0.61)	1.20 (0.49)	1.23 (0.63)	21.48 (3.82)
3.0	TyrPhe + BAd- α -Glc at 4°C	9.40 (1.08)	1.10 (0.32)	0.94 (0.61)	17.90 (3.98)
3.0	TyrPhe	4.23 (1.40)	NM ^a	NM ^a	NA ^b
3.0	BAd- α -Glc	NA ^b	NM ^a	NM ^a	22.43 (4.18)
3.0	Blank (4°C + 37°C)	NA ^b	1.02 (0.50)	0.90 (0.40)	NA ^b
4.5	TyrPhe + BAd- α -Glc	1.66 (0.93)	4.04 (0.87)	3.27 (1.10)	7.48 (1.21)
4.5	TyrPhe + BAd- α -Glc + Phenanthroline	0.94 (0.40)	3.90 (1.20)	4.10 (1.60)	12.50 (4.70)
4.5	TyrPhe + BAd- α -Glc at 4°C	2.80 (0.18)	1.93 (0.65)	1.53 (0.38)	22.63 (5.20)
4.5	BAd- α -Glc	NA ^b	NM ^a	NM ^a	24.10 (5.18)
4.5	Blank (4°C + 37°C)	NA ^b	1.45 (0.50)	1.06 (0.43)	NA ^b
7.2	BAd- α -Glc	NA ^b	NM ^a	NM ^a	22.53 (5.84)

^a NM not measured^b NA not applicable

Table 3. Enzymatic degradation of TyrPhe (reflection set-up) after 70 hours with Standard Error of the Mean, SEM, (n=3-4)

pH		degraded concentration in μM	measured concentration in μM	measured concentration in μM of blank experiments	concentration in μM resulting from TyrPhe degradation
3.0	TyrPhe	0.15 (0.034)			
3.0	Tyr		0.99 (0.023)	0.74 (0.035)	0.13 (0.023)
3.0	Phe		0.85 (0.012)	0.69 (0.020)	0.16 (0.012)
4.5	TyrPhe	0.55 (0.044)			
4.5	Tyr		1.53 (0.032)	0.86 (0.043)	0.67 (0.032)
4.5	Phe		1.26 (0.024)	0.66 (0.023)	0.60 (0.024)

Table 4. Flux, J, of BAd- α -Glc with Standard Error of the Mean, SEM, at pH 3.0 and 4.5 (n=3-9)

pH	Donor composition	J and SEM x 10 ⁵ (in ug/sec/cm ²)		
		Passive I	Iontophoresis	Passive I ^a
3.0	BAd- α -Glc + TyrPhe	0.57 (0.35)	2.52 (2.18)	0.39 (0.27)
3.0	BAd- α -Glc + TyrPhe + Phenanthroline	0.25 (0.15)	-0.057 (0.055)	0.065 (0.019)
3.0	BAd- α -Glc + Phenanthroline	3.67 (2.60)	1.15 (0.76)	0.23 (0.084)
3.0	BAd- α -Glc + TyrPhe at 4°C	0.064 (0.018)	0.039 (0.047)	0.035 (0.0065)
3.0	BAd- α -Glc	0.40 (0.11)	0.20 (0.32)	0.57 (0.28)
4.5	BAd- α -Glc + TyrPhe	0.15 (0.030)	0.69 (0.25)	0.30 (0.026)
4.5	BAd- α -Glc + TyrPhe + Phenanthroline	0.063 (0.012)	0.22 (0.074)	0.043 (0.012)
4.5	BAd- α -Glc + TyrPhe at 4°C	2.61 (1.48)	2.26 (1.97)	0.36 (0.017)
4.5	BAd- α -Glc	0.75 (0.35)	0.41 (0.16)	0.40 (0.12)
7.2	BAd- α -Glc	4.13 (1.90)	24.9 (5.45)	0.37 (0.10)

^a Flux of Passive I phase interpolated to a membrane resistance of 60 kOhm*cm²

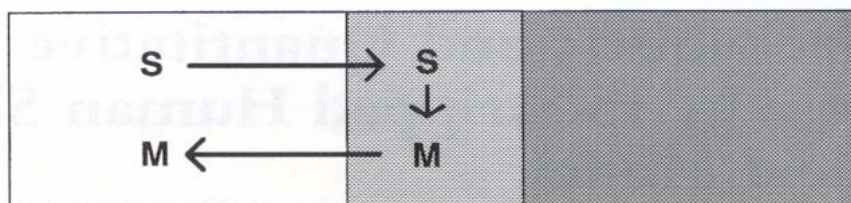


Figure 1. Reflection set-up consisting of donor compartment (left), heat separated epidermis (middle) and impermeable barrier (right; plastic foil). S, substrate; M, metabolite

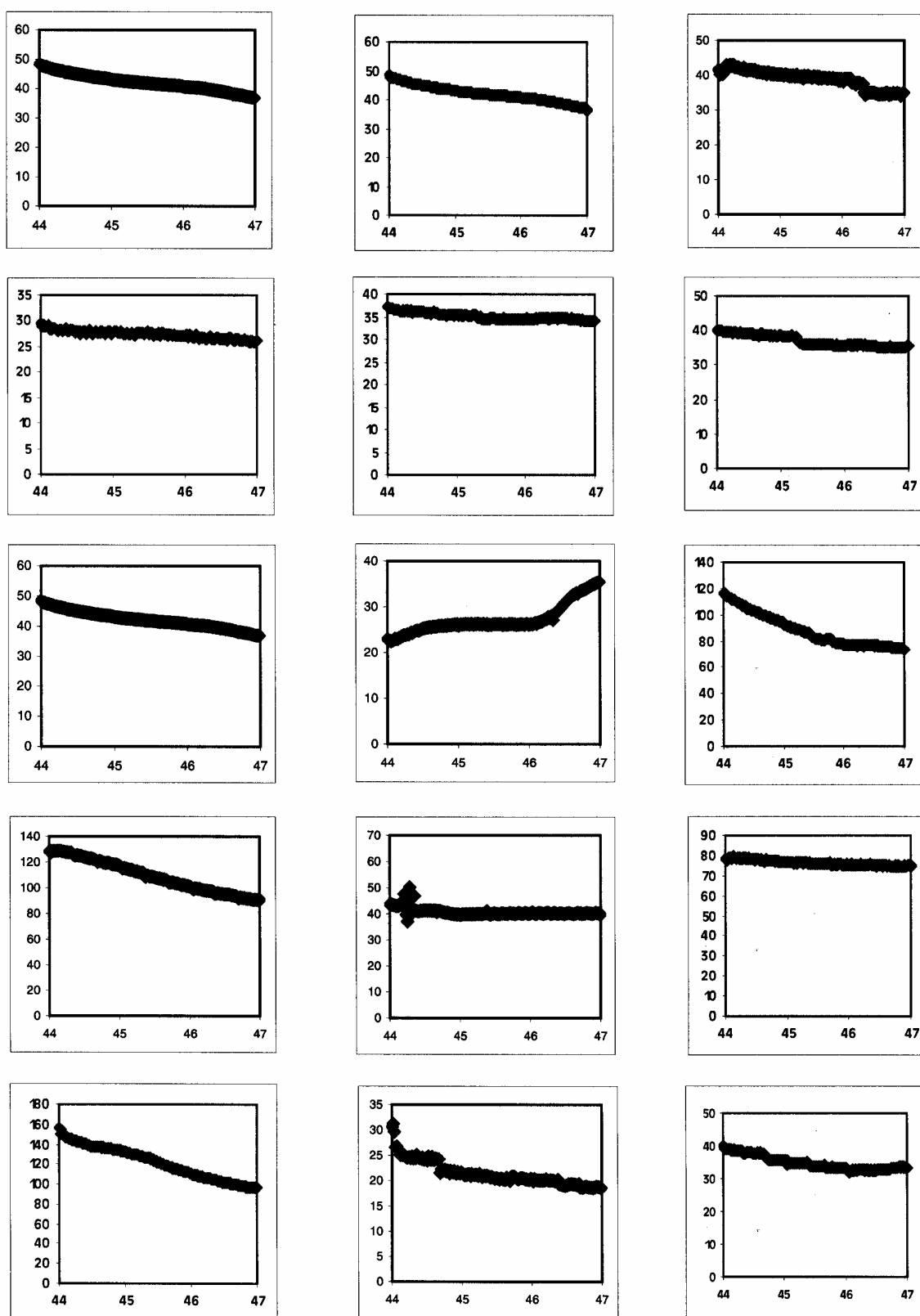


Figure 2. Resistance course during iontophoretic phase (250 mV, 3 hours) of different permeation arrangements; the first three rows are experiments at pH 3, the last two rows at pH 4.5; x-axes show time in hours and y-axes the membrane resistance in $k\Omega \cdot cm^2$

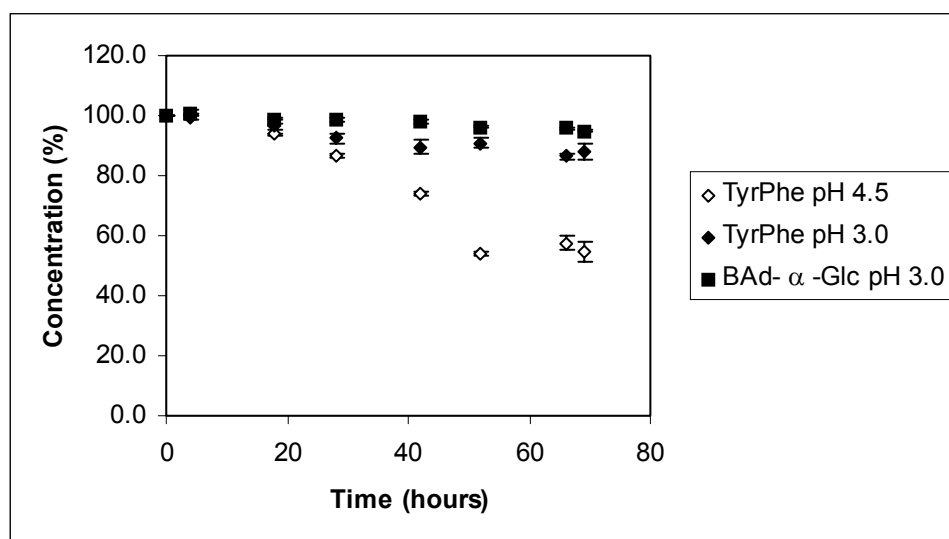


Figure 3. Reflection boundary set-up. Concentration decrease in % of TyrPhe and BAd- α -Glc over 70 hours at pH 3.0 and pH 4.5 with error bars showing SEM (n=4)

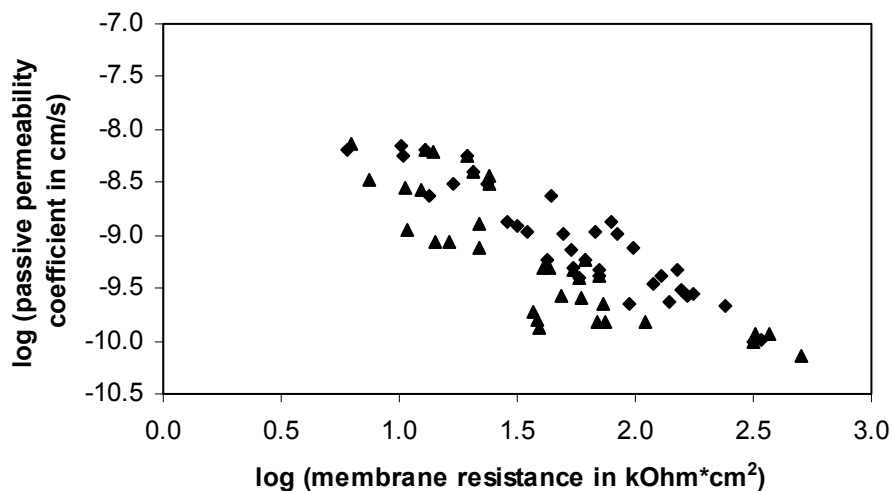


Figure 4. Correlation between Bad- α -Glc passive permeability and electrical resistance. Each point represents the data from one diffusion cell of a permeation experiment (\blacklozenge pH 3.0, \blacktriangle pH 4.5). Regression through the points gave a slope of -1.08 and $r=0.70$ for pH 3.0 and -1.09 and $r=0.86$ for pH 4.5

D.2 Simultaneous assessment of tissue retention, lipophilicity of permeant and electroosmosis as factors affecting iontophoretic enhancement

Abstract

Passive and iontophoretic transport of the dipeptide Tyrosine-Phenylalanine (TyrPhe), the protected amino acid Tyrosine (Tyrosine- β -Naphthylamide (Tyr β -NA)) and the glucose derivative, Benzyl-2-Acetamido-2-deoxy- α -D-glucopyranoside (BAd- α -Glc) across heat-separated human epidermis in vitro was investigated at pH 3 and 4.5, at which the substances carried a positive or zero charge. The three substances were used separately or in combination. The influence of tissue retention and lipophilicity of the permeant and of electroosmosis on iontophoretic permeation was examined. A change of tissue retention affected iontophoretic enhancement. The presence of Tyrosine (Tyr) and/or Phenylalanine (Phe) elicited a decrease of BAd- α -Glc amount retained in the epidermis and an increase of iontophoretic permeation of BAd- α -Glc. The use of Tyr and Phe was motivated by a previous study (Altenbach et al. J Pharm Sci submitted). So far only Tyr and Phe were able to show this effect. Tyr and Phe did not affect iontophoretic permeation of TyrPhe and Tyr β -NA. The effect of lipophilicity and electroosmosis was assessed simultaneously for all three permeants, which spanned a 70-fold range of lipophilicity, excluding the effect of extraneous Tyr and Phe. A theoretical model for the enhancement factor was used that was based on the modified Nernst-Planck Equation, extended by the ratio of permeability coefficients for lipid and aqueous pathway and including an estimate of the ionic valence of permeants in the aqueous domain of the tissue. At pH 4.5 a very weak electroosmotic flow from cathode to anode was observed, indicating an isoelectric point of the skin slightly above 4.5. At pH 3 electroosmotic flow was approximately 10-fold stronger than at pH 4.5. The ratio of the permeability coefficients for lipid and aqueous pathways resulted for all compounds at both pHs in values much smaller than 1, indicating that the aqueous pathway dominated transepidermal permeation. The simultaneous analysis of the results of all substances shows that the applied model evaluation affords a quantitative assessment of the effect of ionic valence, lipophilicity and electroosmosis and makes possible to predict the outcome of iontophoresis.

Introduction

Iontophoresis is an extensively investigated technology to enhance transdermal delivery of drugs by an electric field. Next to the direct effect of the electrical field driving ionic permeants into the skin, secondary phenomena such as electroosmosis and membrane alterations contribute to iontophoretic flux of charged and uncharged permeants.

The direction of the electroosmotic flow may be with the current flow or against, depending on the nature of the membrane. The skin is a permselective membrane with an isoelectric point (pI) above 4^{1,2,3}. At physiological pH the membrane is negatively charged and electroosmotic flow contribute the current flow of an anodal delivery while cathodal delivery is retarded^{4,5}. At a pH close to the pI of the membrane, a neutral membrane and therefore no electroosmotic flux occurs. At a pH smaller than the pI, the membrane carries a positive charge and the electroosmotic flow is against the current flow of an anodal delivery^{1,10,11}.

Compounds may permeate the skin through the aqueous and/or the lipid pathways¹². The aqueous pathways are thereby responsible for the conductance of electric current. The importance of each pathway depends on the ionic state of the compound. Therefore iontophoretic permeation of a compound depends on its ionization. A model based on the modified Nernst-Planck Equation was expanded to include the relative permeation through lipid and aqueous domains of the skin¹³.

In a previous paper⁷ the amino acids Tyrosine (Tyr) and Phenylalanine (Phe) appeared to decrease epidermis retention of the glucose derivative Benzyl-2-Acetamido-2-deoxy- α -D-glucopyranoside (BAd- α -Glc), used as an electroosmosis marker, and increase thereby its iontophoretic delivery at pH 3 and 4.5. When BAd- α -Glc was present alone at the same pH values, iontophoresis elicited a flux retardation of this compound indicating electroosmotic flow occurring in the cathode-to-anode direction in accordance with the accepted view of positive fixed epidermis charges prevailing in this pH range. In those experiments, Tyr and Phe were the products of the metabolism of the model dipeptide TyrPhe in the epidermis. The mechanism, by which the metabolic products of TyrPhe reduced the amount of BAd- α -Glc retained by the tissue upon iontophoresis has not been adequately understood.

In this paper the influence of Tyr and/or Phe on skin retention and iontophoretic permeation of the dipeptide Tyrosine-Phenylalanine (TyrPhe), the protected amino acid Tyrosine (Tyrosine- β -Naphthylamide (Tyr β -NA)) and the glucose derivative Benzyl-2-Acetamido-2-deoxy- α -D-glucopyranoside (BAd- α -Glc), which vary widely in their lipophilicity, was investigated. Permeation experiments were carried out across heat-separated human epidermis at pH 3 and 4.5. At those pH values TyrPhe and Tyr β -NA are positively charged, whereas BAd- α -Glc is uncharged. A theoretical model for the enhancement factor was

applied to quantify the influence of lipophilicity and electroosmosis on iontophoretic enhancement.

Materials and Methods

Materials

Benzyl-2-acetamido-2-deoxy- α -D-glucopyranoside (BAd- α -Glc), neutral at pH 3 and 4.5, was added in a concentration of 13 mM to the donor solution. BAd- α -Glc has a molecular weight of 311.3 and was purchased from Toronto Research Chemicals, North York, Canada. Tyrosine- β -Naphthylamide (Tyr β -NA) an amino acid, which is protected at the C-terminus, with a molecular weight of 306.4 and Tyrosine-Phenylalanine (TyrPhe) a dipeptide with a molecular weight of 328.4 were purchased from Bachem AG (Bubendorf, Switzerland). pK_a of TyrPhe and Tyr β -NA was determined by potentiometric titration to be 3.50 and 4.78, respectively. TyrPhe and Tyr β -NA concentration used in the donor was 3 mM at pH 3 and 2 mM at pH 4.5. The amino acids Tyrosine (Tyr) with a molecular weight of 181.2 (pK_a 2.2, 9.1, 10.1) and Phenylalanine (Phe) with a weight of 165.2 (pK_a 2.2, 9.2) were purchased from Fluka BioChemika (Buchs, Switzerland) and Sigma Chemical CO (St. Louis, USA), respectively. The used donor concentrations for both amino acids were 3 mM at pH 3 and 2 mM at pH 4.5.

Universal buffer was used at pH 3 and 4.5. It was composed of citric and phosphoric acid (6.67 mM each), and boric acid (11.5 mM), which were all dissolved in double distilled water and titrated to the desired pH using sodium hydroxide. For an osmolarity of 300 mosmol the adequate amount of sodium chloride was added to the donor and acceptor solutions. All the chemicals used were of analytical reagent grade or better.

Human skin was obtained from the Department of Pathology, University Hospital, Basel. Heat-separation of the skin, the fitting in the diffusion cell, a gravitational leaking test and an electrical test of the barrier properties were carried out as described in⁶.

Custom-made glass diffusion cells connected to a four-electrode system developed in our laboratories⁶ were used for the permeation experiments. The anode was placed in the donor, the cathode in the acceptor compartment.

The current source (built in the Department of Physics, University of Basel) supplied direct current only and could maintain voltage constant. While keeping voltage constant, the current

was measured and recorded on a disk with Digital Chart Recorder (DCR 520, W + W Instruments AG, Basel, Switzerland).

Methods

Assay

Tyr, Phe, BAd- α -Glc, Tyr β -NA and TyrPhe were assayed by LC/MS (Agilent 1100 and Hewlett Packard 1100 system). A chiral chromatography column (125 x 2 mm, 5 μ m, Spherisorb) was used for quantification. MS parameters were as followed: Mode: SIM, Polarity: Positive, Ionization mode: API-ES, Peak width: 0.2 min, Cycle time: 1.2 s/cycle, Mass range: Tyr 182, 204, 226, Phe 166, BAd- α -Glc 312, Tyr β -NA 307 and TyrPhe 329, Fragmentor: 40-80 Volt, Drying gas flow: 10l/min, Nebulizer pressure: 30 psig, Drying gas temperature: 350°C, Capillary Voltage: 4000, mobile phase for Tyr, Phe, TyrPhe and BAd- α -Glc: acetonitrile 5%, double distilled water 95%, ammonium acetate 10 mM and acetic acid 50% to pH 3.2 and for Tyr β -NA: acetonitrile 20%, double distilled water 80%, ammonium acetate 10 mM and acetic acid 50% to pH 3.2

UV-detection was used to analyze the samples of the partition coefficient determination of TyrPhe, Tyr β -NA and BAd- α -Glc (Perkin Elmer Lambda 5 System). The detailed parameters are as followed: Wavelength: TyrPhe 275 nm, Tyr β -NA 279 nm, BAd- α -Glc 216 nm

Protocol of permeation experiments

In Passive I a passive transport run over 44 hours was carried out, followed by an applied voltage of 250 mV across the membrane over three hours and a second passive run (Passive II) over 22 hours. All the samples were analyzed with no previous treatment against a set of standard solutions by LC/MS. At the beginning of each stage samples were taken of the donor chamber and diluted 400 fold before analyzed. Details of the procedure can be found elsewhere⁷. At the end of Passive I and II a voltage drop of 250 mV was applied for 5 minutes to record the electrical resistance and to check the integrity of the barrier. At the end of each experiment the absence of significant pH and osmolarity changes in both chambers was verified. The cumulative amount of the substances permeating the membrane was determined as a function of time. Permeability coefficients for each permeant were calculated during each experimental stage using the equation:

$$P = \frac{dQ}{dt} \frac{1}{Ac_D} \quad \text{Equation 1}$$

where dQ/dt is the slope of the cumulative permeating amount versus time curve, A is the area of diffusion and c_D is the average donor concentration during the phase. The ratio of the

permeation coefficients of iontophoretic phase and Passive I results in the enhancement factor for the respective substance.

Protocol of TyrPhe permeation experiments with inhibition

To inhibit cutaneous metabolism of TyrPhe the corresponding experiments were carried out at 4°C⁸.

Skin extraction

After each permeation experiment, the skin samples were pulverized and extracted in order to determine the skin retention of the substances, which were dissolved in the donor solution. Details of the procedure can be found elsewhere⁷.

Partition coefficient

Partition coefficients were determined at room temperature in n-octanol/aqueous buffer at pH 3 and 4.5 using shaking flask method⁹. Equilibrium concentration were determined in the aqueous and the organic phase and analyzed with no previous treatment against a set of standards by UV/VIS spectrophotometry.

Results and Discussion

Tissue retention and its modulation

The retention of the glucose derivative BAd- α -Glc in the epidermis was reported previously to be markedly affected by the presence of the amino acids Tyr and Phe during iontophoresis⁷. BAd- α -Glc, an unionized compound, was serving in those experiments as a reporter of electroosmotic flow and Tyr and Phe were the product of the metabolism of the model dipeptide TyrPhe in epidermal tissue. Upon production of Tyr and Phe, iontophoresis at pH 4.5 and pH 3 caused a considerable amount of BAd- α -Glc to be released from the tissue into the receiver solution evoking the impression of permeation enhancement taking place. By comparison, when BAd- α -Glc was present alone at the same pH values, iontophoresis elicited a flux retardation of this compound indicating electroosmotic flow occurring in the cathode-to-anode direction in accordance with the accepted view of positive fixed epidermis charges prevailing in this pH range. The mechanism, by which the metabolic products of TyrPhe reduced the amount of BAd- α -Glc retained by the tissue upon iontophoresis has not been adequately understood⁷.

The a priori addition of Tyr and Phe to the donor solution produced the same effect as the metabolism of TyrPhe (Table 1). For BAd- α -Glc used alone, an enhancement factor <1 (at

pH 4.5) or even negative iontophoretic fluxes (at pH 3) were found, while the addition of Tyr and Phe yielded enhancement factors of BAd- α -Glc much greater than one. The negative fluxes are an expression of the cathode-to-anode electroosmotic flow dominating over the diffusive flux due to concentration difference between donor and receiver compartment. The >1 enhancement factors correlated with the strong reduction of the amount of BAd- α -Glc recovered from the tissue at the end of the experiment, that was observed in the presence of the amino acids (Table 2). This further confirms that these amino acids are responsible for discharging BAd- α -Glc from the epidermis into the receiver solution during iontophoresis thus having a profound effect on its apparent permeation behavior. It is interesting to notice that, at the employed concentrations, the amount of Tyr and Phe recovered from the epidermis is comparable between the two situations, i.e., when these were added a priori to the donor solution and when they were produced by metabolism of the dipeptide TyrPhe in the tissue⁷. The amino acids had no influence on the passive permeability of BAd- α -Glc. This is concluded by inspecting the permeability coefficients which were adjusted to an electrical membrane resistance of 60 kOhm*cm² in order to be corrected for inherent differences between membrane specimens⁷ (Table 1). The added amino acids permeated from the donor into the receiver solution. Both, the average amino acid fluxes (Table 1) and the amount of amino acids recovered from the tissue (Table 2) were significantly greater than the respective values of the blank runs.

Tyr and Phe exerted separately the same effect in qualitative terms as their mixture used at the same concentration (Table 1). The apparent enhancement factor of BAd- α -Glc in the presence of each of the amino acids was >1 and the amount of BAd- α -Glc retained by the tissue was reduced compared to BAd- α -Glc used alone. The magnitude of these effects, however, was smaller for the individual amino acids compared to their mixture. Other than that, the amino acids themselves showed separately the same behavior with respect to epidermis permeation and accumulation as their mixture. This demonstrates that Tyr and Phe share the property of displacing BAd- α -Glc from the epidermis upon iontophoresis. No difference in their potency in this respect was obvious within experimental error. The experiments with the individual amino acids were carried out at pH 4.5. It is considered unlikely that the reached conclusions will be different at pH 3 where the effects are, if anything, stronger as judged by the studies with the Tyr and Phe mixture.

The Tyr derivative Tyr β -NA and the dipeptide TyrPhe did not exert the same effect as Tyr and Phe in terms of reduction of tissue retention of BAd- α -Glc and iontophoretic enhancement at both pH values (Tables 1 and 2). Tyr β -NA is enzymatically stable and TyrPhe is used at 4°C in order to prevent metabolism⁷. Moreover, Tyr β -NA and TyrPhe did not interfere with the action of Tyr and Phe on the iontophoretic behavior of BAd- α -Glc. This property, therefore, seems so far to be unique to these amino acids. It is not possible based

on the present data to ascertain the chemical characteristics that are required for this property. Since Tyr and Phe have very similar lipophilic and ionized groups as Tyr β -NA and TyrPhe, it seems that only the smaller molecular size of the amino acids distinguishes them from the other compounds.

The effect of adding Tyr and Phe to the donor solution on epidermis permeation and iontophoresis of Tyr β -NA and TyrPhe (4°C) is depicted in Tables 3 and 4, respectively. The amino acids had no impact on the electrical resistance-corrected passive permeability coefficients or the iontophoretic enhancement of both compounds. Also, the amino acids had no impact on the epidermis retention of the compounds (Tables 5 and 6). This effect was examined at pH 3 because this is where it was expected to be the strongest based on the BAd- α -Glc results. The result was independent of the presence of BAd- α -Glc (shown for Tyr β -NA). Further, BAd- α -Glc did not influence Tyr β -NA permeability, enhancement and tissue retention at either pH (Table 3). These results are consistent with the BAd- α -Glc results inasmuch as the effect, or lack thereof, of the amino acids on tissue retention correlates with their effect on the measured iontophoretic enhancement.

Notably, in the same experiments which showed no influence of Tyr and Phe on tissue retention and iontophoretic enhancement of Tyr β -NA and TyrPhe, these amino acids did have a major impact on the behavior of BAd- α -Glc. This demonstrates that this effect of Tyr and Phe is not universal but depends on the permeant in question. The three permeants differ in that one of them contains a hexose structure and is uncharged while the other two are peptides that are positively charged at the used pH values. Interestingly, BAd- α -Glc, for which the effect was observed, exhibited by far the largest tissue retention of the three compounds when no amino acids were present. The limited sample size does not allow, of course, to reach a conclusion as to the structural characteristics that may be relevant for this type of interaction with Tyr and Phe. Clearly, a larger study is required for this purpose. Nevertheless, these results draw one's attention to the possible role of tissue retention of permeants and drugs for iontophoretic transport and its modulation by physiological substances.

Permeant lipophilicity and electroosmosis

Representative iontophoretic enhancement factors of the three model permeants Tyr β -NA, TyrPhe and BAd- α -Glc are collected in Table 7 (last column). BAd- α -Glc values only in the absence of extraneous Tyr and Phe are given. Tyr β -NA exhibited the strongest enhancement, which was greater at pH 4.5 than at pH 3 while for TyrPhe the opposite was true. These data are evaluated taking into account, in addition to the ionic valence, the lipophilicity of the permeants and the effect of electroosmotic flow. The ionic valence within the aqueous domain of the epidermis is relevant in this respect because this domain

constitutes the effective pathway that is responsible for electric current conduction and hence iontophoretic transport. The ionic valence of the permeants in the aqueous pathway may differ from that in the (aqueous) bulk because of the electrical charges being present in the epidermis that, on one hand, give rise to the electroosmotic flow but may also create a pH shift in the aqueous micro-environment of the epidermis. Permeant lipophilicity determines its comparative partitioning to the non-aqueous (lipid) and aqueous domains of the epidermis and thus the relative significance of the respective pathways for permeation. Since the contribution of non-aqueous pathways to current conduction is probably insignificant, the ratio of aqueous to non-aqueous epidermis permeability should influence iontophoretic enhancement. Electroosmotic solvent flow, finally, affects the transport across the membrane of all permeants to an extent that depends on the molecular size of the permeant. The contribution of these factors to iontophoretic enhancement is assessed simultaneously for all three permeants at the applied pH values in a quantitative fashion. For this purpose, the following theoretical expression for the enhancement factor derived previously is employed¹³.

$$E = \frac{\frac{-\bar{z}_{ad} B + Pe}{1 + (P_{ld}/P_{ad})^{passive}}}{1 - \exp\left[-\frac{-\bar{z}_{ad} B + Pe}{1 + (P_{ld}/P_{ad})^{passive}}\right]} \quad \text{Equation 2}$$

where, \bar{z}_{ad} is the average net ionic valence of the permeant in aqueous tissue domains, $B = \frac{F\Delta\psi}{RT}$ with F the Faraday constant, R the gas constant, T the absolute temperature and

$\Delta\psi$ the electrical potential difference applied to the membrane, $Pe = \frac{vh}{D_{ad}}$ (Peclet number)

with v the linear convective velocity of the solvent, h the thickness of the membrane and D_{ad} the diffusion coefficient in aqueous domains, and $(P_{ld}/P_{ad})^{passive}$ is the ratio of the permeability coefficients for lipid (P_{ld}) and aqueous membrane domains (P_{ad}) under passive conditions.

In this equation, membrane alteration at the used potential difference of 250 mV was assumed to be negligible, as verified in earlier studies⁶. Equation (2) was fitted simultaneously to all experimental enhancement factors (except for BAd- α -Glc at pH 3, see below) and the numerical values of the parameters Pe and $(P_{ld}/P_{ad})^{passive}$ were estimated using a least squares optimization procedure (MINSQ software, MicroMath, Inc., Salt Lake City, UT, USA). For these calculations, the following assumptions were made: (i) Pe , an expression for electroosmotic flow, depends on pH and temperature but not on the permeant since the three permeants studied here have approximately the same molecular weight, (ii)

the pH difference between epidermis aqueous domain and bulk is between 0.05 and 0.4 units resulting from a surface charge density of tissue of 0.0035 and 0.035 C/m², respectively^{13,14,15}; accordingly, calculated values of \bar{z}_{ad} based on the pK_a of the compounds differed from the average ionic valence in the bulk, \bar{z}_b ; (iii) the relative value of $(P_{id}/P_{ad})^{passive}$ using, for example, BAd- α -Glc pH 4.5 as a point of reference, can be approximated based on the n-octanol/aqueous buffer partition coefficient, $K_{oct/aq}$ (Table 7), and the aqueous domain/bulk partition coefficient given by Equation (3).

$$K_{ad/b} = \frac{10^{(pK_a - pH_{ad})} + 1}{10^{(pK_a - pH_b)} + 1} (10^{(pH_b - pH_{ad})z_2}) \quad \text{Equation (3)}$$

where, pK_a is ionization constant of the permeant, pH_b is the pH of the bulk solution, pH_{ad} refers to the aqueous membrane domain and z₂ is the smallest of the two ionic valences of the permeant.

Fitting of Eq. (2) to the data was performed successively for \bar{z}_{ad} and $K_{ad/b}$ values corresponding to the two surface charge densities given above. The best fit was obtained for the parameter values reported in Table 7. The enhancement factors that were calculated using the estimated parameters showed an excellent agreement with the experimental ones. The best approximation was reached for the high surface charge density at pH 3 and the low one at pH 4.5. These correspond to small to moderate shifts of the ionic valence in the tissue domain compared to the bulk. Pe values were slightly negative at pH 4.5 indicating a small cathode-to-anode electroosmotic flow, which implies an isoelectric point of the tissue of somewhat above 4.5. At pH 3, a ten-fold stronger electroosmotic flow was found compared to pH 4.5 suggesting a larger positive charge of the tissue. This is consistent with the surface charge densities that gave the best fit. No clear dependence of Pe on temperature was seen. This calculation of the contribution of electroosmotic flow to the enhancement agrees with previous reports on the role of this factor for iontophoresis^{1,10,11} and provides a quantitative basis for its assessment. $(P_{id}/P_{ad})^{passive}$, although it differed considerably between permeants, reached a maximal value of 0.018, indicating that the aqueous pathway vastly dominated transepidermal permeation. Thus, this factor was not found to significantly affect iontophoretic enhancement for the studied compounds. This might be because even the most lipophilic of them was not lipophilic enough to exhibit a pronounced lipid pathway permeation.

The presented analysis has yielded remarkably congruent results in that the estimated parameter values could be reasonably interpreted and the calculated enhancement factors closely matched the experimental data of all simultaneously analyzed compounds. This verifies the validity of the used model based on Eq. (2) and the underlying mechanistic

understanding of the iontophoresis process. It further demonstrates that this approach, besides affording a quantitative evaluation of iontophoretic enhancement, may be used as a basis for predicting its outcome.

Passive epidermis permeability of the studied compounds varied considerably following the order Tyr β -NA < BAd- α -Glc < TyrPhe (Tables 1, 3 and 4). Permeability coefficients did not correlate with the lipophilicity of the compounds as expressed by their octanol/aqueous buffer partition coefficient. This is not surprising in light of the finding of the iontophoretic enhancement analysis according to which the aqueous pathway dominated passive epidermis permeation. Hence, permeability differences should be attributable to the different accessibility of the aqueous domain for the three permeants. This is subject to charge-charge interactions, whereas in the present situation size considerations did not play a role because the used compounds had all approximately the same molecular weight. The resulting partition coefficient for the aqueous membrane domain may be expressed by Eq. (3). While this equation predicted a lower partitioning of Tyr β -NA compared to TyrPhe, the difference based on the assumed surface charge densities did not account for the full magnitude of the effect in terms of permeability. Also, the prediction of Eq. (3) of a smaller partitioning at pH 3 compared to pH 4.5 was merely tentatively reflected in the smaller permeability coefficients at the former pH. BAd- α -Glc expectedly exhibited no pH dependence of permeability. Finally, no correlation between passive permeability and tissue retention of the permeants was found. Thus, the present data did not allow a full quantitative understanding of the passive permeability of the employed permeants to be established.

The negative iontophoretic fluxes and hence negative enhancement factors obtained for BAd- α -Glc at pH 3 (Table 7) could be quantitatively analysed only by relaxing the boundary condition of sink in the receiver compartment assumed for the derivation of Eq. (2). The resulting enhancement factor for zero ionic valence applying to BAd- α -Glc is given by Eq. (4).

$$E = \frac{Pe \left(C_D - \frac{C_R}{\exp(Pe)} \right)}{(1 - \exp(-Pe))(C_D - C_R)} \quad \text{Equation (4)}$$

where, C_D and C_R is concentration in the donor and the receiver compartment, respectively. Eq. (4) was used to estimate the magnitude of electroosmotic flow expressed by Pe that would lead to a flux from the receiver to the donor compartment and thus against the prevailing concentration gradient. Since the molecules leaving the receiver solution probably accumulate in the membrane, an estimated permeant concentration in the outer membrane layer facing the receiver solution of 20 $\mu\text{g/ml}$ was used as C_D . This corresponds to 0.5% of the concentration in the donor solution, i.e., reflects an outer layer thickness of 0.5% of the

membrane. With this value and the measured receiver concentration, Pe values ranging between -40 and -0.2 and averaging approximately -15 were calculated. Using the actual donor concentration, no reasonable estimates of Pe could be obtained. The extremely high variability of the data and the required assumptions precluded a meaningful quantitative interpretation of the negative flux data. The value of these data lies in the inference that the electroosmotic flow can completely abolish flux originating from a considerable concentration gradient.

Acknowledgments

We wish to thank Ralf Schoch (Department of Pathology, University Hospital, Basel, Switzerland) for the generous donation of human cadaver skin.

References

1. Marro D, Guy RH, Delgado-Charro MB. 2001. Characterization of the iontophoretic permselectivity properties of human and pig skin. *J Cont Rel* 70: 213-217
2. Luzardo-Alvarez A, Rodriguez-Fernandez M, Blanco-Ménedez J, Guy RH, Delgado-Charro MB. 1998. Iontophoretic permselectivity of mammalian skin: characterization of hairless mouse and porcine membrane models. *Pharm Res* 15:984-987
3. Hoogestraate AJ, Srinivasan V, Sims SM, Higuchi WI. 1994. Iontophoretic enhancement of peptides: behaviour of leuprolide versus model permeants. *J. Cont Rel* 31:41-47
4. Brunette RR, Ongpipattanakul B. 1987. Characterisation of the permselective properties of excised human skin during iontophoresis. *J of Pharm Sci* 76:765-773
5. De Nuzzio JD, Berner B. 1990. Electrochemical and iontophoretic studies of human skin. *J Cont Rel* 11:105-111
6. Kochhar C, Imanidis G. 2003. In vitro transdermal iontophoretic delivery of Leuprolide-Mechanisms under constant voltage application. *J of Pharm Sci* 92: 84-96

7. Altenbach MP, Imanidis G, Schnyder N, Zimmermann C. Simultaneous assessment of tissue binding, lipophilicity and electroosmosis as factors affecting iontophoretic enhancement. *J Pharm Sci* to be submitted.
8. Higo N, Hinz RS, Lau DTW, Benet LZ, Guy RH. 1992. Cutaneous metabolism of nitroglycerin in vitro. II. Effects of skin condition and penetration enhancement. *Pharm Res* 9:303-306
9. Leo A, Hansch C, Elkins D. 1971. Partition coefficients and their uses. *Chem Rev* 71:525-616
10. Nicoli S, Cappellazzi M, Colombo P, Santi P. 2003. Characterization of the permselective properties of rabbit skin during transdermal iontophoresis. *J Pharm Sci* 92:1482-1488
11. Bath BD, White HS, Scott ER. 2000. Visualization and analysis of electroosmosis flow in hairless mouse skin. *Pharm Res* 17:471-475
12. Peck KD, Higuchi WI. 1997. Characterization of the passive transdermal diffusion route of polar/ionic permeants. In Potts RO, Guy RH, editors. *Mechanism of transdermal drug delivery*. New York: Marcel Dekker Inc., p 267-290
13. Lütolf P. 1997. *Transdermale Iontophorese einer amphoteren Verbindung: Einfluss der Molekülladung und Interaktion mit menschlicher Epidermis*. Ph D Thesis, University of Basel
14. Pikal MJ. 1990. Transport mechanisms in iontophoresis. I. A theoretical model for the effect of electroosmotic flow on flux enhancement in transdermal iontophoresis. *Pharm Res* 7: 118-126
15. Aguilera V, Kontturi K, Murtoimäki L, Ramirez P. 1994. Estimation of the pore size and charge density in human cadaver skin. *J Cont Rel* 32: 249-257

Table 1. Permeability coefficient, P, and enhancement factor, E, of BAd- α -Glc, and Flux, J_{69h} , of Tyr and Phe at pH 3.0 and 4.5 with Standard Error of the Mean, SEM, (n=3-8)

pH	Donor composition	P of BAd- α -Glc and SEM x 10 ⁹ (in cm/s)			E of BAd- α -Glc	J_{69h} ^c of Tyr and Phe and SEM x 10 ⁶ (in ug/s/cm ²)	
		Passive I	Iontophoresis	Passive I ^b		Tyr	Phe
3.0	BAd- α -Glc	1.55 (0.45)	<i>d</i>	1.71 (0.89)	<i>d</i>	NM ^a	NM
3.0	BAd- α -Glc + Tyr + Phe	20.03 (14.15)	102.4 (86.85)	2.78 (1.25)	4.76 (2.01)	33.55 (19.87)	30.00 (13.05)
3.0	BAd- α -Glc + Tyr β -NA	5.56 (5.35)	<i>d</i>	2.18 (1.98)	<i>d</i>	NM ^a	NM ^a
3.0	BAd- α -Glc + TyrPhe at 4°C	2.16 (0.63)	<i>d</i>	0.12 (0.022)	<i>d</i>	1.21 (0.21)	0.92 (0.13)
3.0	BAd- α -Glc + Tyr β -NA + Tyr + Phe	3.28 (1.77)	11.28 (4.43)	1.98 (1.49)	4.01 (0.76)	10.19 (4.28)	5.76 (2.96)
3.0	BAd- α -Glc + TyrPhe + Tyr + Phe at 4°C	5.08 (4.56)	16.17 (13.44)	2.41 (0.46)	3.92 (1.84)	7.84 (2.69)	9.24 (1.15)
3.0	Blank	NA ^b				1.02 (0.23)	0.74 (0.012)
4.5	BAd- α -Glc	2.92 (1.46)	1.39 (0.56)	1.08 (0.30)	0.78 (0.18)	NM ^a	NM ^a
4.5	BAd- α -Glc + Tyr + Phe	5.88 (3.40)	18.49 (10.25)	1.81 (0.47)	3.08 (0.40)	2.96 (0.95)	1.78 (0.11)
4.5	BAd- α -Glc + Tyr	2.50 (0.91)	3.12 (0.92)	2.50 (1.11)	1.75 (0.49)	7.59 (0.33)	NM ^a
4.5	BAd- α -Glc + Phe	1.19 (0.39)	2.17 (0.49)	1.30 (0.38)	2.35 (0.66)	NM ^a	2.72 (0.74)
4.5	BAd- α -Glc + Tyr β -NA	0.20 (0.089)	0.13 (0.023)	1.59 (1.56)	0.89 (0.35)	NM ^a	NM ^a
4.5	BAd- α -Glc + TyrPhe at 4°C	8.32 (3.81)	6.85 (5.04)	1.61 (0.95)	0.86 (0.31)	1.94 (0.53)	0.72 (0.11)
4.5	Blank	NA ^b				1.91 (0.21)	0.84 (0.14)

^a NM not measured, ^b NA not applicable, ^c Permeability coefficients of Passive I interpolated to a membrane resistance of 60kOhm*cm²

^d Permeability coefficients and enhancement factors with positive and negative values

Table 2. Skin extraction of BAd- α -Glc with Standard Error of the Mean, SEM, (n=3-10)

pH	Donor composition	Amount ug/skin sample (SEM)		
		BAd- α -Glc	Tyr	Phe
3.0	BAd- α -Glc	22.43 (4.18)	NM ^a	NM ^a
3.0	BAd- α -Glc + Tyr + Phe	3.30 (0.79)	3.08 (0.49)	2.53 (0.78)
3.0	BAd- α -Glc + Tyr β -NA	23.78 (4.82)	NM ^a	NM ^a
3.0	BAd- α -Glc + TyrPhe at 4°C	17.90 (3.98)	1.10 (0.32)	0.94 (0.61)
3.0	BAd- α -Glc + Tyr β -NA + Tyr + Phe	8.15 (2.79)	3.95 (0.85)	3.15 (0.40)
3.0	BAd- α -Glc + TyrPhe + Tyr + Phe at 4°C	24.63 (4.55)	3.94 (1.65)	2.82 (1.34)
3.0	Blank	NA ^b	1.02 (0.50)	0.90 (0.40)
4.5	BAd- α -Glc	24.10 (5.18)	NM ^a	NM ^a
4.5	BAd- α -Glc + Tyr + Phe	11.20 (3.02)	4.35 (1.56)	4.13 (0.92)
4.5	BAd- α -Glc + Tyr	13.53 (4.12)	3.85 (0.73)	1.40 (0.38)
4.5	BAd- α -Glc + Phe	13.38 (3.99)	1.53 (0.52)	3.75 (0.78)
4.5	BAd- α -Glc + Tyr β -NA	23.03 (6.48)	NM ^a	NM ^a
4.5	BAd- α -Glc + TyrPhe at 4°C	22.63 (5.20)	1.93 (0.65)	1.53 (0.38)
4.5	Blank	NA ^b	1.45 (0.50)	1.06 (0.43)

^a NM not measured, ^b NA not applicable

Table 3. Permeability coefficient, P, and enhancement factor, E, of Tyr β -NA at pH 3.0 and 4.5 with Standard Error of the Mean, SEM, (n=3-8)

pH	Donor composition	P of Tyr β -NA and SEM x 10 ⁹ (in cm/s)			E of Tyr β -NA
		Passive I	Iontophoresis	Passive I ^a	
3.0	Tyr β -NA	0.36 (0.058)	1.20 (0.23)	0.41 (0.052)	3.38 (0.73)
3.0	Tyr β -NA + BAd- α -Glc	1.32 (0.70)	7.29 (4.33)	0.45 (0.095)	4.46 (0.91)
3.0	Tyr β -NA + Tyr + Phe	0.98 (0.87)	2.65 (1.88)	0.60 (0.37)	4.72 (2.27)
3.0	Tyr β -NA + BAd- α -Glc + Tyr + Phe	0.61 (0.29)	4.58 (2.34)	0.47 (0.32)	4.56 (1.48)
4.5	Tyr β -NA	0.96 (0.53)	4.76 (2.44)	1.02 (0.63)	5.65 (0.62)
4.5	Tyr β -NA + BAd- α -Glc	0.88 (0.035)	4.73 (0.89)	1.53 (0.057)	5.35 (0.84)

^a Flux of Passive I phase interpolated to a membrane resistance of 60 kOhm*cm²; Regression through the points gave a slope of -1.03 and r=0.66 for pH 3.0 and 4.5

Table 4. Permeability coefficient, P, and enhancement factor, E, of TyrPhe at pH 3.0 and 4.5 with Standard Error of the Mean, SEM, (n=3-4)

pH	Donor composition	P of TyrPhe and SEM x 10 ⁹ (in cm/s)			E of TyrPhe
		Passive I	Iontophoresis	Passive I ^a	
3.0	TyrPhe + BAd- α -Glc at 4°C	14.86 (13.37)	22.57 (20.3)	10.01 (8.84)	1.57 (0.23)
3.0	TyrPhe + BAd- α -Glc + Tyr + Phe at 4°C	26.21 (25.74)	51.13 (50.44)	11.83 (10.84)	1.62 (0.17)
4.5	TyrPhe + BAd- α -Glc at 4°C	46.75 (43.12)	74.25 (68.36)	11.59 (9.58)	1.06 (0.43)

^a Flux of Passive I phase interpolated to a membrane resistance of 60 kOhm*cm²; Regression through the points gave a slope of -1.04 and r=0.67 for pH 3.0 and 4.5

Table 5. Skin extractions of Tyr β -NA with Standard Error of the Mean, SEM, (n=3-8)

pH	Donor composition	Amount ug/skin sample of Tyr β -NA (SEM)
3.0	Tyr β -NA	12.38 (2.41)
3.0	Tyr β -NA + BAd- α -Glc	12.90 (2.32)
3.0	Tyr β -NA +Tyr + Phe	10.43 (3.82)
3.0	Tyr β -NA + BAd- α -Glc +Tyr + Phe	12.65 (4.45)
4.5	Tyr β -NA	17.45 (3.85)
4.5	Tyr β -NA + BAd- α -Glc	16.85 (2.60)

Table 6. Skin extractions of TyrPhe with Standard Error of the Mean, SEM, (n=4-11)

pH	Donor composition	Amount ug/skin sample of TyrPhe (SEM)
3.0	TyrPhe + BAd- α -Glc at 4°C	9.40 (1.08)
3.0	TyrPhe + BAd- α -Glc + Tyr + Phe at 4°C	9.03 (2.47)
4.5	TyrPhe + BAd- α -Glc at 4°C	2.80 (0.18)

Table 7. Parameters calculated using the model

pH	Temperature (in °C)		\bar{z}_b	\bar{z}_{ad}	$K_{oct/ad}$	$(P_{ld}/P_{ad})^{passive}$ $\times 10^4$	Pe	$E_{calculated}$	$E_{experim}$
3.0	37	Tyr β -NA	0.98	0.96	4.81	175.6	-4.83	4.15	4.15
	37/4	BAd- α -Glc	0.00	0.00	0.13	2.4	<i>a</i>	<i>a</i>	<i>a</i>
	4	TyrPhe	0.76	0.56	0.80	22.2	-4.83	1.6	1.60
4.5	37	Tyr β -NA	0.66	0.63	7.28	146.0	-0.36	5.48	5.50
	37	BAd- α -Glc	0.00	0.00	0.11	2.0	-0.36	0.83	0.78
	4	TyrPhe	0.091	0.082	0.61	11.3	-0.58	1.15	1.06
	4	BAd- α -Glc	0.00	0.00	0.11	2.0	-0.58	0.74	0.86

^a Experimental enhancement factors partly negative for separate evaluation see text

E Appendix

This chapter contains the additional procedures and validation experiments, which are not yet described in the original papers of the previous section.

Choice of pH-values and buffer system

It was decided to carry out the permeation experiments at pH 3, where the skin is suspected to carry a net positive charge indicating an electroosmotic flow from cathode to anode and at pH 4.5, which lies in the region of the isoelectric point of the skin and consequently no electroosmotic flow occurs (Hoogestraate et al. 1994, Luzardo-Alvarez et al. 1998, Marro et al. 2001).

On the basis of these considerations it was decided to use Teorell-Stenhagen buffer system for both pHs (Wissenschaftliche Tabellen Geigy 1979).

Composition of buffer solutions

Universal buffer	Citric acid monohydrate	30.5 mM
	Boric acid	57.3 mM
	Phosphoric acid 85%	50.0 mM
	1M NaOH	343 ml
	Double distilled water	657 ml
Buffer pH 3	Teorell-Stenhagen Universal buffer	200 ml
	1M HCl	57 ml
	Double distilled water	743 ml
Buffer pH 4.5	Teorell-Stenhagen Universal buffer	200 ml
	1M HCl	48 ml
	Double distilled water	752 ml

For the donor solutions the substances were dissolved in one of the buffer. Then the buffer solution and the donor solution were isotonized by an extra of an adequate amount of sodium chloride.

E.1 Assay of TyrPhe, Tyr β -NA, BAd- α -Glc, Tyr, Phe and Benzyl alcohol

Solubility and partition coefficient

UV-detection was used to analyze TyrPhe, Tyr β -NA and BAd- α -Glc. Therefore a Perkin Elmer Lamda 5 System was used.

The detailed parameters are as follows:

Wavelength:

TyrPhe	275 nm
Tyr β -NA	279 nm
BAd- α -Glc	216 nm

Permeation and stability experiments

MS combined with HPLC was used to analyze TyrPhe, Tyr β -NA, BAd- α -Glc, Tyr and Phe. Agilent 1100 and HP 1100 system combined with an autosampler and an UV detector was used to analyze the compounds.

The detailed parameters are as follows:

HPLC

Column:	CC 125/2 Spherisorb 80-5 ODS-2
Flow Rate:	0.25 ml/min
Pressure:	approx. 90 bar
Retention time (minutes):	
TyrPhe	10-11
Tyr	2.0–3.0
Phe	2.5–3.5
BAd- α -Glc:	
- alone	12-13
- plus TyrPhe	12-13
- plus Tyr and/or Phe	12-13
- plus Tyr β -NA	2.5-3.5
Tyr β -NA	12-13

Wavelength:

TyrPhe	214 nm
BAd- α -Glc	214 nm
Tyr	214 nm
Phe	214 nm
Tyr β -NA	245 nm

Injection volume: 100 μ l

Solvent system:

TyrPhe, BAd- α -Glc, Tyr and Phe	Acetonitrile 5% Double distilled water 95%, Ammonium acetate 10 mM Acetic acid 50% to pH 3.2
--	---

Tyr β -NA	Acetonitrile 20% Double distilled water 80% Ammonium acetate 10 mM Acetic acid 50 % to pH 3.2
MS	
Mode:	SIM
Polarity:	Positive
Ionization mode:	API-ES
Peak width:	0.2 min
Cycle time:	1.2 s/cycle
Time filter:	on
Mass range:	
TyrPhe	329
Tyr	182, 204, 226
Phe	166
BAd- α -Glc:	312
Tyr β -NA	307
Fragmentor (V):	
TyrPhe	80
Tyr	40
Phe	40
BAd- α -Glc:	40
Tyr β -NA	70
Gain:	1
SIM resolution:	low
Drying gas flow: 10 l/min	
Nebulizer pressure: 30 psig	
Drying gas temperature: 350°C	
Capillary Voltage (V): 4000	

Enzymatic stability of BAd- α -Glc

HPLC was used to analyze benzyl alcohol. Agilent 1100 and HP 1100 system combined with an autosampler and a UV detector was used to analyze the compounds.

The detailed parameters are as follows:

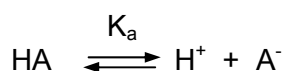
Column:	CC 125/2 Lichrospher 100-5 RP-18ec
Flow Rate:	0.25 ml/min
Pressure:	approx. 80
Retention time (minutes):	6-7
Wavelength:	258 nm
Injection volume:	100 μ l
Solvent system:	Acetonitrile 15% Double distilled water 85%

E.2 Physico-chemical characterization of TyrPhe, Tyrβ-NA and BAd-α-Glc

E.2.1 Ionization constants

Ionization constants are used to measure the strength of acids and bases. They reveal the proportion of the different ionic species of a compound at any pH.

HA is ionized as follows:



The ionization constant is defined as

$$K_a = \frac{[\text{H}^+][\text{A}^-]}{[\text{HA}]}$$

and as inversed log

$$\text{p}K_a = \text{pH} + \log \frac{[\text{HA}]}{[\text{A}^-]}$$

$\text{p}K_a$ is defined as pH where $[\text{HA}]$ and $[\text{A}^-]$ are equal (point of half-neutralization) and thus the log of their ratio is zero.

Experimental procedures

TyrPhe (1.2 mM) and Tyrβ-NA (0.11 mM) were dissolved separately in double distilled water with an equivalent of HCl. The solutions were then titrated with 10 mM NaOH and 1 mM NaOH, respectively. The titrations with Tyrβ-NA had to be gassed with argon because of greater variations of pH values.

The point of half-neutralization was determined by the tangent procedure (Hartke and Mutschler 1989).

Results

Table 1. Determination of $\text{p}K_a$ for TyrPhe and Tyrβ-NA with Standard Error of the Mean, SEM, (n=4)

	$\text{p}K_a$	SEM
TyrPhe	3.50	0.00
Tyrβ-NA	4.78	0.03
Tyr*	2.20, 9.11, 10.13	-
Phe*	2.16, 9.18	-

*The $\text{p}K_a$ values for Try and Phe were taken from literature (Vollhardt 1990)

E.2.2 Solubility of TyrPhe and Tyr β -NA

To decide the donor concentration, the saturation concentration was determined.

Experimental procedures

The component was added in surplus to Teorell-Stenhagen buffer pH 3 and pH 4.5. The suspensions were shaken by magnetic stirrer and heated up to 37°C by water bath. Each 24 hours samples were withdrawn and the amount determined by UV-detection as described above. This process was repeated until the concentration measured did not rise on successive measurements.

Results

Table 2. Solubility of TyrPhe and Tyr β -NA

	Solubility mg/ml	
	pH 3	pH 4.5
TyrPhe	1.4	0.8
Tyr β -NA	1.1	0.6

The aqueous solubility of BAd- α -Glc is 50 mg/ml (Certificate of Analysis, Aldrich, Switzerland).

E.2.3 Stability

The stability of TyrPhe and BAd- α -Glc should be ensured during storage and throughout the experiment. Tyr β -NA was assumed to be stable due to the side-chain protecting group at the C-terminus.

E.2.3.1 Chemical stability

The chemical stability was determined for TyrPhe and BAd- α -Glc dissolved in buffer at pH 3 and 4.5.

Experimental procedures

At pH 3 and pH 4.5 TyrPhe solutions (3.8 mM) were put in a water bath and shaken continuously by magnetic stirrer at 37°C over a period of 95 hours. Every 10-12 hours the pH values was monitored and samples were withdrawn and analyzed as described above.

The same procedure was carried out with BAd- α -Glc solutions (1.5 mM).

Results

The pH of all solutions remained constant during the period of the experiment (maximum variations were ± 0.2 pH units).

TyrPhe and BAd- α -Glc concentration remained stable (see Figure 1) and no degradation products were measured after 95 hours.

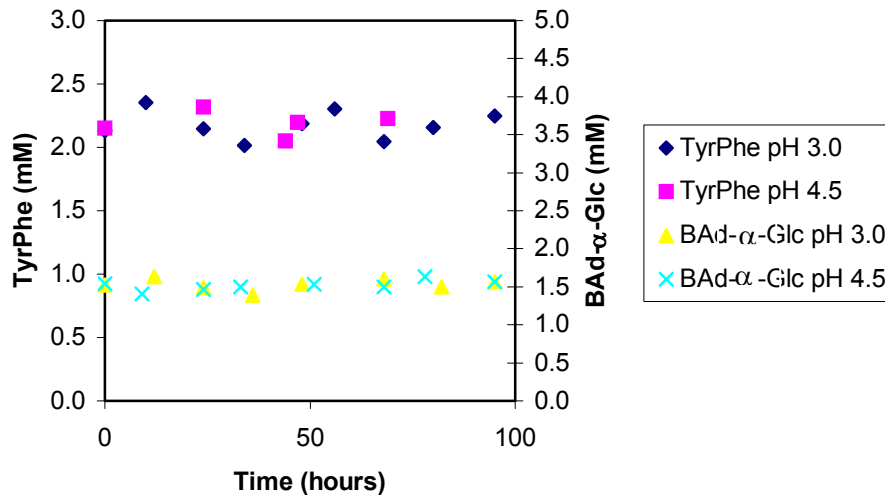


Figure 1. Chemical stability of TyrPhe and BAd- α -Glc over 95 hours

E.2.3.2 Enzymatic stability of TyrPhe

The stability was determined by measuring the decrease of TyrPhe concentration and the increase of the generated degradation products Tyr and Phe.

The experimental procedure was carried out using reflection method (Boderke et al. 1998). Therefore, the heat-separated epidermis was interposed between two half-cells, the viable epidermis facing the donor chamber. Between the receiver chamber and the stratum corneum, a plastic foil was mounted as an impermeable barrier (see Figure 2).

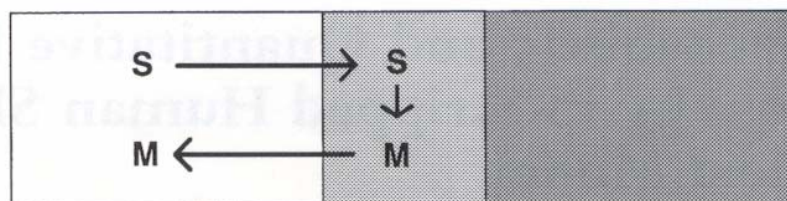


Figure 2. Reflection set-up consisting of donor compartment (left), heat-separated epidermis (middle) and impermeable barrier (right; plastic foil). S, substrate; M, metabolite

Experimental procedures

After the membrane was clamped between donor compartment, plastic foil and receiver compartment, 7.5 ml of TyrPhe solution (1.2 mM) at pH 3 or pH 4.5 was filled in the donor compartment. Analogue to permeation experiments the cells were stirred at 400 rpm with teflon paddles in a water bath at 37°C over a period of 70 hours. Every 10-15 hours samples were withdrawn and analyzed as described above.

Results

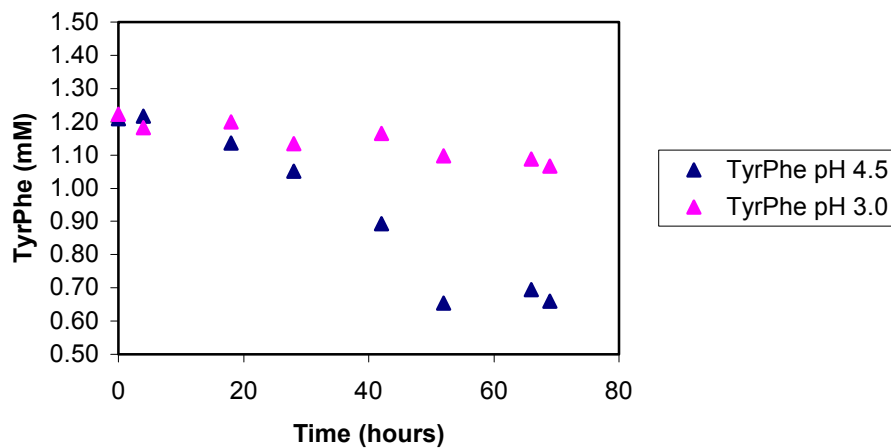


Figure 3. Reflection boundary set-up: Decrease of the TyrPhe concentration in the presence of human epidermal membrane

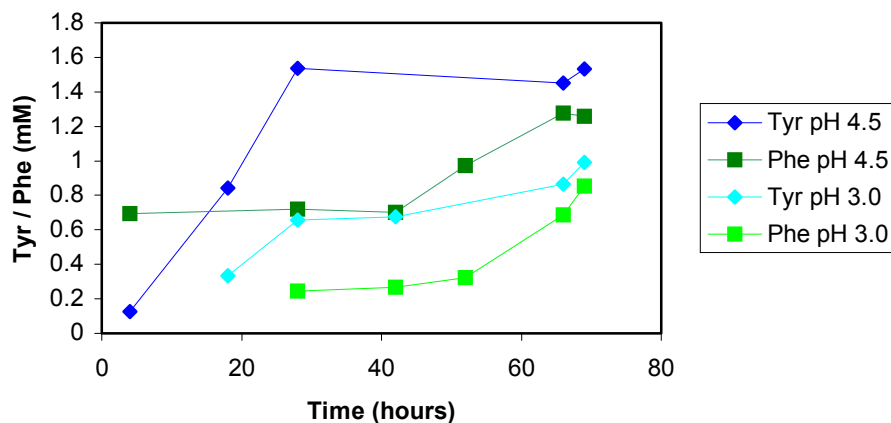


Figure 4. Generation of the degradation products Tyr and Phe in the compartment at pH 3 and 4.5

Reflection experiments showed a decrease of TyrPhe concentration of 12% at pH 3 and 45% at pH 4.5 after 70 hours. Both degradation products appeared within the first 20-30 hours at pH 3 and the first 5 hours at pH 4.5, respectively (see Figure 3 and 4).

As explained in details in the original papers in the previous section, the amount of generated Tyr and Phe accounted exactly for the concentration decrease of TyrPhe.

E.2.3.3 Enzymatic stability of BAd- α -Glc

Instead of analyzing the decrease of BAd- α -Glc concentration it was decided to determine the stability of BAd- α -Glc by measuring the degradation product benzyl alcohol.

Experimental procedures

1 ml of BAd- α -Glc solution (1.5 mM) at pH 3 or pH 4.5 was added to a piece of heat-separated epidermis of the same size like those of the permeations experiments. During 70 hours samples of 100 μ l were withdrawn every 8-17 hours and analyzed as described above.

Results

The degradation product was measured in a concentration less than 0.5% at pH 3 and pH 4.5 indicating no enzymatic degradation of BAd- α -Glc.

E.2.3.4 Stability during voltage application of 250 mV

The stability of the dipeptide TyrPhe during voltage application of 250 mV was investigated.

Experimental procedures

Instead of human epidermal membrane, 75 membrane filters (Isopore™ Membrane Filter, Filter Type 0.1 μ m VCTP, Milipore AG) with a pore size of 0.1 μ m were used. Each half-cell was filled with TyrPhe solution at pH 4.5, which was analogue to the permeation experiment. During 8 hours a voltage of 250 mV was applied and each hour a sample was withdrawn.

Results

No decrease of TyrPhe concentration (see Figure 5) and no generation of any degradation products (Tyr or Phe) were recognized. Therefore, TyrPhe was regarded as stable during a voltage application of 250 mV over 8 hours.

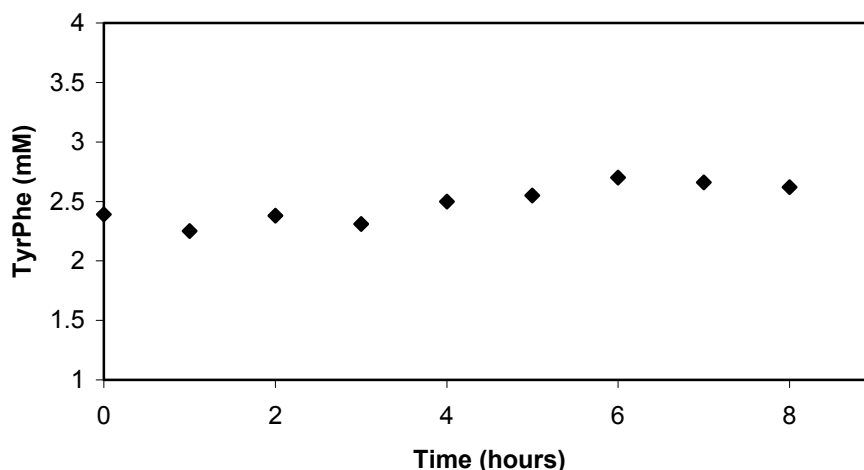


Figure 5. Stability of TyrPhe during voltage application of 250 mV over 8 hours

E.2.4 Partition coefficient

Partition coefficient is a measure of partitioning of non-ionized substances between two immiscible phases. For most purposes these phases are an organic solvent and water. The partition coefficient K of a substance is defined as the ratio of the concentration in the two phases at equilibrium.

$$K = \frac{C_o}{C_w}$$

where C_o is the concentration in the organic and C_w the concentration in the aqueous phase. Sometimes the partition coefficient is determined under conditions where the substance is partially ionized. In this case the ratio of the concentrations is termed *apparent partition coefficient* to distinguish from the *real partition coefficient* for the totally non-ionized compound.

The real partition coefficient was measured for BAD- α -Glc and the apparent partition coefficient was measured for TyrPhe and Tyr β -NA at pH 3 and 4.5, using n-octanol and Teorell-Stenhagen buffer as organic and aqueous phase. n-octanol has been widely used as model for biological membranes (Lund 1994). Its long non-polar carbon atom chain represents the bound or free fatty acid chains and the polar heads of a membrane.

It is expected that the apparent partition coefficient of Tyr β -NA at pH 3 is smaller than at pH 4.5 because of the lack of the carboxyl group. This leads to a greater amount of ionized molecules at pH 3. In contrast, TyrPhe carries more charge at pH 4.5 (amino group and

carboxyl group) and should therefore have a higher partition coefficient at pH 3. With the uncharged BAd- α -Glc the partition coefficient should be the same for both pHs.

The real and the apparent partition coefficient were measured using flask shaking method. Therefore the two immiscible solutes were shaken and analyzed for content (Leo et al. 1971).

Experimental procedures

Each substance was dissolved in the medium (n-octanol or buffer) in which it was less soluble by stirring it continuously over 48 hours followed by ultrasonic for 15 minutes. The overstanding solution was centrifuged and 20 ml were added to an equal volume of buffer (pH 3 or pH 4.5) or n-octanol. This mixture was shaken 20 times during one minute by inverting the flask at 180°. This procedure was carried out every 10 minutes during the first hour. Then it was shaken 20 times in a minute once in an hour for the following 5 hours. The mixture was allowed to stand 10 minutes before the two phases were separated, centrifuged at 4000 rpm for 15 minutes and analyzed by UV-detection as described above.

Results

Table 3. Determination of partition coefficients of TyrPhe, Tyr β -NA and BAd- α -Glc at pH 3 and 4.5 with Standard Error of the Mean, SEM, (n=4-8)

		Partition coefficient K (SEM)	
pH 3	BAd- α -Glc	0.11	(0.071)
	TP	0.80	(0.170)
	Tyr β -NA	4.81	(0.086)
pH 4.5	BAd- α -Glc	0.13	(0.062)
	TP	0.61	(0.074)
	Tyr β -NA	7.28	(0.160)

E.3 Validation for transport studies

The diffusion cells used in this project were already used in our laboratory. They have been described and validated in detail in earlier PhD thesis's (Lütolf 1997 and Kochhar 2001).

E.4 Experimental determinations

E.4.1 Determination of the transport area

The transport area of both half-cells is relevant for the calculation of the flux of the permeants. Therefore, the inner diameter was measured at 3 different positions by a Vernier Capiller.

Table 4. Transport area of the half-cells

Transport cell	Mean inner diameter (d) (cm)			Transport area (cm ²) $= \pi \left(\frac{d}{2}\right)^2$
	Donor	Receiver	Mean	
Cell a	1.617	1.600	1.608	2.03
Cell b	1.600	1.600	1.600	2.01
Cell c	1.600	1.600	1.600	2.01
Cell d	1.617	1.563	1.590	1.99
Cell e	1.620	1.622	1.621	2.06
Cell f	1.600	1.625	1.613	2.04
Cell h	1.600	1.500	1.550	1.89
Cell l	1.600	1.625	1.613	2.04
Cell k	1.654	1.649	1.615	2.14
Cell y	1.625	1.600	1.613	2.04

E.4.2 Determination of the thickness of heat-separated epidermal membrane

The thickness of the epidermis was measured by micrometer direct after the heat separation.

Experimental procedures

After the heat separation, the skin specimens were lying on a piece of aluminium foil. These two layers were mounted between two cover-glasses (18x18 mm, thickness 0.28 mm) and measured by micrometer on 3 different positions in triplicate in order to investigate reproducibility. The thickness of the two cover-glasses and the aluminium foil was measured and subtracted from the mean thickness of the whole before measured system (Lütolf 1997).

Results

This method showed reproducibility and a mean thickness of $43 \mu\text{m} \pm 5 \mu\text{m}$ (n=16).

E.4.3 Osmolarity and pH during permeation experiment

As a control the osmolarity and the pH of donor and receiver solutions was measured before and after each permeation experiment by an osmo- and a pH-meter. If the difference of the values before and after the permeations experiment was greater than 15 mosmol and 0.2 pH units the transport data of that cell was not included in the results.

E.4.4 Pulverization of skin

E.4.4.1 Determination of the membrane extraction

After each permeation experiment, the skin sample was pulverized in order to determine the amount of the substances, which were dissolved in the donor solution and their possible degradation products.

Experimental procedures and results are described in chapter C 'Publications'.

E.4.4.2 Recovery from epidermal membrane

This procedure was performed to estimate the accuracy of the substance extraction of the skin pulverization experiments.

Experimental procedures

BAd- α -Glc solution was applied on epidermal membrane and paper filter as a control. After drying, the samples were pulverized and diluted in HPLC eluant and then extracted as described above. The ratio of the determined BAd- α -Glc concentration in the epidermal membrane to the BAd- α -Glc concentration in the paper filter gave the recovery of 59%.

E.4.5 Time dependent resistance changes of the membrane

Experimental procedure

The assessment of this experiment corresponded to the permeation experiments. Buffer solution pH 3 (cell 1 and cell 2) or pH 4.5 (cell 3) was filled in both compartments. Every 10-15 hours a voltage of 250 mV was applied during 10 minutes. The current flow of each skin specimen was measured and recorded and though the corresponding resistance calculated.

Results

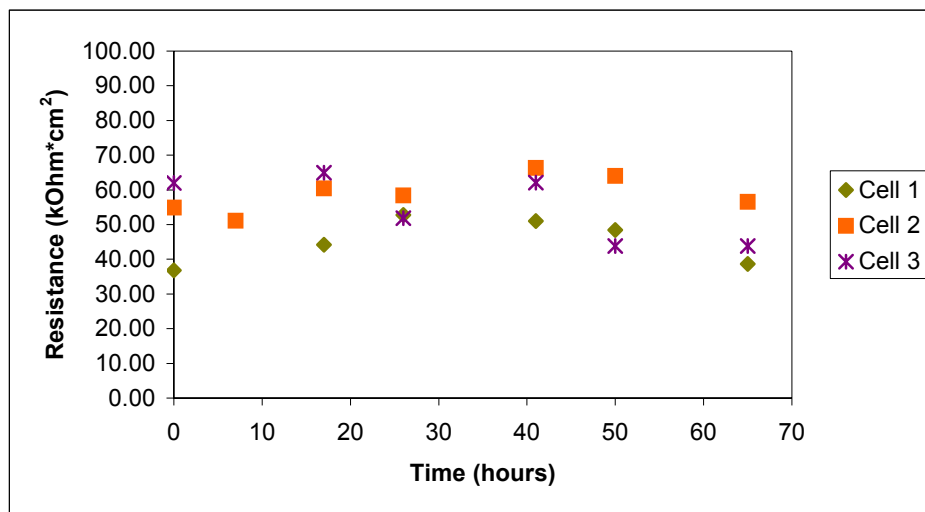


Figure 6. Resistance changes of three membrane specimens over 70 hours

The resistances of the membranes remained constant over 70 hours at both pHs.

E.4.6 Procedure of the permeation experiments

Setting the cells

Full thickness skin was heat separated at 60°C as described by Sims et al. 1991. The epidermal membrane was cut into pieces using a circular punch with a diameter of 2.5 cm. The skin piece was put in buffer with the stratum corneum facing the upper side. The receiver half-cell was immersed into the buffer and lifted out the membrane with the stratum corneum on its exposed side. The receiver half-cell with the membrane was covered carefully by the donor half-cell. The two half cells were pressed one on the other and sealed with teflon tape. The whole cell was then secured further with teflon covers from donor and receiver side, which were screwed together to fix the cell tightly. The donor cell was filled with approximately 3 ml of buffer solution and held in upright position for 15 minutes to check any leaking.

Meanwhile, buffer was degassed in the ultrasonic bath and filled in the Luggin capillaries without any bubbles. The capillaries were carefully fitted in the leak proved and dried cells and secured with teflon clamps.

The cell was then screwed to a teflon board, which rested in a water bath at 37°C and could hold five of such cells. Reference and working electrodes as well as stirrers were fitted in the cell. The stirrers were connected with a beaded chain, which was connected to a motor operated at 400 rpm. The donor and receiver half-cells were filled with 7.5 ml of donor or buffer solution, respectively. Samples of 50 μ l in the donor and 200 μ l in the receiver

compartment were withdrawn. The volume drawn from the receiver compartment was replenished with buffer solution only. Samples were withdrawn regularly at determined intervals and analyzed against a set of standard solutions. The cumulative amount was calculated as shown in the next section.

E.4.7 Cumulative amount permeation

As an example an experiment with TyrPhe, BAd- α -Glc, Tyr and Phe dissolved in the donor solution is shown.

C₁: concentration calculated from the calibration curve

C₂: concentration in the receiver compartment at time x (in 7.5 ml)

C₃: concentration drawn from the cell at time x (in 0.2 ml)

C₄: corrected cumulative amount at time x

Calibration curve used for TyrPhe: $y = 1909247x + 137101$

$$r^2 = 1.00$$

Table 5. The cumulative amount of TyrPhe over 69 hours

Stage	Time	Area	C ₁ ($\mu\text{g/ml}$)	C ₂ ($\mu\text{g}/7.5\text{ml}$)	C ₃ ($\mu\text{g}/0.2\text{ml}$)	C ₄ (in μg)
	0.00					
	1.50	290718	0.100	0.752	0.020	0.752
	3.00	334143	0.115	0.864	0.023	0.884
	16.50	3584440	1.236	9.267	0.247	9.310
	18.00	3597650	1.240	9.301	0.248	9.591
	19.50	3579150	1.234	9.253	0.247	9.791
Stage I	21.00	3597170	1.240	9.300	0.248	10.085
	22.50	3576030	1.233	9.245	0.247	10.278
	24.00	3625980	1.250	9.374	0.250	10.654
	25.50	3649710	1.258	9.436	0.252	10.965
	26.50	3656810	1.261	9.454	0.252	11.235
	41.50	4277500	1.474	11.059	0.295	13.092
	42.00	4289880	1.479	11.091	0.296	13.419
	43.50	4294530	1.480	11.103	0.296	13.727
	44.00	4239520	1.461	10.961	0.292	13.880
	44.67	4166490	1.436	10.772	0.287	13.984
	45.00	4188780	1.444	10.829	0.289	14.329
Stage II (250 mV)	45.33	4045650	1.395	10.459	0.279	14.248
	45.67	4064940	1.401	10.509	0.280	14.576
	46.33	4021330	1.386	10.396	0.277	14.744
	46.67	4054170	1.398	10.481	0.280	15.106
	47.00	3896490	1.343	10.074	0.269	14.978
	48.50	3706040	1.278	9.581	0.256	14.754
	50.00	3773690	1.301	9.756	0.260	15.184
Stage III	65.50	3998770	1.378	10.338	0.276	16.027
	66.00	3938130	1.358	10.181	0.272	16.145
	67.50	4068260	1.402	10.518	0.280	16.753
	69.00	4029250	1.389	10.417	0.278	16.933

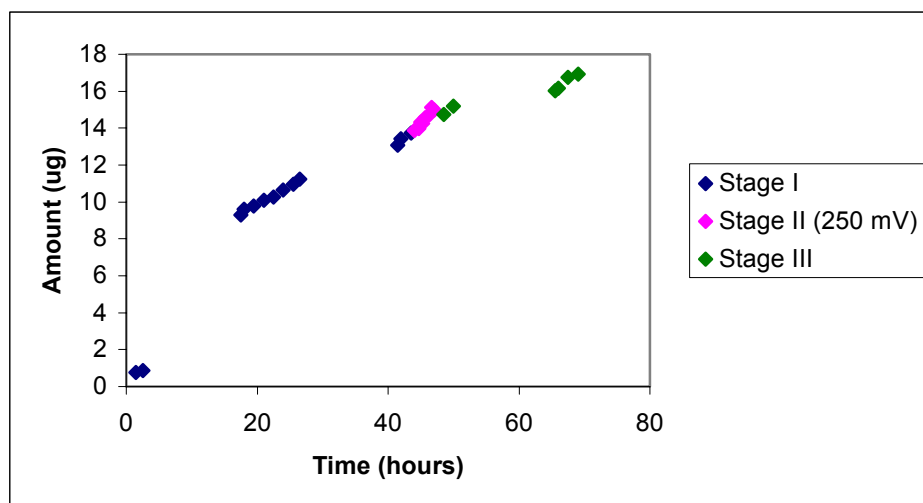


Figure 7. Permeation profile of TyrPhe

Table 6. Calculation of the permeability coefficient P and enhancement factor E of TyrPhe

Stage	Slope (in $\mu\text{g}/\text{h}$)	Donor conc. (in $\mu\text{g}/\text{ml}$)	Permeability coefficient P	Enhancement factor E
Stage I	7.97E-5	579	6.67E-8	
Stage II (250 mV)	1.16E-4	556	1.01E-7	1.52
Stage III	2.45E-5	540	2.20E-8	

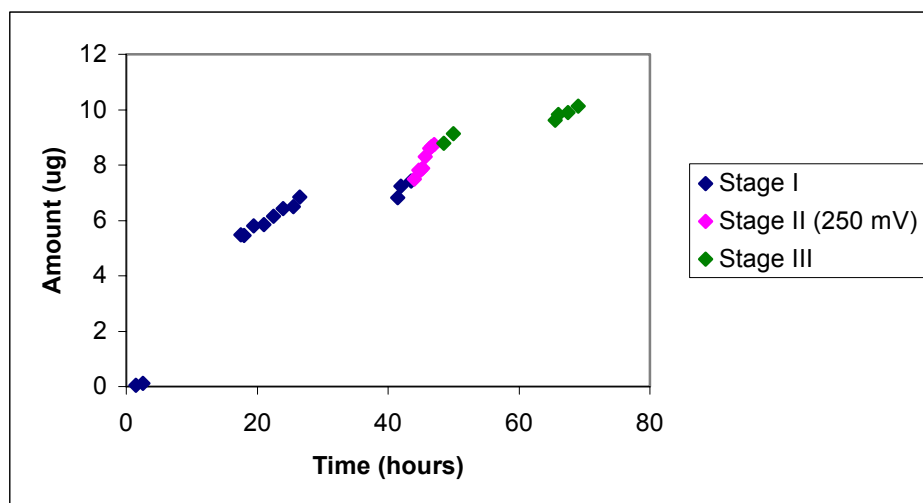
Area of the cell used: 2.064 cm^2

Appendix

Calibration curve used for BAd- α -Glc: $y = 1966630x + 147091$
 $r^2 = 1.00$

Table 7. The cumulative amount of BAd- α -Glc over 69 hours

Stage	Time	Area	C ₁ ($\mu\text{g/ml}$)	C ₂ ($\mu\text{g}/7.5\text{ml}$)	C ₃ ($\mu\text{g}/0.2\text{ml}$)	C ₄ (in μg)
	0.00					
	1.50	157528	0.005	0.040	0.001	0.040
	3.00	178874	0.016	0.121	0.003	0.122
	16.50	1583460	0.730	5.478	0.146	5.482
	18.00	1538750	0.708	5.307	0.142	5.458
	19.50	1594910	0.736	5.521	0.147	5.813
Stage I	21.00	1562840	0.720	5.399	0.144	5.838
	22.50	1609770	0.744	5.578	0.149	6.161
	24.00	1642560	0.760	5.703	0.152	6.435
	25.50	1618520	0.748	5.611	0.150	6.495
	26.50	1668900	0.774	5.804	0.155	6.837
	41.50	1626460	0.752	5.642	0.150	6.830
	42.00	1695530	0.787	5.905	0.157	7.244
	43.50	1698710	0.789	5.917	0.158	7.414
	44.00	1678650	0.779	5.841	0.156	7.495
	44.67	1718770	0.799	5.994	0.160	7.804
	45.00	1680110	0.780	5.846	0.156	7.816
Stage II (250 mV)	45.33	1657340	0.768	5.760	0.154	7.885
	45.67	1724730	0.802	6.017	0.160	8.296
	46.33	1763570	0.822	6.165	0.164	8.604
	46.67	1736650	0.808	6.062	0.162	8.666
	47.00	1711770	0.796	5.967	0.159	8.733
	48.50	1685280	0.782	5.866	0.156	8.791
	50.00	1734260	0.807	6.053	0.161	9.134
Stage III	64.50	1817060	0.849	6.369	0.170	9.611
	66.00	1828050	0.855	6.411	0.171	9.823
	67.50	1801470	0.841	6.309	0.168	9.893
	69.00	1818070	0.850	6.372	0.170	10.124

Figure 8. Permeation profile of BAd- α -GlcTable 8. Calculation of the permeability coefficient P and enhancement factor E of BAd- α -Glc

Stage	Slope (in $\mu\text{g}/\text{h}$)	Donor conc. (in $\mu\text{g}/\text{ml}$)	Permeability coefficient P	Enhancement factor E
Stage I	4.40E-5	3505	6.08E-9	
Stage II (250 mV)	1.24E-4	3403	1.77E-8	2.91
Stage III	1.46E-5	3332	2.12E-9	

Area of the cell used: 2.064 cm^2

Calibration curve used for Tyr: $y = 21396x + 1597.8$
 $r^2 = 0.999$

Table 9. The cumulative amount of Tyr over 69 hours

Stage	Time	Area	C ₁ ($\mu\text{g/ml}$)	C ₂ ($\mu\text{g}/7.5\text{ml}$)	C ₃ ($\mu\text{g}/0.2\text{ml}$)	C ₄ (in μg)
Stage I	0.00					
	1.50					
	3.00					
	16.50	10656.2	0.423	3.175	0.085	3.175
	18.00	10663.9	0.424	3.178	0.085	3.263
	19.50	10742.7	0.427	3.206	0.085	3.375
	21.00	10908.7	0.435	3.264	0.087	3.519
	22.50	11478.7	0.462	3.464	0.092	3.806
	24.00	11778.9	0.476	3.569	0.095	4.003
	25.50	11975.2	0.485	3.638	0.097	4.167
	27.00	12068.6	0.489	3.670	0.098	4.297
	40.50	13824.6	0.571	4.286	0.114	5.010
	42.00	14112.4	0.585	4.387	0.117	5.225
43.50	14299.4	0.594	4.452	0.119	5.408	
Stage II (250 mV)	44.00	15453.1	0.648	4.857	0.130	5.931
	44.67	14826	0.618	4.637	0.124	5.841
	45.00	14727.2	0.614	4.602	0.123	5.930
	45.33	14300.8	0.594	4.453	0.119	5.903
	45.67	14263	0.592	4.440	0.118	6.009
	46.33	13869.7	0.574	4.302	0.115	5.989
	46.67	13616.9	0.562	4.213	0.112	6.015
47.00	13485.1	0.556	4.167	0.111	6.081	
Stage III	48.50	11517.1	0.464	3.477	0.093	5.503
	50.00	11803.6	0.477	3.577	0.095	5.696
	64.50	14202	0.589	4.418	0.118	6.632
	66.00	14374.2	0.597	4.479	0.119	6.810
	67.50	14095.9	0.584	4.381	0.117	6.832
	69.00	14724.1	0.613	4.601	0.123	7.169

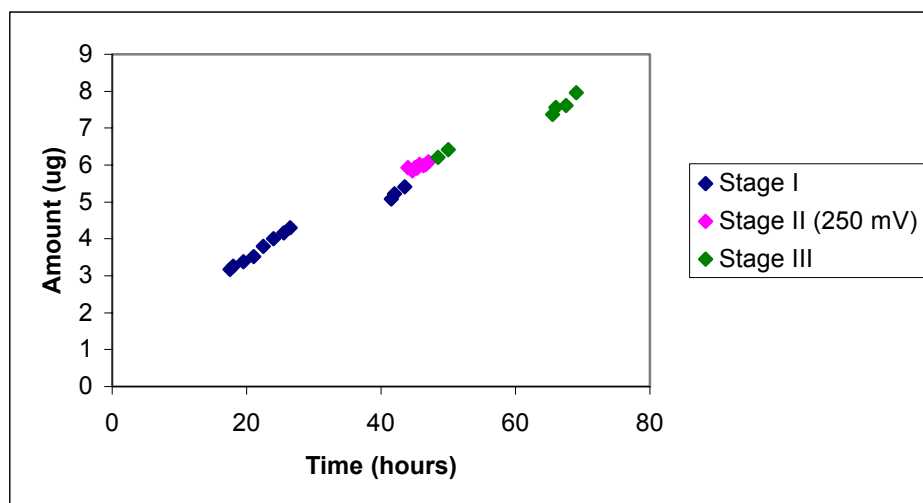


Figure 9. Permeation profile of Tyr

Table 10. Calculation of the permeability coefficient P and enhancement factor E of Tyr

Stage	Slope (in $\mu\text{g}/\text{h}$)	Donor conc. (in $\mu\text{g}/\text{ml}$)	Permeability coefficient P	Enhancement factor E
Stage I	7.97E-5	579	6.97E-8	
Stage II (250 mV)	1.16E-4	556	1.18E-7	1.22
Stage III	2.45E-5	540	739E-8	

Area of the cell used: 2.064 cm^2

Appendix

Calibration curve used for Phe: $y = 1465831x + 237088$
 $r^2 = 0.999$

Table 11. The cumulative amount of Phe over 69 hours

Stage	Time	Area	C ₁ ($\mu\text{g/ml}$)	C ₂ ($\mu\text{g}/7.5\text{ml}$)	C ₃ ($\mu\text{g}/0.2\text{ml}$)	C ₄ (in μg)
	0.00					
	1.50	192295	0.062	0.466	0.012	0.466
	3.00	220206	0.071	0.533	0.014	0.546
	16.50	1748900	0.565	4.236	0.113	4.263
	18.00	1723830	0.557	4.175	0.111	4.315
	19.50	1680400	0.543	4.070	0.109	4.321
Stage I	21.00	1651760	0.533	4.001	0.107	4.360
	22.50	1578860	0.510	3.824	0.102	4.291
	24.00	1480820	0.478	3.587	0.096	4.155
	25.50	1457440	0.471	3.530	0.094	4.194
	26.50	1434550	0.463	3.475	0.093	4.233
	41.50	1523080	0.492	3.689	0.098	4.540
	42.00	1449060	0.468	3.510	0.094	4.459
	43.50	1494390	0.483	3.620	0.097	4.662
	44.00	1458600	0.471	3.533	0.094	4.672
	44.67	1401290	0.453	3.394	0.091	4.628
	45.00	1465690	0.473	3.550	0.095	4.874
Stage II (250 mV)	45.33	1420650	0.459	3.441	0.092	4.860
	45.67	1395730	0.451	3.381	0.090	4.891
	46.33	1434570	0.463	3.475	0.093	5.075
	46.67	1382900	0.447	3.350	0.089	5.043
	47.00	1303500	0.421	3.157	0.084	4.940
	48.50	1201090	0.388	2.909	0.078	4.776
	50.00	1226260	0.396	2.970	0.079	4.914
Stage III	64.50	1709790	0.552	4.141	0.110	6.165
	66.00	1758250	0.568	4.259	0.114	6.393
	67.50	1647800	0.532	3.991	0.106	6.239
	69.00	1637770	0.529	3.967	0.106	6.321

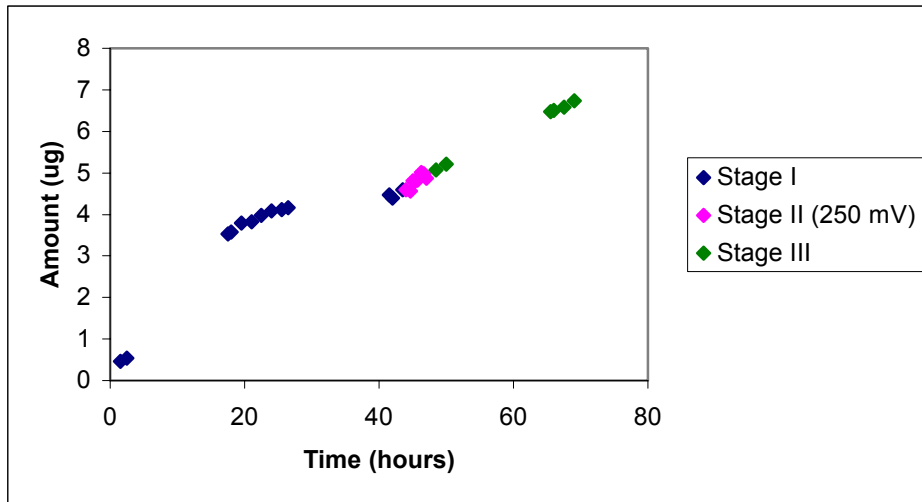


Figure 10. Permeation profile of Phe

Table 12. Calculation of the permeability coefficient P and enhancement factor E of Phe

Stage	Slope (in $\mu\text{g}/\text{h}$)	Donor conc. (in $\mu\text{g}/\text{ml}$)	Permeability coefficient P	Enhancement factor E
Stage I	2.35E-5	500	4.53E-8	
Stage II (250 mV)	3.62E-5	483	7.21E-7	1.59
Stage III	2.21E-5	472	4.52E-8	

Area of the cell used: 2.064 cm^2

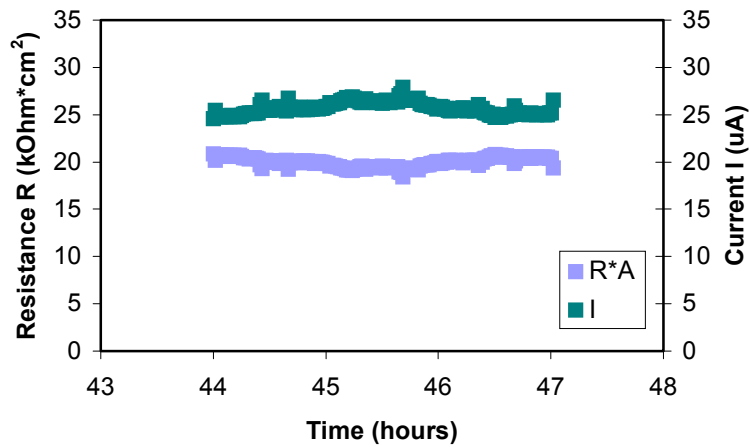


Figure 11. Electrical profile during stage II (250 mV)

Table 13. Electrical data

Stage	Resistance (in $\text{k}\Omega \cdot \text{cm}^2$)	Current (in μA)
Stage I	19.81	25.9
Stage II (250 mV)	19.88	25.8
Stage III	18.10	28.3

E.5 List of instruments

Balance, Mettler AT 261DeltaRange®, No. P27846, Mettler Toledo AG, Greifensee ZH, Switzerland

Centrifuge, Centrifuge Sigma 302K, No. 22644, Sigma, Osterode/Harz, Germany

Destillationsapparatur, Büchi Laboratoriums-Technik AG, Flawil/SG, Switzerland

Freeze mill, 6750, No. 98060, SPEX CertiPrep, Incorporated, New Jersey, USA

HPLC-MS, Hewlett Packard HPLC/MS-System, Serie 1100, Hewlett Packard, Switzerland

Isocratic pump:	Type G1310A Serie No. DE52700102
Vacuum degasser:	Type G1322A Serie No. JP52900335
Autosampler:	Type G1329A Serie No. DE23909716
UV-Detector:	Type G1314A Serie No. JP55100233
Massdetector:	Type G1946C Serie No. US11811027
Software:	LC/MSD ChemStation Rev. A.09.01 [1206]
HPLC Column:	CC 125/2 SPHERISORB 80-5 ODS-2 Kat No. 728007.02 Serie No. 9081978, Batch 123 Macherey-Nagel, Schweiz

Glas cells and capillaries (Iontophoresis), Glastechnik Rahm, 4132 Muttenz, Switzerland

Micrometer, Isomaster® (0-25 mm, 0.01 mm), No. 028374, Tesa SA, Renens VD, Switzerland

Osmometer, Roebbling Osmometer Type 4B, No. 8606007, Auer Bittmann Soulié AG, Dietikon ZH, Switzerland

Perkin Elmer Spectrometer Lambda 20, No. 20029, Perkin Elmer, Überlingen, Germany

pH-meter, Metrohm 744 pH meter, Type 1.744.0010, No. 12190, Metrohm, Herisau, Switzerland

Potentiostat, Potentiostat für Gleichstrom, Institut für Physik der Universität Basel, Switzerland

Potentiostat writer, model DCR 520C, Instruments AG, Münchenstein, Switzerland

Reference electrodes, Metrohm Ag, Ag/Cl-Elektroden/0...80°C, Type 6.0724.140, Metrohm, Herisau, Switzerland

Stirring system (Iontophoresis), RE 162 IKA Motor, No. 725921, Janke & Kunkel, IKA-Labortechnik, Staufen i.Br., Deutschland

Synthetic membranes, Isopore™ Membrane Filters, Filter type 0.1 µm VCTP, No. VCTP02500, Lot No. R3CN98135, Millipore AG, Volketswil ZH, Switzerland

Vernier Calliper, Etalon 75-115821 T, Pierre Roch, Rolle GmbH, Switzerland

Waterbath (Iontophorese), Julabo 36B, Type VC/3, No. 1099332668 Julabo Labortechnik GmbH, Seelbach, Germany

Waterbath, Variomag® Electronicrührer, Type E, No. 00202320951, Julabo Labortechnik GmbH, Munich, Germany

Ultrasonic bath, Retsch Type URG, No. 306059007, Retsch GmbH&Co., Haan, Germany

E.6 References

Boderke P, Boddé HE, Ponce M, Wolf M, Merkle HP. 1998. Mechanistic and quantitative prediction of aminopeptidase activity in stripped human skin based on the HaCaT cell sheet model. *J Invest Dermatol* 3: 180-184

'Certificate of analysis' from Aldich, Switzerland

Hartke K and Mutschler E. 1989. Chapter V.6.14 Potentiometrie. In *Deutsches Arzneimittelbuch Kommentar Band 4*. Ninth edition. Wissenschaftliche Verlagsgesellschaft mbH Stuttgart/Govi-Verlag GmbH Frankfurt. 3693-3694

Hoogstraate AJ, Srinivasan V, Sims SM, Higuchi WI. 1994 Iontophoretic enhancement of peptides: behaviour of leuprolide versus model permeants. *J. Cont Rel* 31:41-47

Kochhar C, Imanidis G. 2003. In vitro transdermal iontophoretic delivery of leuprolide-Mechanism under constant voltage application. *J Pharm Sci* 92: 84-96

Leo A, Hansch C, Elkins D. 1971. Partition coefficients and their uses. *Chem Rev* 71: 525-616

Lütolf P. 1997. Transdermale Iontophorese einer amphoteren Verbindung: Einfluss der Molekülladung und Interaktion mit menschlicher Epidermis. Ph D Thesis, University of Basel

Lund W. 1994. *The Pharmaceutical Codex 1994*. Twelfth edition. London. The Pharmaceutical Press. 188-189

Luzardo-Alvarez A, Rodriguez-Fernandez M, Blanco-Méendez J., Guy RH, Delgado-Charro MB. 1998. Iontophoretic permselectivity of mammalian skin: characterization of hairless mouse and porcine membrane models. *Pharm Res* 15: 984-987

Marro D, Guy RH, Delgado-Charro MB. 2001 Characterization of the iontophoretic permselectivity properties of human and pig skin. *J Cont Rel* 70: 213-217

Sims SM, Higuchi WI, Srinivasan V. 1991 Skin alteration and convective flow effects during iontophoresis I. Neutral solute transport across human skin. *Int J Pharm* 69: 109-121

Vollhardt K.P.C. 1990. *Organische Chemie*. Weinheim. VCH Verlagsgesellschaft mbH. 1263

Wissenschaftliche Tabellen Geigy. 1979. Teilband Hämathologie und Humangenetik. 8. Auflage. Basel. Ciba Geigy AG. 60-61

Curriculum vitae

Name Melanie Pamela Altenbach

Date of birth 30.4.1973

Place of birth Basel, Switzerland

Education

12/1992 Matura, Gymnasium Münchenstein, Switzerland

11/1993 Registration at University of Basel, Basel, Switzerland
Department of Pharmacy

7/1995 - Practical year
7/1996 City Apotheke, Basel, Switzerland

11/1998 Academic degree in Pharmacy
University of Basel, Basel, Switzerland

PhD study

5/1999 - PhD study under the supervision of PD Dr. G. Imanidis and
4/2004 Prof. Dr. H. Leuenberger at the Institute of Pharmaceutical
Technology, Department of Pharmacy, University of Basel,
Switzerland

Poster 'Effect of metabolism of a dipeptide on iontophoretic
enhancement' (SGPhW-Award 2003)

Lectureship in practical courses of semi solide dosage forms

Supervision of the following diploma thesis:

'Lipophilieeinfluss auf den Peptidtransport bei transdermaler
iontophoretischer Applikation'
performed by R. Mirsaidi

'Simultane Iontophorese einer Aminosäure und eines Markers'
performed by Ch. Zimmermann

'Transdermale Iontophorese: Einfluss des Hautmetabolismus auf
die Transportrate eines Dipeptids und eines Markers'
performed by N. Schnyder
(Amedis Förderpreis 2003)

